Multimodal self-motion integration for multilevel control of walking in Drosophila

Tomás Lopes da Cruz

Dissertation presented to obtain the Ph.D degree in Neuroscience

Instituto de Tecnologia Química e Biológica António Xavier | Universidade Nova de Lisboa

Oeiras,
June, 2022

UNIVERSIDADE NOVA DE LISBOA

Multimodal self-motion integration for multilevel control of walking in Drosophila

Tomás Lopes da Cruz

Dissertation presented to obtain the Ph.D degree in Neuroscience

Instituto de Tecnologia Química e Biológica António Xavier | Universidade Nova de Lisboa

Research work coordinated by:

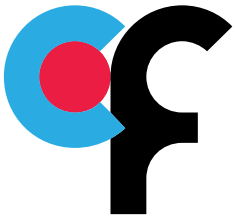

Oeiras, June, 2022

Acknowledgements

This thesis represents the culmination of a project that spanned over the last 7 years, and a journey that started even before that. Compiling the work from all these years I am moved not by the sequence of scientific production but by the sequence of wonderful people that have contributed in one way or another to this work. My deepest gratitude goes to (not by order of importance):

Para toda a minha família, pelo exemplo que são, pelos valores que me passaram, e especialmente porque mesmo quando não entendiam o significado do meu trabalho sempre me monstraram um orgulho incondicional. É esse tipo de apoio que permite dar 100% e avançar sem olhar para trás.

A tota la meva família catalana, per tot l'amor i suport al llarg dels anys.

Eugenia Chiappe first for years ago taking the change to hire someone with no clue of biology or neuroscience as the first person in her lab. Second for the continuous trust, teaching, guidance, mentoring and inspiration. Lastly for being an exemplar scientist whose high standards I hope to take with me for my whole life and career.

To all members of the Chiappe Lab, past and present, for being such a stimulating and nourishing group of people. Special thanks to Teru, Jimmy, Mert, André, Nuno, Nélia, Ece, Wynne, Seba, Rita, Marga and Corinna for all the coffee, cake, laughs, support, friendship and scientific insights.

All the friends that shared this journey with me and made the all the good moments better and all the bad ones not relevant. I can't thank you all by name here, but a special mention to: Rodrigo, Cachitas, Inês, Vivek, Julia, Vero, Paco, Tati, Bruno, Pietro.

The Champalimaud community, who have received me like family.

Lady and Kedi, for the fluff.

And Vicky, my love and inspiration, for always bringing me up when I am down and grounding me when I am obsessed. T'estimo.

Abstract

Locomotion in natural environments is under constant adversities like terrain inhomogeneities or noise in neuromuscular systems. Still, animals are capable of maintaining a tight coordination of movement across their body to reach their desired goals. In both vertebrates and insects, the neural control of locomotion is distributed across multiple areas in the central nervous system which provide different levels of control. To guarantee a successful locomotion, self-motion information is thought to be important at these multiple levels. However how self-motion information is processed in natural scenarios and how it modulates the selection and/or execution of locomotor movements is still unclear.

In the present thesis, we employed multiple strategies to explore how self-motion signals are integrated and used at multiple levels of locomotor control. We combined virtual reality tools with quantitative analysis of behavior to examine how *Drosophila melanogaster* uses self-generated visual information (visual feedback) to control gaze during exploratory walking. We observed that flies execute distinct motor programs coordinated across the body to maximize gaze stability. The performance of gaze stability is highly dependent on the ability of the fly to sense self-motion. We found that self-generated visual signals tune postural reflexes to rapidly prevent turns rather than to promote corrective steering, a long-standing idea for visually guided course control. We also describe a novel role of self-motion signals to flexibly modulate steering actions, and we partially identified a new neural pathway that could support this function. This neural pathway links the integration of self-motion signals during natural locomotion with action-selection/command centers in the fly brain. Finally, we used

whole-cell patch-clamp recordings while flies walked in virtual reality environments to gain a deeper understanding of the computations underlying self-motion integration. We found that multiple sources of congruent self-motion information converge in single neurons. Genetically targeted recordings of these neurons show that they perform an optimal integration of the unimodal signals to improve the reliability of self-motion estimation.

These findings have important implications for our understanding of how animals use self-motion information to achieve high-performance locomotion given the hardships created by natural scenarios.

Keywords: Locomotion control; Self-motion signals; Noise; Gaze stability; Posture stability; Multimodal integration

Resumo

A locomoção em ambientes naturais está sob constantes adversidades como as heterogeneidades no terreno ou o ruído inerente aos sistemas neuromusculares. Ainda assim, os animais conseguem manter uma fiável coordenação de movimentos em diferentes partes do corpo que lhes permite alcançar os seus objetivos. Tanto em vertebrados como em insectos, a parte neuronal do controlo da locomoção é distribuída por várias áreas do sistema nervoso central que fornecem diferentes tipos de controlo. Para garantir uma locomoção bem-sucedida, a constante monitorização do movimento é importante nesses vários níveis. No entanto, a questão de como o movimento é monitorizado em cenários naturais e como essa informação modula a seleção e/ou execução dos movimentos ainda permanece em aberto. Nesta tese, empregamos várias estratégias para explorar como os sinais relacionados com o movimento são integrados no sistema nervoso e usados em vários níveis do controlo da locomoção. Aqui, combinamos novas ferramentas de realidade virtual com análises quantitativas de comportamento para investigar como a mosca da fruta Drosophila melanogaster usa informações visuais provenientes do próprio movimento (feedback visual) para controlar a direção do seu olhar enquanto explora o ambiente. Observamos que as moscas executam diferentes programas motores suportados por distintas coordenações de várias partes do corpo para maximizar a estabilidade do olhar. Descobrimos que o desempenho da estabilidade do olhar é altamente dependente da capacidade da mosca em medir o próprio movimento. Descobrimos ainda que os sinais visuais causados pelo próprio movimento ajustam os reflexos posturais por forma a evitar desvios do olhar. Esta nova função aparece em alternativa à promoção de desvios corretivos, uma ideia de longa data no campo do controlo visual da locomoção. Descrevemos

ainda um novo papel da monitorização do movimento para a modulação das ações que alteram a direção do olhar e identificamos parcialmente um novo circuito neuronal que apoia essa função. Esse circuito neuronal liga a integração de sinais periféricos de movimento durante a locomoção com os centros de seleção/comando de ações no cérebro da mosca. Por fim, usamos whole-cell patch-clamp para medir a actividade de neurónios enquanto as moscas caminhavam em ambientes de realidade virtual, com o objectivo de atingir uma compreensão mais profunda das computações subjacentes à monitorização de movimento. Descobrimos que sinais de várias modalidades contendo informação acerca do movimento convergem em neurónios individuais. Medições da actividade desses neurónios mostram que eles realizam uma integração ideal dos sinais unimodais para melhorar a confiabilidade das estimativas de movimento. Essas descobertas têm implicações importantes para a nossa compreensão de como os animais usam a monitorização de movimento para obter alto desempenho na sua locomoção, dadas as dificuldades criadas pelos cenários naturais.

Palavras-chave: Controlo da locomoção; Monitorização do movimento; Ruído; Estabilidade do olhar; Estabilidade da postura; Integração multimodal

Contents

Chapter 1

Introduction

1.1 The hardships of locomotor systems

All our movements are defined by an interplay between behavioral goals, the reasons why movements are executed in the first place, and mechanical stability mediated by postural reflexes which keep our body balanced as we move through complex and unpredictable environments (Bernstein, 1967; Dickinson et al., 2000; Matthis et al., 2018). Thus, both external factors like terrain heterogeneity or internal factors like muscle fatigue or noise in sensorimotor systems can quickly compromise the stability of movements and jeopardize their intended goal. Still, simply observing a common housecat elegantly scamper through the tilted roofs of an abandoned house as it looks for possible victims, shows that evolution has equipped animals with the necessary tools to deal with the aforementioned hardships.

Locomotion in its different forms (e.g. flying, walking, swimming, etc.) is generally produced by the rhythmic oscillation of appendages that exert forces on the external environment to propel the animal in space (Dickinson et al., 2000; Herman, 2017). In comparison to other rhythmic movements like chewing or grooming, locomotion must be performed in a very rapid

and flexible manner (Bizzi et al., 1991; Foster & Higham, 2014). In the following sections we will briefly explore in more detail how locomotor systems work and the importance of locomotor control to allow for stable but flexible behavior.

1.2 Locomotor control in vertebrates and insects

Locomotor control systems are widely distributed through the nervous system of both vertebrates and insects. A common synthesis of the neural control of locomotion is to consider it as a multilevel process with different areas of the nervous system acting as interacting processing units. For instance, in both animal systems we can divide general movement control into 3 different levels: action selection (goal), command, and execution (Fig. 1.1, Arber and Costa, 2018).

1.2.1 Execution

Locomotion requires well coordinated rhythmicity. In its most basic form, the propulsion of the body through space requires a repeating sequence of alternating movements. For most animals, locomotion can be accomplished by a precise rhythmic coordination of antagonistic muscle pairs shaping movements around different joints. The neural circuits responsible for generation and coordination of the locomotor rhythm are located in the spinal cord in vertebrates and in the ventral nerve cord (VNC) in insects. These networks are typically known as central pattern generators (CPGs) and are thought to be sufficient to activate the different motor neurons in the appropriate sequence to generate locomotion (Grillner, 2006; Marder & Bucher, 2001; Marder & Calabrese, 1996). As long as they have sufficient drive, these spinal circuits alone can generate coordinated walking or swimming movements in mammals, fish or insects (Forssberg & Grillner, 1973; Gal & Libersat, 2006; Grillner & Wallén, 1982; Kien, 1983).

In both vertebrates and insects, the spinal cord/VNC are thought to be composed of multiple CPGs, each capable of generating independent rhythms of periodic bursting coordinated through inhibitory and excitatory interactions (Grillner, 1981; Grillner, 1985). The interaction between CPGs acting on different muscle groups around each joint forms microcircuits that can elicit different types of movements. The organization in specialized

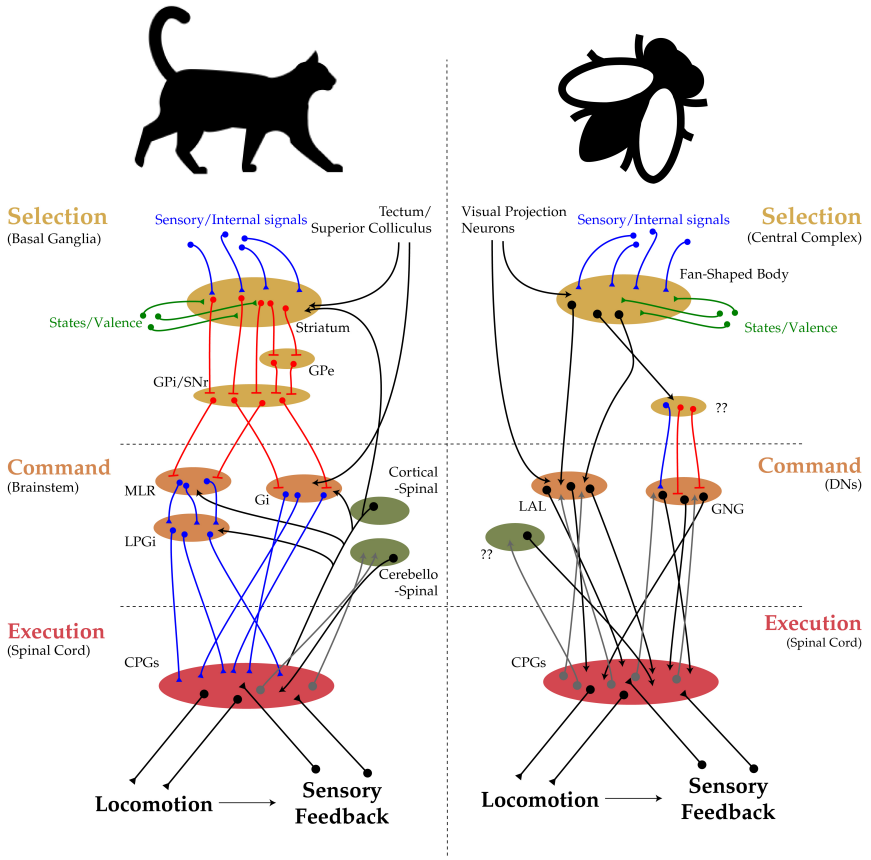

Figure 1.1: Schematic of goal directed locomotion circuits in vertebrates and insects. Locomotion control circuits were divided into selection (yellow), command (orange) and execution (red). Areas depicted in green are responsible for the fine-tuning of movement. Blue links correspond to known excitatory connections, red links to known inhibitory connections, green links to known neuromodulatory connections, black and grey links to other connections.

spinal microcircuits can allow for external signals to flexibly recruit and regulate the interaction between CPGs in order to shape the behavior to the animal's needs.

Multi-limbed animals need to coordinate movement around both single joints and across multiple joints, including across the left-right axis (Büschges et al., 2008). Within spinal cord/VNC circuits multiple sets of excitatory and inhibitory local interneurons have been found to mediate this interaction. An important class of interneurons conserved within vertebrates are the commissural V0 interneurons that control left-right limb alternation (Goulding, 2009). As an example of the versatility of these circuits, two V0 subclasses have been found to differentially coordinate left-right movements depending on the locomotive speed (Björnfors & El Manira, 2016).

In large insects, mostly unidentified VNC interneurons have also been found and proposed to mediate coordination within executive circuits (Brunn & Dean, 1994; Laurent & Burrows, 1989). However, in these systems, targeted functional experiments are still difficult. With its genetic toolkit, the insect model *Drosophila melanogaster* will surely help to find and test the role of specific intersegmental neurons at coordinating the execution of movement across the body. While the evidence for circuits with CPG-like activity is present for larger insects, there is still no conclusive evidence for their existence in smaller insects like Drosophila (Bidaye et al., 2018; Büschges, 1995; Fuchs et al., 2011). This lack of knowledge stems from the challenging electrophysiological access to the VNC in these animals. Once these technical challenges are surpassed, the genetic tools available for this organism will turn it into a promising system to study the neural topology underlying these networks and their interaction with descending neurons or other coordinating interneurons.

An important feature of CPGs is their recurrent relationship with proprioceptive and tactile feedback (Fig. 1.1). In some examples, CPG rhythmic activity and consequent muscle alternation do not depend on proprioceptive feedback (Dubuc et al., 1988; Grillner & Zangger, 1984), even though it is unclear to which degree these findings generalize to locomotion per se. Proprioceptive self-movement information plays a major role in regulating and adapting different phases of the locomotor cycle based on the state of different muscles and joint positions. This afferent sensory information

exerts a critical influence on the coordination of movements in both vertebrates and insects (Anderson & Grillner, 1981; Bässler & Büschges, 1998; Cruse et al., 2007). In legged animals, the multiple mechanoreceptors in the legs are constantly signaling every joint angle, velocity and acceleration (Tuthill & Azim, 2018; Tuthill & Wilson, 2016; Windhorst, 2007). In Chapter 3 of this thesis, we will further explore how this self-motion information is modulated in a step cycle dependent way (Pearson, 1995; Wolf & Burrows, 1995) to regulate multiple aspects of limb movement (Cruse, 1985, 1990; Dean, 1984).

The precise execution of locomotor movements is ensured by the continuous adaptation of the rhythmic activity of the CPGs by self-motion sensory feedback. Although the peripheral sensorimotor machinery is sufficient to execute coordinated locomotion, experiments with lesioned or decerebrated vertebrates (Orlovsky et al., 1999) and insects (Ridgel et al., 2007; Yellman et al., 1997) show the necessity of information from the brain in order to command initiation and termination of locomotion (Gal & Libersat, 2006), as well as to command its speed and direction (Berg et al., 2018; Graham, 1979).

1.2.2 Command

Even if well coordinated, locomotion in decerebrated animals is rather purposeless since the animal can't actively guide its locomotion towards a particular goal. The modulation of spinal cord/VNC executive circuits by higher brain areas is brought about by descending neurons (DNs). Multiple classes of DNs have been identified in both vertebrates and insects. In vertebrates, brain areas like the brainstem, the cortex or the cerebellum are the major sources of input to the spinal cord. Interestingly, of the aforementioned spinal tracts, the brainstem is the only one that has been shown as necessary and sufficient to command locomotion, with the cortical and cerebellar pathways being attributed a modulatory role that we will explore later (Grillner & El Manira, 2020).

The brainstem location at the intersection between higher motor centers and the spinal cord makes it a major candidate for commanding body movements. This role became especially evident with the discovery of a brainstem region that could induce locomotion in a decerebrate animal (Shik et al., 1969). This brain area was later called the mesencephalic locomotor

region (MLR) and it turned out to be a highly conserved command structure controlling locomotion in vertebrates. While some MLR neurons respond to locomotion, other MLR neurons have been found to be recruited during other spontaneous behaviors like rearing, grooming or food handling, suggesting a more diversified function for the MLR (Ferreira-Pinto et al., 2021). Still, unilateral activation of MLR induces laterally symmetric locomotor movements (Brocard et al., 2010) through its connections to brainstem reticulospinal neurons that can directly modulate spinal CPGs (Garcia-Rill & Skinner, 1987; Steeves & Jordan, 1980).

The spatial intermingling of brainstem circuits makes it challenging to understand the role of particular neural populations. At the same time, electrical stimulation and lesion experiments are too coarse to draw a clear picture of the contribution of the multiple intermingled neural populations. With more recent genetic and tracing tools, brainstem organization started to be unveiled (Arber & Costa, 2022; Caggiano et al., 2018; Josset et al., 2018). In particular, the role of MLR as locomotion command is connected to another brainstem area called lateral paragigantocellular nucleus (LPGi) (Fig. 1.1). The glutamatergic neural population in this brainstem area receives MLR inputs and is both sufficient and required for eliciting high speed locomotion (Capelli et al., 2017). Recently, a nearby brainstem population has been proposed to command the direction of locomotion. A specific genetically identifiable population in the nucleus gigantocellularis (Gi) has been implicated in ipsilateral turning behavior when unilaterally manipulated (Cregg et al., 2020). Neurons in the Gi receive major inputs from the tectum/superior colliculus, an area responsible to elicit approach or evasive behaviors (Usseglio et al., 2020). Still, how these neurons relate to turning (Bouvier et al., 2015; Schwenkgrub et al., 2020) in more general locomotor contexts is still unclear. A complete picture will require better genetic neuronal subtype specification together with targeted physiology in behaving animals to understand how the context for turning relates to recruitment of activity from different neural populations.

Gi and LPGi are just two example brainstem populations that exist in close proximity and control different aspects of locomotion. In general, brainstem sub-areas and populations of DNs are thought to operate as command lines for diverse types of actions of the body. Information from different brainstem circuits is then likely to be combined in the spinal cord, where local circuits and sensory feedback contribute to further processing

towards execution.

In insects, even with the numerically simpler nervous system and extensive anatomical information, the organization of descending pathways is not much more evident. As with vertebrates, fully decapitated insects are still capable of coordinated locomotion. Still, they have similar problems with the self-initiation of walking as well as at speed and direction control. These early observations were followed by precise lesion studies in large insects. These legion studies indicate that descending neurons situated in the gnathal ganglion are sufficient for initiating forward walking, whereas higher brain regions like the lateral accessory lobe (LAL) are necessary for control of walking speed and direction (Gal & Libersat, 2006; Graham, 1979; Ridgel & Ritzmann, 2005). Interestingly, lesions where most of the brain is removed but the gnathal ganglion is left intact result in insects that exhibit long bouts of coordinated walking, suggesting an inhibitory influence from the rest of the brain on this premotor brain region (Bässler & Wegner, 1983; Kien, 1983; Ridgel & Ritzmann, 2005). In contrast, lesions to the gnathal ganglion dramatically reduced spontaneous locomotion (Kien, 1983).

In the last decades, the powerful genetic tools of the fruit fly *Drosophila melanogaster* have been successfully put to the service of systems neuroscience, allowing for highly specific manipulations and recordings from genetically identified cells or cell populations. In recent years, a collaborative effort (Namiki et al., 2018) has systematically identified and generated genetic access for a large number of DN cell types. Purely anatomical analysis revealed a similarity in the numbers and spatial distribution of DNs across insect species (Hsu & Bhandawat, 2016). While DNs could be found through most of the fly brain, they have an especially high density of dendrites in the more ventral-posterior parts of the brain, with special emphasis on the areas around the LAL, the posterior slope (PS) and the gnathal ganglion. Interestingly, the same study revealed that some premotor areas including the LAL-PS form a coarse cluster of DNs that project into integrative VNC areas while another premotor area that includes the gnathal ganglion has its own cluster of DNs that mainly project to all leg-related neuropils in the VNC (Namiki et al., 2018). These projection patterns in combination with the previous activation experiments are consistent with the hypothesis that the gnathal ganglion (in a loose analogy to LPGi) elicits and maintains generic coordinated locomotor movements, while LAL-PS (perhaps more analogous to Gi and other modulatory descending pathways) instructs goal-oriented

steering behaviors. We will further explore this apparent organization of locomotor circuits and what it might do for the animal's natural behavior in Chapter 2 and 4 of this thesis.

In line with this idea, recent electrophysiological recordings from descending neurons with dendrites in the LAL-PS associated areas (Rayshubskiy, 2020; Schnell et al., 2017) have shown strong correlations between their activity and the steering maneuvers of the fly. Moreover, neurons projecting close to the gnathal ganglia have been shown to induce non-directional straight, forward walking (Bidaye et al., 2020). Full brain imaging has further shown a correlation between the activity in the gnathal ganglia and forward walking whereas activity in LAL-PS areas correlated more strongly with lateral movements (Brezovec et al., 2022). To better understand the role of these different command lines, it will be important to consistently record and manipulate the same neuron or neural population in the context of locomotion while knowing their synaptic inputs. In Drosophila, specific DNs have been implicated in behaviors like landing (Ache, Namiki, et al., 2019), courtship (Von Philipsborn et al., 2011), evasive take-off (Von Reyn et al., 2014) or freezing (Zacarias et al., 2018). Additional physiological and functional studies will be necessary to link the genetic diversity of descending neuron populations with their role in locomotion control.

In both vertebrates and insects, descending pathways are thought to function as the relay between selected goal-related actions and the activation of the desired executive spinal/VNC circuits. One of the important, as of yet unanswered, questions is how do diverse descending pathways interact and modulate spinal/VNC circuits. We will tackle this question in Chapter 3 and 6 of this thesis.

1.2.3 Selection

As important as being able to move in space, it is to do so based on when and where the animal so desires. In both vertebrates and insects, multiple brain circuits give input to the previously mentioned command areas and can select different movement patterns based on the desired action. In vertebrates, a brain area that deserves special attention for its role in action selection are the basal ganglia. In insects, a similar role has been attributed to the central complex as a potential important upstream contributor to movement selection (Fig. 1.1).

The basal ganglia comprise highly conserved areas within the vertebrate brain that strongly connect to the brainstem and have been proposed to be critical for selection of or commitment to different movements.

Basal ganglia output nuclei (GPi/SNr) provide tonic inhibition to different brainstem motor command centers including the MLR (Stephenson-Jones et al., 2011). Classical models suggest that for movement selection to happen, a coincident excitatory activation and disinhibition of command centers from basal ganglia output structures has to occur. This disinhibitory mechanism for the release of a motor program has been demonstrated in multiple species (Garcia-Rill et al., 1983; Grillner et al., 2005; Hikosaka & Wurtz, 1983; Roseberry et al., 2016; Takakusaki et al., 2003) and is mediated by direct and indirect inputs to GPi/SNr from another basal ganglia structure call the striatum. Striatal neurons receive excitatory inputs from cortical and thalamic areas as well as dopaminergic modulation. Even though the information about specific actions is inherited from upstream circuits, striatal neurons can convey their vigor and selection (Thura & Cisek, 2017). Importantly, activation of the direct connections from striatum to GPi/SNr leads to activation of glutamatergic MLR neurons and consequent initiation of locomotion (Mogenson et al., 1985; Roseberry et al., 2016). In opposition, net activation of the indirect connections results in enhanced activity in GPi/SNr, which further inhibits downstream motor centers (Cui et al., 2013). Consistently, activation of the indirect pathway can result in a reduction of locomotion (Roseberry et al., 2016). These results contribute to an understanding of basal ganglia's role in motor control as a "center surround for actions" (Arber & Costa, 2022). In this model, the inhibited population of SNr neurons target the specific brainstem neurons required for execution of the desired movement, while the activated population of SNr neurons project to other brainstem neurons to inhibit competing non-desired movements (Freeze et al., 2013). In line with this idea, different populations of SNr neurons target different brainstem command areas, even though the actual level of specification of these targets is still not known.

Within this simplified depiction of the basal ganglia, an important element deserving of special attention is dopamine. Dopamine has a major role in the functioning of basal ganglia circuits. A classical role of dopaminergic input from VTA is related to the signaling of rewards. The purpose of these

dopaminergic signals is to reinforce motor programs based on external rewards or perception of success. More recently, the activity of SNc dopaminergic neurons has been associated with locomotor events. Furthermore, SNc dopaminergic neurons have been shown to be critical for both movement initiation and vigor (Da Silva et al., 2018; Howe & Dombeck, 2016). It has been proposed that these non-specific locomotor-related dopaminergic input could set internal contexts that increase the excitability of specific locomotor striatal ensembles. Within this hypothesis, dopaminergic input influences action selection by influencing the magnitude and specificity in which striatum communicates with its targets.

In insects, a set of anatomical, behavioral and physiological results have placed the central complex as potential brain region linking sensation and action (Pfeiffer & Homberg, 2014; Turner-Evans & Jayaraman, 2016). The central complex has been suggested to perform partially analogous functions to multiple areas of the vertebrate brain. In this brief description we will focus mostly on its role as a premotor center that has the ability to flexibly select actions to control locomotion.

The central complex is composed of multiple areas, namely the protocerebral bridge (PB), ellipsoid body (EB), fan-shaped body (FB), and the noduli (Nod). These regions are further connected to several support areas including the LAL and the bulb (Turner-Evans & Jayaraman, 2016). Over recent years, many studies have focused on how the central complex integrates multimodal sensory information related to the insect's orientation in space to generate abstract representations of heading (Green et al., 2017; Okubo et al., 2020; Seelig & Jayaraman, 2015). The abstract representations are maintained by a ring attractor-like network existent in the PB-EB (Kim, Rouault, et al., 2017). This representation physically exists as a bump of activity that can be understood as a vectorial representation of heading. These orientation vectors propagate and are further processed in different areas of the central complex until they reach the fan-shaped body and further output areas (Lu et al., 2022; Lyu et al., 2022). It is, however, unclear what the animals do with these orientation vectors, or more generally, how exactly they convert this abstract information into action.

Another body of literature (collected mostly in large insects) has observed that the central complex is important for the initiation and maintenance of walking activity (Bender et al., 2010). The central complex is also crucial for the fine-tuning of motor patterns, like unilateral alterations in

stride length that lead to curve walking (Harley & Ritzmann, 2010; Strausfeld, 1999). The premotor role of the central complex has expanded to other motor behaviors like flight (Strauss & Heisenberg, 1993)), acoustic communication (Popov et al., 2005), and courtship (Sakai & Kitamoto, 2006). Through extracellular recordings, Martin et al., 2015 showed that activity within central complex neurons can predict different locomotor movements hundreds of milliseconds in advance, suggesting the direct involvement of this area in the generation of different motor commands. Even though the connection between more sensory/representational functions of the central complex and its premotor functionality is still being investigated (probably as this thesis is being written), some suggestions on how central complex wiring may integrate both functions have arisen from anatomical studies (Hulse et al., 2021).

The fan-shaped body in particular is organized in a 2D grid (Hulse et al., 2021; Strausfeld & Hirth, 2013), with different columnar cell types operating as phase shifted vector representations of the fly's movement direction, and possibly also representing other ongoing motor variables. This anatomical configuration (allied to the columnar structure of fan-shaped body outputs) is proposed to be well suited to generate detailed goal-directed motor commands (Stone et al., 2017). Orthogonal to this sensory-motor columnar structure, the fan-shaped body is innervated by many dopaminergic tangential neurons. These tangential neurons receive inputs from, among others, Mushroom Body (MB) output neurons that encode valence-related signals, including reward, punishment, behavior goal or motivation (Scaplen et al., 2021). These dopaminergic neurons have also been implicated in experience-dependent behaviors (Ojelade et al., 2019). Moreover, different fan-shaped tangential neurons have been shown to encode more broad internal states like locomotion, hunger, sleep or aggression (Liu et al., 2016; Pimentel et al., 2016; Sareen et al., 2020; Weir & Dickinson, 2015). The organization of this brain structure combined with an analysis of the programs of gene expression and regulation in place have suggested some analogy to the vertebrate striatal structure where connections between sensory/representational pathways and specific actions are promoted/reinforced by dopaminergic signals coding for valence, locomotion and internal state information (Fig. 1.1, Strausfeld and Hirth, 2013). This hypothesis of how the central complex might support action selection still raises questions about how central complex output neurons modulate command areas, in

particular the LAL-PS. In Chapter 4 of the present thesis We will explore the factors involved in eliciting and modulating locomotor decisions.

1.3 Self-motion integration for multilevel locomotor control

The largely feedforward scheme for locomotion control presented in the previous section can generate locomotion patterns and adapt them based on the goals of the animal (Fig. 1.1). However, this simplified scheme would be insufficient to explain the complexity of animal locomotion in natural scenarios. As alluded previously, the dynamic nature of natural environments pose challenges to an animal's locomotion. Such challenges can relate to extrinsic factors like terrain heterogeneity, weather events, or intrinsic factors like the state of the animal's body, muscle fatigue or sensorimotor noise. For all these challenges that animals encounter as they locomote, feedback systems have to be in place to help achieve its desired goals.

Nervous systems across the animal kingdom developed strategies to monitor self-movement. Many sensory systems signal self-motion: vestibular systems inform the brain about head movements, proprioceptive systems inform the nervous system about the movement and position of different body parts, motion vision conveys information about eye, head and body movements. In addition, premotor circuits route copies of motor commands to different brain areas, including sensory pathways. These internally generated signals, known as corollary discharge (Sperry, 1950) or efference copies (von Holst & Mittelstaedt, 1950) have been largely thought of as an inhibitory mechanism acting on incoming reafference streams to cancel out the effects of self-motion (Crapse & Sommer, 2008). This type of inhibitory effect is often observed in reflexive systems that must be prevented from self-activation (Cullen, 2004; Davis et al., 1973; Kim et al., 2015a; Sillar & Roberts, 1988; Voss et al., 2006).

Under certain circumstances, however, self-motion information becomes crucial and should not be canceled out. For example, in the context of navigation and other oriented behaviors, the brain relies on an accurate internal estimate of self-movement to update internal representations of both ongoing movement and space (Franklin & Wolpert, 2011; Requarth

et al., 2014; Sommer & Wurtz, 2002; Whitlock et al., 2008).

Locomotion generates self-motion information from multiple independent sources. How different sources are jointly integrated to control locomotion is still unknown. During locomotion different body parts have to be coordinated together for posture control, simultaneous with the control of direction and speed of movement. Self-motion information is not only critical for navigation but also to be able to orchestrate the successful coordination across body parts and to fine-tune the behavior of the animal in dynamic conditions.

1.3.1 Reconciling posture and command

Locomotion in natural environments is marked by constant trade-offs between different aspects of behavior that are generally modulated by the environment. For example, an exploring cat might prefer to walk on a more difficult and energy intensive burrowed path than on a much easier but more exposed one. Another major tradeoff animals and in general locomotor systems have to make is the one between maneuverability and passive stability (Dickinson et al., 2000). The need to coordinate movement across body parts while ensuring the stability of the whole body relies on being able to align the movement command with postural adjustments. This alignment depends on constant regulation of the motor output by both neural and mechanical feedback (Gandevia & Burke, 1992). Thankfully, evolution has equipped animals with multiple arrays of neuromechanical sensors that monitor the forces and shape changes in the musculoskeletal system throughout each cycle of locomotion (Duysens et al., 2000). Self-motion feedback from these structures is essential for the operation of CPG circuits, with both central and sensory systems operating as a single unit in natural conditions (Pearson, 1995).

A striking example comes from limbed locomotion. Across species, the step cycle is divided in four phases: stance (support), lift-off, swing and landing. The moment of lift-off is particularly reliant on information about the limb's position and the the load and forces it encounters (Büschges, 2005; Grillner & Rossignol, 1978; Noah et al., 2004) in order to prevent a lift-off from a leg that is currently supporting body weight, which would cause the animal to fall. Interestingly, this load and position information not only modulates the stepping at the VNC/spinal level but is also transmitted to

the cerebellum through the dorsal spinocerebellar tract.

In vertebrates, the cerebellum is particularly well placed to aid spinal postural reflexes that maintain locomotion stability. In addition to all the information it receives directly from the spinal cord and other brain centers (Miall & Wolpert, 1996), it can also directly target CPGs or motoneurons through descending pathways. Adding to the ability of the cerebellum to continuously monitor and correct ongoing locomotor activity, it is also capable of adapting movements through learning (Darmohray et al., 2019; De Zeeuw & Yeo, 2005; Miles & Lisberger, 1981). An equivalent system in insects has not yet been found, even though they are also capable of movement adaptation through learning (Isakov et al., 2016). In addition, cerebellar associated nuclei are critical to mediate the use of sensory information for movement or postural adjustments. An example of this are vestibulo-collic reflexes, that function to stabilize the head in the presence of a vestibular disturbance through the activation of neck muscles (Gdowski & McCrea, 1999; Wilson et al., 1995).

An asymmetric activation of the vestibular system leads to posture changes during standing and locomotion (Deliagina et al., 2008; Deliagina et al., 2006). These effects are mediated by the vestibulospinal neurons, which themselves can excite motoneurons (Grillner et al., 1971; Murray et al., 2018). In particular, a lateral perturbation is compensated by a lateral movement of the limbs during the next swing phase so that they land in a more lateral position. There are, however, only limited effects on overall limb trajectory (Karayannidou et al., 2009). An important aspect of many of these stabilizing mechanisms is their context dependency. For example, the vestibulo-collic reflexes don't occur during active head movements (Cullen, 2019) and the responses to lateral perturbations diminish with the vigor of locomotion (Orlovsky & Pavlova, 1972).

In summary, fast supraspinal sensorimotor loops, as well as local circuits within the spinal cord/VNC, use self-motion information to perform rapid adjustments tailored to the step cycle to control posture in the presence of internally and externally generated noise. These adjustments can be context-dependent and under the modulation of other executive pathways through efference copies or other unknown mechanisms. In fact, how animals align their selected goals sent through command circuits with their posture stability requirements given by spinal/VNC or modulatory circuits is largely unknown.

1.3.2 Visuomotor fine tuning of movements

Self-motion information is used not only for reflexive-like modulation of movement execution but also in conjunction with higher order processing to fine tune the movement of animals in natural environments. Visuomotor information takes a especially important role in this context both to avoid or approach elements of the environment and to fine-tune the placement of the limbs in complex and dynamic environments.

In vertebrates, steering actions to orient or avoid particular obstacles depend to a large extent on the activity of the tectum/superior colliculus. This brain structure receives visual input in its top layers arranged in a retinotopic map of the surrounding space (Isa et al., 2021). The retinotopic map can be used to spatially align other sensory information like auditory or olfactory signals in the intermediate layers (Isa et al., 2021). In the bottom layer, the multisensory maps are then transformed into a motor map that can be understood as having two types of efferents, one producing evasive and other producing orienting movements (Helmbrecht et al., 2018; Kardamakis et al., 2015; Saitoh et al., 2007). The tectum/colliculus efferents project to the thalamus and to the brainstem (including Gi nucleus), the latter conveying steering signals to the spinal cord.

Visuomotor coordination is also mediated by the motor cortex through the corticospinal system in mammals, which enables them to modify the step cycle and provide very precise placement of the feet when walking (Beloozerova & Sirota, 1993; Drew et al., 2008). Corticospinal neuronal activity is highly modulated during both precision walking and reaching tasks (Beloozerova & Sirota, 1993; Drew & Marigold, 2015). Interestingly, these premotor pathway establishes extensive axon collaterals to multiple regions (Kita & Kita, 2012) like the basal ganglia, superior colliculus and the brainstem before descending to the spinal cord. The specific role of these collaterals in the modulation of other premotor circuits still remains an open question.

In insects, visual processing happens within the retinotopically organized optic lobe. From there, the large majority of visual projection neurons exit from the Lobula Complex towards the central brain. Once most visual projection neural populations reach the insect central brain they lose their retinotopic arrangement and form compact glomeruli-like structures

(Strausfeld, 1976; Strausfeld & Okamura, 2007; Wu et al., 2016). This organization led to the belief that visual pathways in insects are specialized for coarsely modulating specific behaviors (Ache, Polsky, et al., 2019; Keleş & Frye, 2017; Klapoetke et al., 2022; Ribeiro et al., 2018; Wu et al., 2016). Further anatomical and functional exploration of visual projection pathways together with mapping their connectivity to DNs and premotor areas is necessary to get a clearer picture of how visuomotor information informs the fine tuning of the insect's locomotion.

The most well studied region involved in the visual steering of insect locomotion is the Lobula Plate, in particular its optic-flow sensitive large tangential cells (LPTCs, reviewed in Borst and Haag, 2002). LPTCs function as matched filters for the complex optic-flow patterns associated with the insect's own movements (Krapp & Hengstenberg, 1996; Krapp et al., 1998). A more detailed exploration of these self-motion sensitive cells can be found in Chapter 5 of this thesis. Importantly, even though optic-flow is generally thought to be critical for controlling body rotations in the presence of perturbations (Borst, 2014; Brandt et al., 1971; Srinivasan, 2011; Turano & Wang, 1994; Warren et al., 2001), its role in natural walking control remains contested (Cutting et al., 1992; Götz & Wenking, 1973; Harris & Bonas, 2002; Katsov & Clandinin, 2008; Prokop et al., 1997; Rushton et al., 1998; von Holst & Mittelstaedt, 1950; Warren & Hannon, 1988; Warren et al., 2001). Moreover, even though optic-flow sensitive neurons are found universally across species, from insects to non-human primates (Duffy & Wurtz, 1991; Grasse & Cynader, 1982; Hengstenberg et al., 1982; Joesch et al., 2008; Kubo et al., 2014; Morgan & Frost, 1981; Soodak & Simpson, 1988), the full pathways that link this self-motion feedback to movement selection and execution remain largely unknown in any species.

1.4 Thesis aim and structure

In the previous sections we examined the systems for locomotion control with emphasis on the functional parallels between the vertebrate and insect neural pathways to guide locomotion in naturalistic conditions. We started from a mostly feedforward and hierarchical understanding for the generation of purposeful locomotion. Through the acknowledgement of the real challenges of natural scenarios, we further explored the important role of self-motion feedback at multiple levels to allow for stable and precise

locomotion.

It is important to note that the simple scheme of the hierarchical control composed of goal-command-execution is constantly challenged by new anatomical and functional data that shows a much deeper recurrence and inter-connectivity between these premotor areas in both vertebrate and insect systems. The purpose of the observed recurrence and how much the actual control scheme deviates from this simplified version are big questions still unanswered in any system. In the previous sections we further posed some important questions that are deeply intertwined with the research presented in this thesis:

- How do command level signals interact with ongoing executive circuits, specially in conflicting situations?

- Through which pathways is self-motion information used to inform and modulate behavior decisions?

- How are multiple sources of self-motion information interacting within central circuits to modulate behavior?

Finally, we also emphasized the promising role that Drosophila has in tackling some of the major questions related to locomotor control. The well-established large genetic toolkit available in this organism, combined with the recent connectomic efforts and the development of novel paradigms that allow for targeted neural recordings and manipulation during behavior, will help us better understand the complexity and beauty of the neural mechanisms that allow animals to seamlessly move through their natural environments.

The present thesis further includes four chapters of results and a general discussion. The first results chapter (Chapter 2) aims at establishing the newly developed paradigms and analytical methods to understand the elements structuring fly locomotion. The following three chapters tackle the three questions pointed out above.

Chapter 3 explores how flies balance different level goals during locomotion. Namely how the need for posture stability is balanced with other goals. We further examine the role of visual-motion feedback at orchestrating this balance. Chapter 4 investigates the internal and external factors that modulate the animal's behavior decisions and describes a novel neural pathway that brings self-motion information into premotor goal-related areas.

In Chapter 5, the experimental paradigm is changed in order to allow for whole-cell patch clamp recording in walking flies. This chapter shows that neurons classically considered to be visual-motion sensitive actually integrate multimodal self-motion signals in a statistically optimal fashion. This reliable multimodal self-motion estimation explains some of the behavior results obtained in the earlier chapters.

Finally, in the last chapter, the main insights arising from our results will be discussed together with the new lines of inquiry they suggest.

CHAPTER 2

GAZE STABILITY AS LOCOMOTOR GOAL DURING EXPLORATORY WALKING

2.1 Overview

In the previous chapter, we have explored the crucial role of self-motion signals to guarantee locomotor performance while animals walk in real world scenarios. Furthermore, we asserted Drosophila as a powerful model organism to investigate the mechanisms underlying the interactions between the different levels of locomotor control. In the following sections we will focus on the contribution of visual self-motion information to the walking behavior of the fruit fly *Drosophila melanogaster*.

We approach this question by allowing the fly to express free and spontaneous walking while we continuously monitor its behavior and visual feedback at high detail. By not constraining the animal within the confines of a task we gain access to a more natural repertoire of locomotive motifs. However, the lack of a task structure also makes it harder to set the context for the animal's behavior and therefore we can't directly access its explicit goals. Moreover the monitoring of self-motion clues becomes much harder when animals are not physically constrained. In this chapter,

we will present our strategy and results that allowed to circumvent some of these challenges: starting with (1) the development of novel experimental paradigms; (2) the use of both supervised and unsupervised strategies to understand the coarse dynamics of exploratory walking; and (3) the detailed analysis of coordination across body parts to attribute particular goals to different movement patterns of the freely walking fly.

2.1.1 A general strategy for unconstrained visual exploration

Understanding the structure of the environment is a critical skill for survival. For example, once in a new environment, finding the closest shelter can prevent predation or finding the closest food source can prevent starvation. A common exploratory strategy to extract information from an environment is to interleave quick shifts in gaze with moments of gaze stability (Collett & Land, 1975; Easter & Johns, 1974; Fuchs, 1967; Land, 1973; Land, 1995; Pratt, 1982; Stryker & Blakemore, 1972; Yarbus, 1967). Integral to such strategy is the ability to maintain the position of gaze stable in order to acquire spatial information from the environment (Collett, 1978; Land, 1999; Lehrer et al., 1988; Schuster et al., 2002). Since most animals are also able to smoothly move their gaze (Collett & Land, 1975; Rashbass, 1961), such a fixation-saccade gaze pattern does not emerge from any physical limitation in the way animals are allowed to move their eyes or body/head. A fixation-saccade strategy is generally opted while animals explore a visual scene. This strategy has been proposed to assure essential functions like minimizing the motion blur experienced while moving the gaze or help the disambiguation between rotational and translational visual-flow fields (Land, 1999).

Because of their high spatial resolution and relatively low temporal resolution, vertebrate eyes become especially susceptible to motion blur (Kelly, 1979). Minimizing eye movements in between saccades and reducing saccadic duration decreases the blurring of the image due to gaze change. In the case of insects, the lower spatial resolution and higher temporal resolution makes motion blur relevant only when gaze shifts at high speed (Juusola & French, 1997). Another major motive to maintain a stable gaze is flow field disambiguation. While the optic-flow pattern resulting from a pure gaze rotation does not include spatial information, the optic-flow resultant from

a pure translation is intrinsically linked to the relative distance between observer and objects (Koenderink & van Doorn, 1987). The use of translational optic-flow information to estimate distance has been previously shown in some species (Collett, 1978; Lehrer et al., 1988) and there is even some evidence for it in walking Drosophila (Schuster et al., 2002). While it is still unknown how a tight performance of a fixation-saccade movement pattern influences these spatial behaviors, computational studies have shown that the processing of depth information is crucially dependent on a precise gaze stabilization, being jeopardized if the translational optic-flow is contaminated by rotational information (Koenderink & van Doorn, 1987).

2.1.2 The case of flying insects

An open window on a warm day can lead to some flies flying erratically through a living room. A closer look at the seemingly aimless movement of these insects exposes that they are all roaming in a similar way: they interleave moments of flying straight in some direction with a fast, sharp change in direction, followed by another moment of straight flight. This very recognizable flight scheme in patrolling houseflies (Wagner, 1986; Zeil, 1986) is also observed in hoverflies (Collett & Land, 1975; Geurten et al., 2010), honeybees (Boeddeker et al., 2010; Dittmar et al., 2010), blowflies (Land, 1973; Schilstra & Hateren, 1999) and Drosophila (Buelthoff et al., 1980). Moreover, this flight pattern happens in a large variety of behavior contexts, such as cruising (Collett & Land, 1975), patrolling (Zeil, 1986), searching (Dittmar et al., 2010) or orienting to external landmarks (van Breugel & Dickinson, 2014). The behavior is so robust and innate that it is still observable even under tethered, sensory deprived conditions (Heisenberg & Wolf, 1979; Reichardt & Poggio, 1976). Common across all the aforementioned behaviors is a need of the animal to understand its environment, either to try to escape (Heisenberg & Wolf, 1979; Tammero & Dickinson, 2002), to look for competitors (Zeil, 1986) or to find the appropriate place to land/fly towards (Dittmar et al., 2010; van Breugel & Dickinson, 2014). Noticeably, the highly conserved flight scheme is not a consequence of mechanical constraints, since flying insects are still able of many other flight patterns while engaged in other contexts (Collett & Land, 1975; Schilstra & Hateren, 1999).

It is still unclear whether or under which conditions free walking Drosophila engage in a fixation-saccade exploratory strategy (Geurten et al., 2014). Reaching those conditions can anchor our examination of the elements of locomotor control by establishing the locomotor goal of the fly as to maximize the stability of its gaze.

2.2 A virtual reality setup for freely exploring Drosophila

2.2.1 Free walking virtual reality

We developed a novel virtual reality (VR) system to study the role of self-generated visual information (visual feedback) on walking control. This system allows for precise manipulations of visual feedback while flies walk around freely (Fig. 2.1A).

In our system, single flies with clipped wings moved freely in a 90mm circular arena with walls heated up to 42ºC by an insulated nichrome wire (Pelican Wire P2128N60TFEWT). In order to prevent walking on the ceiling, the arena was covered with a glass plate pre-treated with Sigmacote (Sigma). Individual flies covered the space homogeneously within a few minutes, while avoiding the aversive hot walls of the arena. The fly was video recorded using a near infrared camera (IDS UI-3240CP-NIR) at a frame rate of 60Hz and resolution 900x900 pixels. The camera has attached a 2x expander (Computar EX2C), a wide field lens (Computar 5mm 1:1:4 ½), and a filter against visible light (Thorlabs AC254-100-A-ML). The illumination was set beneath the arena by IR LEDs (850nm SFH 4235-Z), powered by a current power supply (TENMA 72-10480). The position and orientation of the fly were determined via real-time tracking. Simultaneously, custom-made visual stimuli were projected onto the arena's floor, i.e., ventrally to the walking fly. A ventral projection of a visual pattern was sufficient to stimulate the fly's over an area that extended from a ventral region of the eye to above the equator. Previous to starting this project it was still not established whether a ventral projection was sufficient for effective processing of self-generated visual information (an exception can be found here Katsov and Clandinin, 2008). We quickly realized that flies strongly cared about ventral visual flow (see Chapter 3) and therefore kept the visual display configuration. Visual stimuli were projected onto a rear projection material (Da-Lite High Contrast DA-Tex), attached to the floor of the arena.

We used a small LED projector (DLP Lightcrafter 4500, Texas Instruments) at a frame rate of 60Hz and a pixel size of 160px/mm. The achieved pixel size is smaller than the resolution of the eye of the fly as long as it keeps its head elevated at about 10 micrometers. However, the frame rate of 60Hz is slower than the speed of the fly photoreceptor flicker fusion. We tested whether this would be a problem both by checking the fly's behavior responses (Chapter 3) and also by measuring the physiology of neurons that integrate visual feedback information in the fly brain (Chapter 5). None of the tests suggested any effect of the 60Hz framerate in behavior or in neural response.

Following FlyMad (Bath et al., 2014), high-resolution images of the fly were recorded at 120fps and 1024x544 pixel resolution with a near infrared camera (IDS UI-3360CP-NIR-GL) and a telecentric lens (Edmund Optics 1x, 220mm WD CompactTL Telecentric Lens). The camera pointed to a pair of galvo mirrors (Thorlabs GVS012/M - 2D Large Beam (10mm) Diameter Galvo System) whose orientation was controlled by the FlyVRena software based on the instantaneous position of the fly in order to maintain the fly centered in the high resolution frame (Fig. 2.1A).

Our system therefore allows for the precise manipulation of self-generated visual feedback of flies that are free to walk in user-defined visual environments. Furthermore, we can both acquire lower resolution movement trajectories of flies in our large arena while they naturalistically interact with the virtual environment, and also acquire high resolution data of the movement and coordination of the different body parts of the fly (Fig. 2.1C). The link between these two scales of analyzing motor control will be an important aspect of the investigation in the following chapters.

2.2.2 FlyVRena software

A custom-made software (FlyVRena, https://github.com/tlcruz/FlyVRena) (Cruz, 2013) manages the full operation of our experimental apparatus. FlyVRena implements the real time tracking of the position and orientation of the fly. The tracking algorithm first performs a background subtraction using an image of an empty arena, followed by the application of a pixel intensity threshold. From the distribution of pixels within the contour of the thresholded image, the 2D centroid and main orientation are estimated. The final estimate of the position and orientation of the fly is given

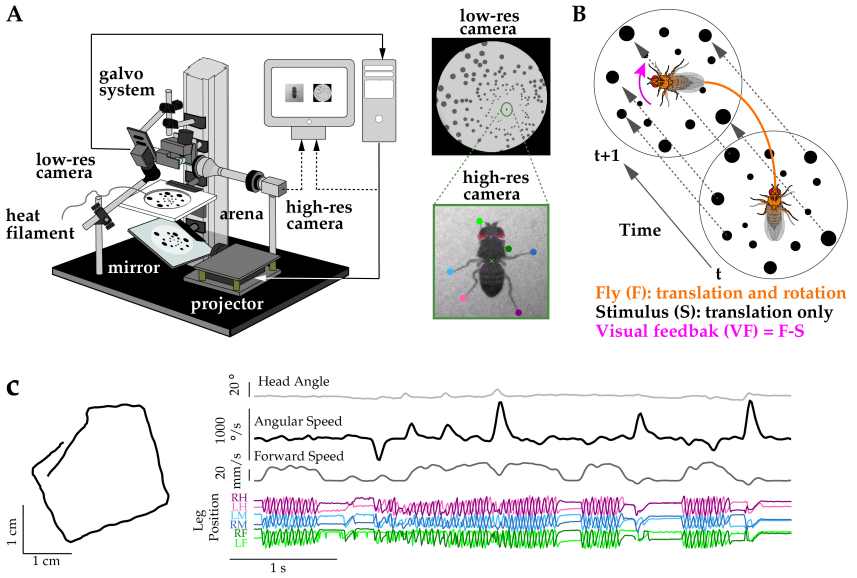

Figure 2.1: **A virtual reality setup for freely exploring Drosophila.** (A) Virtual reality setup for freely walking flies. (B) Virtually constrained visual feedback. A change in the fly position (orange), detected in real-time, elicited an identical translation of the stimulus (dotted lines), such that walking generated rotational-related visual signals only (magenta). (C) Example set of time series measured with the developed system that range from lower resolution exploratory paths, to kinematics of full body movements (angular and forward speed), to detailed movement of different body parts (head and leg positions).

by a Kalman filter, which combines the recorded data with prior knowledge about the system to statistically minimize the difference between the real and estimated values. Computer game development libraries were used to render virtual objects, and update their behavior according to user defined function and/or according to the fly's behavior (closed-loop). The delay between the fly movement and the update of the world is about 40ms (as measured using a photodiode, Vishay BPW21R) and is inherited majorly from the lag of the projection system. In the first version of the software, virtual worlds could be 2D or 3D environments with the 3D models designed in Blender (https://www.blender.org), and the textures generated in MATLAB and Adobe Illustrator. In the second version (FlyVRena2.0), 2D or 3D worlds can be created and drawn through OpenGL libraries within the FlyVRena software.

FlyVRena is also responsible for the communication between the different elements of the setup. Different elements of the experiments (e.g. galvo mirror control, online tracking, LEDs for optogenetics ...) are defined in individual modules that run asynchronously in different threads. FlyVRena implements the communication across modules with a publish/subscribe architecture.

Altogether, FlyVRena provides us with a high-performance, modular and flexible tool to control and manage our experimental virtual reality setups.

2.2.3 Virtual tether

In the following behavioral experiments we focused on the relation between self-generated rotational visual signals and the control of walking direction. In order to decouple the visual feedback resulting from translation and rotation we used real time tracking of the fly to update the position of the stimulus, such that it was "clamped"to the fly's position. While likely both rotational and translational optic flow are useful for course control and visual stabilization, this "virtual tether"largely facilitates the control of the visual feedback that the fly receives (Fig. 2.1B). In our conditions, only the fly body rotations largely generated visual feedback, and henceforth, for brevity, rotational visual feedback will be referred to as simply visual feedback.

2.3 Exploratory walking paths reveal two distinct motor contexts

To examine the effect of visual feedback on the exploratory behavior of the fly, we first need to understand the structure of the behavior. To elucidate the organization of body movement underlying the exploratory walking, we followed two different strategies. In the first one, we obtained an unbiased description of critical body kinematics linked to the motor programs at play. This project was spearheaded by Sebastián Malagon-Párez under mine and Eugenia Chiappe's supervision and will be briefly described in the following section. In the second strategy we used our previous knowledge of typical exploratory walking paths, and characterized them by either translations with high speed and fixed direction, and rapid rotations with

spike-like angular velocity profile known as body saccades (Geurten et al., 2014; Schilstra & Hateren, 1999; Zeil, 1986).

2.3.1 Body kinematics during exploratory walking

The continuous character of the locomotion of most animals poses a challenge for an unbiased segmentation of body kinematics. Therefore, we implemented an unsupervised segmentation of multivariate time series using a principled adaptive approach (Costa et al., 2019) (Fig. 2.2A). Briefly, we model local dynamics in variable time windows with first-order linear models, using the forward and angular velocities and respective accelerations as inputs. In line with previous work (Katsov et al., 2017), body kinematics were segmented into a set of windows ranging from 180 to 500ms. To group similar dynamics, we ran pairwise comparisons across all the segments to construct a dissimilarity matrix. Subsequently, we applied hierarchical clustering followed by a principled merging method via a logistic regression model (5-fold cross-validated binary classification, separability > 99%, Fig 2.2A). Applying this method on our dataset (84 flies, 441 minutes of recordings) led to 10 clusters representing body kinematics during continuous walking and 17 clusters for non-continuous locomotion. The clusters were organized into five main branches (Fig. 2.2B). Two of these branches (named "a"and "b") contained kinematics with prominent angular velocity profile accompanied by forward velocity profiles displaying decelerations followed by accelerations (Fig. 2.2C “cyan”, “magenta”, “dark violet”, “dark green”). In addition, these branches contained clusters with prominent angular bias and high forward velocity profiles (Fig. 2.2C “black”, “blue”, “orange”, and “spring green”). In contrast, the third branch for continuous locomotion ("c") contained clusters that on average lacked prominent angular velocity profiles and were accompanied by high and steady forward velocity profiles (Fig. 2.2C “dodge blue” and “lime” clusters). Thus, body kinematics during locomotion can be organized into regular sets of dynamics across different time scales revealing characteristic properties of the fly’s exploratory walking.

To examine the temporal organization of clusters, we identified common transition patterns between them (Fig. 2.2D), left. We performed a singular-value decomposition (SVD) on the one-step probability transition matrix between clusters and obtained a ranked description of the most relevant

transitions (transition modes, Mearns et al., 2020) (Fig. 2.2D). Because the first transition mode contains mainly steady-state transitions, we focused our analysis on the subsequent modes. The highest contribution to the second mode corresponds to transitions between angular peak-like rotations and relaxations in the angular velocity (Fig. 2.2D, right). The third and fourth mode highest contributors include transitions from the steady forward velocity clusters to either the same clusters or to initiations of peak-like rotations, respectively (Fig. 2.2D, right).

Altogether, these findings indicated the presence of two main distinctive body motor programs, characterized either by angular spike-like events resembling body saccades (Blaj & Van Hateren, 2004; Geurten et al., 2014) (angular peak plus relaxation) that are executed in about 56% of the time (14978 segments), or by segments with steady high forward velocity (forward runs) executed in about 44% of the total time spent walking (11744 segments). Thus, the organization of the body kinematics during exploration resembles a fixation-saccade strategy in which the fly interleaves fast turning with forward displacements.

2.3.2 Forward runs and body saccade detection

The computational load of the unsupervised analysis grows exponentially with data size. We leveraged the information acquired from this analysis together with previous behavior descriptions (Geurten et al., 2014; Schilstra & Hateren, 1999; Zeil, 1986) and developed a faster, supervised identification of body saccades.

In brief, we used a continuous wavelet transform strategy to classify events as spike-like (Fig 2.3A, Arthur et al., 2013). We computed the continuous wavelet transform of the angular velocity for each walking bout, using Gaussian wavelets, and extracted the signal power at a range of 10-15Hz (frequency signal) (Fig 2.3A). Note that the selection of the frequency band affects the spike detection, but it is not a determinant factor for subsequent analysis (Fig. 2.3B). Next, we calculated the local maxima of the frequency signal and of the absolute value of the angular velocity. If the local maxima coincide between the two sets, then these were labeled as putative spike turns (Fig. 2.3A).

Putative spike turns were winnowed twice: (1) to remove small local

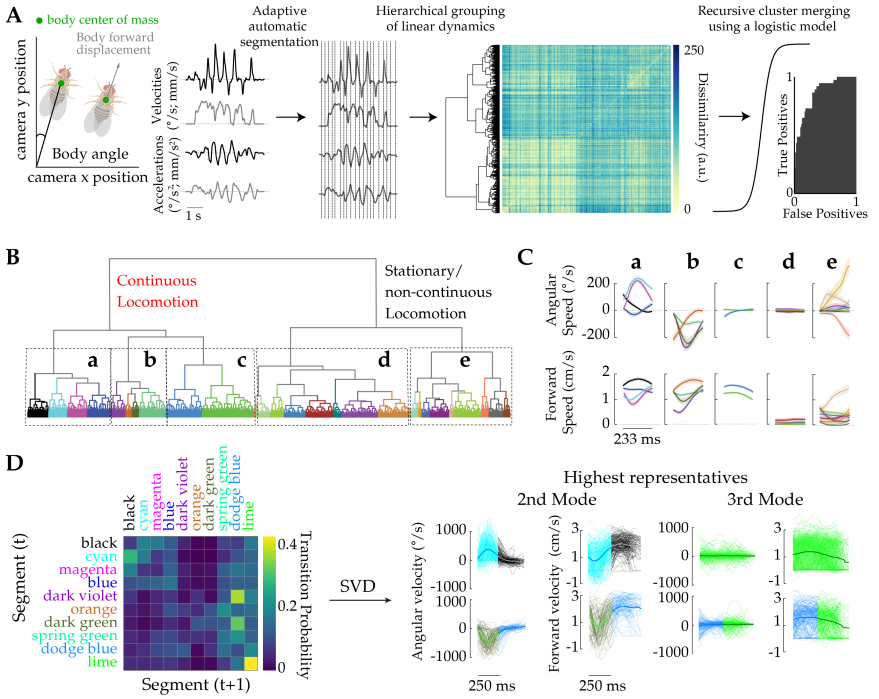

Figure 2.2: **Body kinematics during exploratory walking.** (A) Schematic of the fly's body movement. From the tracked position of the body center of mass we extracted the angular (black) and forward (grey) velocities and accelerations. Using the multivariate time series defined by velocities and accelerations, the unsupervised algorithm identified temporal segments of different length. Hierarchical clustering and logistic regression analysis were applied to the segments to obtain characteristic body kinematics. (B) Dendrogram associated with the hierarchical clustering. Note that a principled strategy was employed to select the final clusters based on their statistical separability. (C) Representative time series for the clusters at a single time window (233ms). (D) Left: One-step probability transition matrix of the continuous walking clusters. Right: Highest representatives of the second and third transition modes.

maxima (<200°/s) that did not disrupt the forward velocity of the fly (variance of forward speed < 3mm/s) and (2) to match the signal with a template obtained via PCA on a subset of pronounced spike-like events (the first principal component explained 90% of the shape variance, and was used as the template, Fig. 2.3C). Those spike turns in which the square distance between the scaled shape and the template was smaller than a cutoff of 0.15 were labeled as angular spike events (Fig. 2.3A).

It is important to note that the dynamics of body saccades were highly stereotyped (Fig. 2.3C), and this property facilitated their identification (Arthur et al., 2013). We will further explore the stereotypy and flexibility properties of saccadic turns in the Chapter 4 of this thesis.

To identify forward walking segments, saccadic events were removed from the walking bout. The remaining segments longer than 333ms, and with average forward velocity larger than 6mm/s were defined as forward runs throughout this study. Our description of behavior was robust within the classifier's parameter space (Fig. 2.3B).

The high stereotypy of the dynamics of saccades complemented previous observations performed in tethered flight (Fig. 2.3C, Bender and Dickinson, 2006a; Heisenberg and Wolf, 1988). In contrast, the dynamics of the angular velocity during forward segments evaluated at a comparable time scale were a lot less regular (Fig. 2.3C). Altogether, our data is compatible with the exploratory walking behavior of the fly being organized by two distinctive motor contexts that are driven by characteristic body dynamics.

2.4 The structure of exploratory walking is configured to maximize gaze stability

2.4.1 Fixation-saccade strategy

A fixation-saccade strategy orchestrates specific motor programs across the body to maintain gaze stable (Bizzi et al., 1971; Blaj & Van Hateren, 2004; Collett & Land, 1975; Collewijn, 1977; Geurten et al., 2014; Gilchrist et al., 1997; Land, 1999; Meyer et al., 2020; Zeil, 1986). For visual animals, such a locomotor strategy is advantageous to minimize motion blur (due to changes in direction), and to maximize acquisition of spatial information for the location of food sources, the detection of other animals, and homing or landing responses (Kim & Dickinson, 2017; Koenderink, 1986; Land,

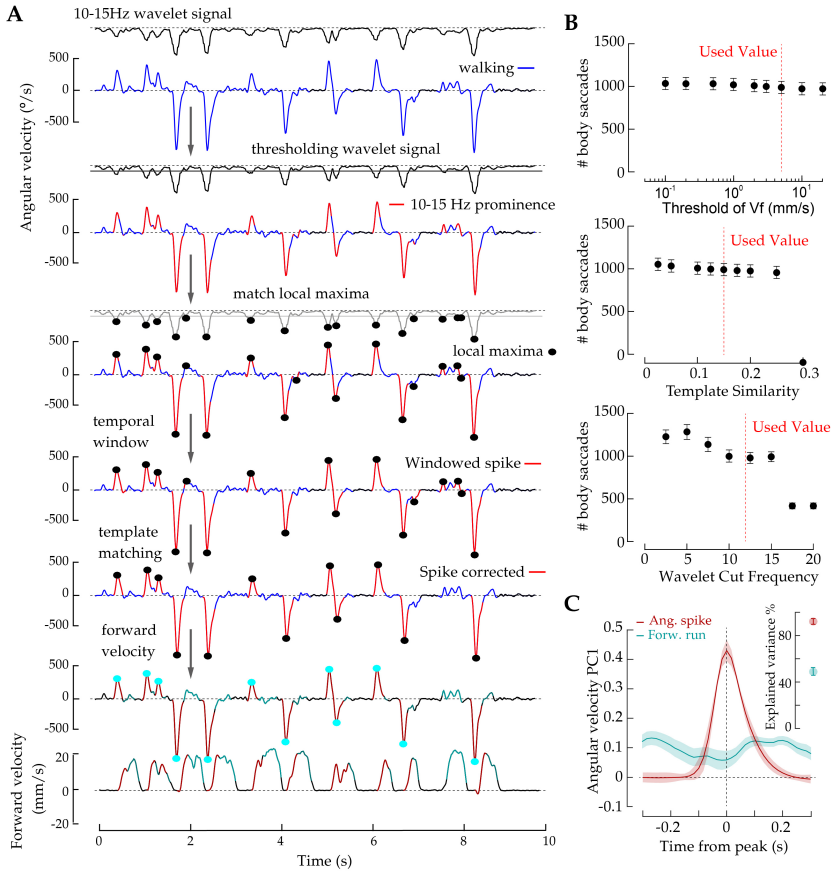

Figure 2.3: **Forward runs and body saccade detection.** (A) Different steps involved in the identification of rapid spikes of angular velocity that are referred to as body saccades in this study. (B) Exploration of the parameter space of the body saccade detection heuristics. Top: the number of saccades detected as a function of the threshold for the forward speed reduction during a body saccade. Middle: the number of body saccades using different thresholds for the template matching. Bottom: number of body saccades using different wavelet frequency cuts. For all the sets of heuristic parameters used, the variations in the number of detected saccades were generally small and did not affect the differences between experimental conditions. (C) Dynamics of the first principal component of the angular velocity during body saccades (red) or during forward runs (cyan). Inset: variance explained by PC1.

1999; Müller & Wehner, 1988; Pfeffer & Wittlinger, 2016; van Breugel & Dickinson, 2014). To test whether the fly attempts to maintain gaze stable as it explores the arena, we analyzed the coordination of movement between the head and the body (Bartz, 1966; Bizzi et al., 1971; Collett & Land, 1975; Meyer et al., 2020) in each motor context of the fly behavior.

2.4.2 Measuring head movement

We use our high resolution system to measure the fly head movements in the yaw axis as it freely explored the large arena. We filtered the high-resolution images with a Gaussian filter (width=16pixels), subtracted the background (Fig. 2.4A). Pixels that belonged to the fly were estimated with an iterative combination of edge detector operations and morphological transformations, until a connected object with dimensions similar to the fly was detected. The centroid and orientation of the object were used to translate and rotate the frame in order to keep a vertical fly at its center (Fig. 2.4A). Next, a fixed-size window around the head was cropped from the frame. The top of the thorax of the fly was masked out from the cropped frame, and the head was segmented using a combination of edge detector operations and morphological transformations. Head rotation was calculated via cross correlation with a template upright head (Fig. 2.4A, Berman et al., 2014). The head tracking error was computed as the squared error between the template and the rotated head. The head angle trace was then smoothed using a lowess algorithm with a window of 83 ms. Frames in which the head tracking error was high (top 2.5%) were removed from the original trace (Fig. 2.4B).

As an alternative strategy, we used DeepLabCut to estimate the rotation of the head with respect to the body of the fly (Mathis et al., 2018). We trained a neural network with a subset of images where the fly was in the upright position with four labels to track: Left Eye, Right Eye, Neck, and Thorax ending. After applying the tracking network to the full dataset, we transformed the positions of the labeled points into head angles. No significant differences were observed when comparing the two methods.

2.4.3 Gaze stability during saccades

We isolated the head and body rotations during body saccades. The head and the body of the fly moved initially in sync, with no lag at a temporal

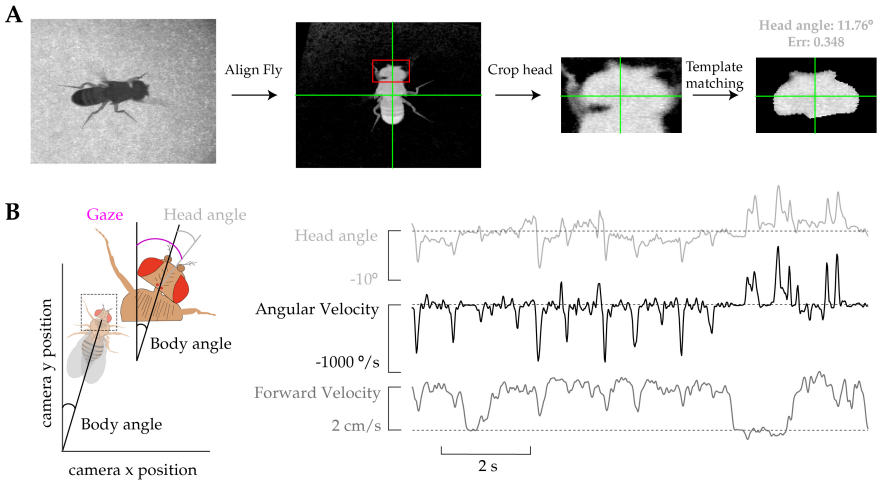

Figure 2.4: **Measuring head movement.** (A) Pipeline for head tracking includes the steps: Background subtraction, body alignment, head cropping and template matching. (B) Left: Definition of head angle, body angle and gaze. Right: example time series of head angle, Angular velocity (calculated based on body angle) and forward velocity.

resolution of about 8ms (120Hz) (Blaj and Van Hateren, 2004; Geurten et al., 2014, Fig. 2.5A), as measured by the cross-covariance between the body angular velocity and the head angle. At the peak velocity of the body saccade, the head velocity changes sign and initiates a counter rotation that facilitates keeping the new gaze position stable as the body completes its rotation (Fig 2.5B). In non-human primates and mice, both the eyes and the head contribute to gaze saccades (Bizzi et al., 1972; Meyer et al., 2020). In contrast, in walking Drosophila we found that the contribution of the head to gaze shifts is minor relative to the body's (Fig 2.5B), perhaps due to the head's limited range of movement ($< 20°$) and/or the body's fast maneuverability.

2.4.4 Gaze stability during forward runs

We also isolated the head and body rotations during forward runs. Like the vertebrate cervical-ocular reflex (Goldberg & Peterson, 1986), the head and body move in opposite directions, as observed in the cross-covariance

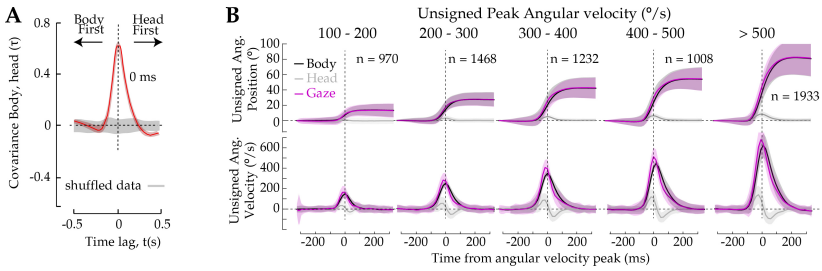

Figure 2.5: **Gaze stability during saccades.** (A) Head-body coordination measured as the cross-covariance between head angle and body angular velocity during body saccades. Gray: cross-covariance between head angle and temporally shuffled body angular velocity. (B) Time series of the angular position (top) and angular velocity (bottom) of the body (black), head (gray) and gaze (purple) during body saccades of varying peak angular velocity.

between the body angular velocity and the head angle. The body movement precedes the head by a 66ms lag (Fig. 2.6A). Importantly, the anti-correlation (Fig. 2.6B) (which is lost when we glued the head to the body (Fig. 2.6D) suggests the presence of a head compensatory response to body angular movements, perhaps to keep a stable gaze while the fly is moving forward (Fig. 2.6C, D). A direct measurement of the gaze deviations when only body or head-plus-body movements are considered shows that the head movement can reduce, but can't perfectly cancel the gaze deviations of the walking fly (Fig. 2.6C,D).

2.5 Discussion

Gaze stability during locomotion is fundamental for visual and spatial perception (Henderson, 2017). However, maintaining gaze stable during walking is not trivial because of uncertainties in the interaction between the body and the terrain. Here, we developed a novel paradigm where walking Drosophila perform a fixation-saccade strategy to explore an arena (Fig. 2.1, 2.2, 2.3). The size of our experimental arena (>50BL) together with its aversive walls, allow to circumvent the fly's innate centerphobism (Götz & Biesinger, 1985) and promote longer excursions through the whole arena, allowing us to identify this behavior pattern.

While saccadic turns have very stereotyped dynamics and associated

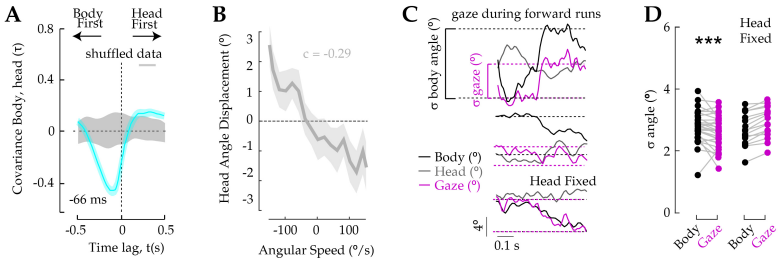

Figure 2.6: **Gaze stability during forward runs.** (A) Head-body coordination measured as the cross-covariance between head angle and body angular velocity during forward runs. Gray: cross-covariance between head angle and temporally shuffled body angular velocity. (B) Anti-correlation between instantaneous angular speed and head angle displacements during forward runs. (C) Top and middle: example traces of the variance in body, head and gaze angles during a forward run. Bottom: same but for a fly with its head fixed to the thorax. (D) Comparison between body vs. gaze deviations during forward runs in natural (left) and head fixed conditions (right).

head movements to curtail the time of gaze shift (Fig. 2.4 ,2.5), during forward runs flies attempt to keep their gaze stable by moving forward in fixed directions while coordinating angular head and body movements in antiphase (Fig. 2.4, 2.6).

2.5.1 Defining actions in spontaneous behavior

The small size of the fly allowed us to acquire high resolution information about all its legs, body, and head movements in a space equivalent to that of a cat running in a large room or a person rushing in a football pitch; all just in the corner of a small, hot, humid and windowless room.

We took the approach of allowing for the spontaneous expression of natural locomotion instead of constraining the behavior by the use of a specific task or physical constrains like a tether. While this approach generates a more natural repertoire of the animal's locomotive motifs, it also creates some challenges. Two of the main identified challenges are the inability to set explicit goals for the animal, and the difficulty to monitor and manipulate self-motion information in free moving animals. While the second challenge was surpassed by the use of a novel VR system that allows for low latency control of projection and galvo systems, the first challenge remains

unresolved. A way to get a window to the animal's goals is by inquiring the details of its behavior. Over the last years multiple supervised and unsupervised techniques aiming at quantitative descriptions of behavior have been been published (Berman et al., 2014; Bohnslav et al., 2021; Kabra et al., 2013; Katsov et al., 2017; Wiltschko et al., 2015). Here we took a mixed approach: we used an unbiased description of the walking dynamics given by our adaptation of Costa et al., 2019, that independently validated our expectation of a fixation-saccade structure during exploratory locomotion in our system.

The use of a fixation-saccade structure is commonly interpreted as having the underlying goal to minimize gaze deviations. Knowing the latent goal of the behavior allows us to define metrics of task performance (Harris & Wolpert, 1998; Pitkow & Angelaki, 2017; Todorov, 2004) even when studying spontaneous behavior. In the following chapters we will use these metrics to investigate how the goal of gaze stability interacts with lower level postural stability or higher level stability of internal representations.

2.5.2 Self-motion feedback for gaze stabilization

Saccades curtail the time spent generating retinal image shifts as a fly changes the direction of locomotion. We confirmed the previous observations that the head and the body of the fly initially move in unison during a saccade (Fig. 2.5) (Blaj & Van Hateren, 2004; Geurten et al., 2014; Heisenberg & Wolf, 1979; Schilstra & Hateren, 1999; Zeil, 1986). In different organisms saccades are thought to represent ballistic movements, unaffected by self-motion feedback (Bender & Dickinson, 2006a; Grossberg & Kuperstein, 2011; Muijres et al., 2015). Even though they are this "simple"movement, saccades are a very versatile way of responding under multiple situations. A clear illustration of the complexity of this action comes from the amount of vertebrate nervous system areas that modulate eye saccades. These include the retina, superior colliculus, parietal cortex, cerebellum, visual cortex, frontal cortex and the oculomotor nuclei (Grossberg & Kuperstein, 2011). In insects, a saccade command circuit is still unknown, even though recent work has described potential descending pathways whose activity correlates with tethered flight saccades (Schnell et al., 2017). This work suggested the LAL/PS as a candidate region generating saccade commands. The very conserved dynamics of body saccades described here is in agreement with the

possibility of them being a ballistic movement in our system as well (Fig. 2.3) (Bender & Dickinson, 2006a; Grossberg & Kuperstein, 2011; Muijres et al., 2015). In the next chapters we will challenge this idea and test the effects of self-motion information in saccade decision and execution, as well as explore novel neural pathways for saccade modulation.

During straight walking, several animal species show compensatory mechanisms among eye, head and body that keep their gaze stable (Imai et al., 2001; Land, 1999). Notably, when flies walk forward, their slow body rotations are accompanied by anti-phase head movements to promote gaze stabilization (Fig. 2.6). Evidence for gaze stabilization has been previously reported in blowflies during walking and flight (Blaj & Van Hateren, 2004; Hateren & Schilstra, 1999; Kern et al., 2006), although the anti-correlated head-body movement coordination has not been previously described. Several mechanosensory systems have been proposed to contribute to gaze stabilization (Bender & Dickinson, 2006b; Preuss & Hengstenberg, 1992). The presence of multiple signals suggests a functional analogy to gaze stabilizations reflexes found in vertebrates, such as vestibulo-ocular reflex (Waespe & Henn, 1987) or the vestibulo-collic reflex (Gdowski & McCrea, 1999; Wilson et al., 1995)

The distinct body dynamics found during exploratory walking are associated with different motor programs across the body and head. This points to a structural organization that is configured to maximize gaze stability, and to minimize the time spent on gaze shifts. Because the body has an important contribution in gaze control, gaze stability must emerge not only via head-body movement coordination, but also through a fine control of course direction. That is, during forward runs, small gaze deviations will occur if unintended angular drifts of the body develop.

Altogether, these findings demonstrate that each of the distinctive phases of the behavior has a specific goal, contributing together to maximizing gaze stability. Therefore, next, we will examine the role of visual feedback on the control of gaze during walking.

2.6 Bonus Discussion: theoretical models of exploration

To directly ask an animal why it moves the way it does is still a strategy that only works for one species. For most cases, our best approach to move

from phenomenological descriptions to more causal and rigorous knowledge is to understand how organisms move and which factors influence their movement.

From rich movement trajectory datasets we can try to infer patterns that can be interpreted based on theoretical frameworks (With, 2019). A range of mathematical models of animal movement has been proposed and tested, from simple Brownian random walks (uncorrelated, unbiased movement), correlated random walks (same, but the heading in each step depends on previous step - e.g. Kareiva and Shigesada, 1983), biased correlated random walks (same, but with a drift e.g. Crone and Schultz, 2008) to Lévy walks (random walks where the step length distribution follows a power law e.g. Viswanathan et al., 1996). The model that would better adjust to a dataset can tell us about the type of search the animal is doing (more local with a characteristic length or more global foraging) or about a possible use of memory or a preference from the animal.

The power-law distribution of a Lévy walk means that occasionally there will be a very large step. The resulting pattern consists of clusters of small steps connected by rare long steps. The clusters themselves consist of smaller clusters of even shorter steps connected by longer steps, and so on to give a repeating pattern at multiple scales (Edwards et al., 2012). The ecological interest arises from the demonstration that a Lévy walk with an exponent of 2 represents an optimal foraging strategy in conditions where targets are sparse and further from the animal and can be visited multiple times (Viswanathan et al., 1999). Lévy walk models have been proposed as a movement strategy in a wide variety of animal movements - including Drosophila (Austin et al., 2004; Bartumeus et al., 2003; Brown et al., 2007; Mårell et al., 2002; Reynolds & Frye, 2007; Viswanathan et al., 1999), albeit with some controversy (Edwards, 2008; Edwards et al., 2007; Sims et al., 2007; White et al., 2008). Even though theory has shown that Lévy walks are a more efficient strategy for locating sparse random targets (Shlesinger, 2009; Shlesinger & Klafter, 1986), brownian random walks can match their efficiency if targets are more local and abundant (Viswanathan et al., 2011). A more recent approach to distinguish these different types of movement is to compare if the distribution of step length follows a power-law (Lévy walk) or an exponential (Brownian motion) (Breed et al., 2015; Edwards et al., 2012; James et al., 2011; Sims et al., 2012).

In the experiments described in this chapter, flies were free to walk in a

large arena (50BL diameter). To distinguish whether flies are using a power law (indicative of a Lévi walk) of an exponential (indicative of Brownian motion) distribution of step length, we extracted all the saccades and measured the distribution of the distance run in between saccades (ISID) as a proxy for step length.

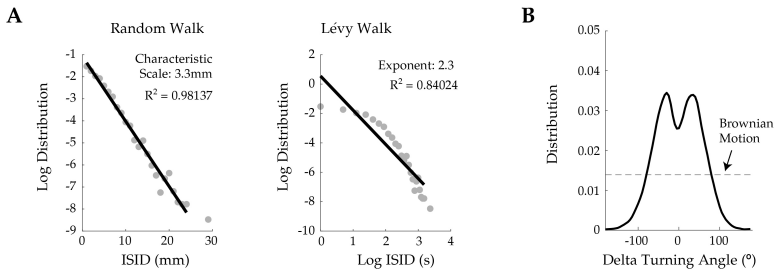

Figure 2.7: **Comparison between theoretical models of exploration.** (A) Distributions of the distance run in between saccades. Left: fit testing the exponential (Random walk) hypothesis; Right: fit testing the power law (Lévy walk) hypothesis. (B) Distribution of the turning angle of saccades. Dashed line represents the expected from fully random (Brownian) motion.

In our data, inter-saccade distances distribute in an exponential fashion, and reject a power law distribution (Fig. 2.7A). Therefore, in our conditions walking paths are better explained by Brownian movement than Lévy walks. This result suggests that flies are more unlikely to be engaging in global foraging for scattered targets but rather doing more local exploration (Bartumeus et al., 2003; Sims et al., 2012).

Within the random walk type of searches, a correlated random walk is a more natural search type for animals (Viswanathan et al., 2011) and has been used to explain realistic animal movements (Bovet & Benhamou, 1988; Kareiva & Shigesada, 1983). In correlated random walks, the turning angles between successive step vectors are usually taken from a non-uniform symmetrical distribution (Bagarti, 2011; Bartumeus et al., 2005; Haefner & Crist, 1994). In our data, we extracted the turning angle of the fly between consecutive saccadic turns. We obtained a non-uniform symmetrical distribution (Fig. 2.7B), suggesting that indeed flies movements resembled a correlated random walk movement.

Overall, our analysis suggests that in our large constrained arena, the exploratory walking resembles a search in which flies might be locally looking

for possible escapes using targeted turning decisions.

2.7 Acknowledgements

The setups and experiments in this chapter were designed with Eugenia Chiappe. The unsupervised analysis was performed by Sebastián Malagon Pérez with inputs from Greg Stephens and António Costa. Alexandre Laborde adviced and wrote some of the libraries used for inter-module communication in the second version of the FlyVRena software. This work was supported by the Champalimaud Foundation and the research infrastructure Congento, LISBOA-01-0145-FEDER-022170, co-financed by Fundação para a Ciência e Tecnologia (Portugal) and Lisboa2020, under the PORTUGAL 2020 Agreement (European Regional Development Fund). This work was also supported by Fundação para a Ciência e Tecnologia FCT PD/BD/105947/2014 (T.C.), by the Marie Curie Career Integration Grant PCIG13-GA-2013-618854 (M.E.Ch), and by the European Research Council Starting Grant ERC-2017-STG-759782 537 (M.E.Ch).

Chapter 3

Visual Control of Course Stability

3.1 Overview

In the previous chapter, we established that, under our experimental conditions, flies perform an exploratory local search organized in a fixation-saccade strategy with the goal of maximizing gaze stability and therefore improve the acquisition of environmental information.

In this chapter, we will examine the direct contribution of visual self-motion feedback during unconstrained, spontaneous locomotion. This question will further lead us to explore how the latent higher goal of gaze stability interacts with lower level goals of postural stability. In particular, we will focus on how self-motion information acts as a coordinating factor between goals at different levels of locomotor control. We will further attempt to identify the neural pathways that could be involved in this novel function of visual self-motion information.

3.1.1 Visual control of locomotion

While vision is the primary beneficiary of gaze stabilization, it is also thought to be an important contributor to its control, complementing non-visual gaze stabilization mechanisms. Experiments in which visual-motion perturbations are presented uncoupled from the animal's behavior have largely contributed to our current understanding of how vision controls gaze. In both vertebrates and invertebrates, this type of perturbations leads to directed rotations of the eyes, known as an optokinetic response (OKR), or rotations of the head or body in which head orientation and course direction are changed as a function of visual motion stimulation (Götz & Wenking, 1973; Kretschmer et al., 2017; Orger et al., 2000; Robinson, 1981). Several models have proposed that OKR and head and body optomotor responses (OMRs) operate via a feedback control system in which visually induced error signals are minimized by compensatory head or body turns, thereby reducing gaze and course deviations (Poggio & Reichardt, 1973; Robinson, 1981; Roth et al., 2012). Much less is known about how vision controls gaze fixations in the absence of external visual perturbations, when visual information is self-generated by the movements of the animal (Collett et al., 1993; Patla, 1997; Warren et al., 2001). Indeed, challenges have been raised to the sufficiency of OMR mechanisms to guarantee gaze stability under self-generated visual conditions. First, the gain of OMRs is low in walking insects, potentially due to the interference between visual and non-visual mechanisms of gaze control (Lönnendonker & Scharstein, 1991). Second, very little is known about OMR function in the coordination of movement across the body for gaze stability (Götz, 1975; Poggio & Reichardt, 1973; Roth et al., 2012; Wolf & Heisenberg, 1990). Third, OMRs depend on visual velocity signals, which must be integrated (in the mathematical sense) to maintain the orientation of head and body fixed (Collett et al., 1993; Skavenski & Robinson, 1973). Indeed, OMRs are modeled by a proportional-integrative feedback control system (i.e. PI controller) (Roth et al., 2012; Schnell et al., 2014; Wolf & Heisenberg, 1990). The integrative aspect of the OMR controller questions whether it is fast enough for a smooth control of gaze. Speed becomes especially relevant in the presence of the stepwise postural adjustments occurring during walking in response to neuromuscular noise. Alternatively, the fly may use unidentified mechanisms other than compensatory rotations to prevent gaze deviations.

3.1.2 Visual flow processing

Locomotion generates optic-flow fields - coherent retinal image shifts induced by instantaneous self-motion. The brain could use these signals to monitor an animal's movement (Pfeffer & Wittlinger, 2016; Warren et al., 2001). This idea is supported by the ubiquitous presence of optic flow sensitive neurons in the animal kingdom, which exhibit large receptive fields that are selective for specific flow fields (Bradley et al., 1996; Duffy & Wurtz, 1991; Grasse & Cynader, 1982; Joesch et al., 2008; Kubo et al., 2014; Morgan & Frost, 1981).

In Drosophila, visual signals are processed in a brain region called the optic lobe. The optic lobe is composed of 5 retinotopically arranged neuropils: retina, lamina, medulla, lobula and lobula plate. Similar to vertebrates, (Borst & Helmstaedter, 2015), visual stimuli are processed through largely independent ON and OFF pathways, which process luminance increases and decreases respectively (Clark et al., 2011; Joesch et al., 2010). The first neurons along these pathways known to encode visual motion are the medulla output neurons T4 (ON), and the lobula output neurons T5(OFF) (Maisak et al., 2013). T4 and T5 cells have preferred motion directions along one of the four cardinal directions, and their preferred directions dictate the lobula plate layer to which they project to (Maisak et al., 2013). There, among others, T4 and T5 cells provide direct excitatory input onto the dendrites of multiple wide-field, motion-sensitive tangential cells (LPTCs, Borst and Haag, 2002). LPTCs function as matched filters for complex optic-flow patterns associated with the animal's own movements (Krapp & Hengstenberg, 1996; Krapp et al., 1998). LPTCs are a major output from the lobula plate and send their wide-field visual self-motion information to higher processing centers in the central brain, as well onto neck motor neurons and descending neurons (Borst & Haag, 2002; Haag et al., 2007; Hausen et al., 1980; Suver et al., 2016; Wertz et al., 2012). Based on their receptive fields, classes of classical LPTCs called HS and VS cells have been thought to function as part of the OMR controller for gaze and course control. Indeed, artificial activation of LPTCs induces ipsilateral head, wing or leg movements (Busch et al., 2018; Fujiwara et al., 2017; Haikala et al., 2013), while their inactivation leads to contralateral movements (Busch et al., 2018; Fujiwara et al., 2022). These experiments support the role of LPTCs in gaze stabilization reflexes; however, the mechanisms

by which LPTCs may control the fly's locomotion remain elusive.

Several models have proposed that OKR and OMR operate via a feedback control system in which visually induced error signals are minimized via compensatory rotations, thereby promoting gaze stability. These models however do not contemplate the interaction between visual signals and the locomotor machinery supporting the continuous locomotion. Furthermore, all these studies assume that the mechanisms by which external visual perturbations control gaze are the same to those induced by self-generated visual information (visual feedback). Given the critical role of gaze stability for internal representations of space, it is important to establish the direct contribution of visual feedback during continuous movements through space during exploration and navigation.

3.2 Role of vision in gaze stabilization

3.2.1 Flies try to maximize gaze stability independent of vision

We previously established that, under our experimental conditions, flies perform an exploratory local search organized in a fixation-saccade strategy in order to minimize gaze deviation and therefore improve the acquisition of environmental information. Here, we question whether the observed strategy is dependent on vision. To this end, we compared flies that were free to walk in darkness or under clear visual conditions. We observed a very similar organization of the behavior in the two conditions, with saccades and forward runs being promptly detected using the previously developed methods (Fig. 3.1A, B).

The independence of the behavioral structure from vision is further emphasized by the maintenance of head-body coordination in both conditions. During saccades the head and the body move in sync to curtail the time of gaze shift while during forward runs the head and body move in opposite directions to help keep the gaze stable (Fig. 3.1C). These results suggest that flies maintain the same general movement patterns that try to maximize gaze stability independent of vision. In the following sections, we will explore the role of vision in the execution of each of the two observed motor contexts.

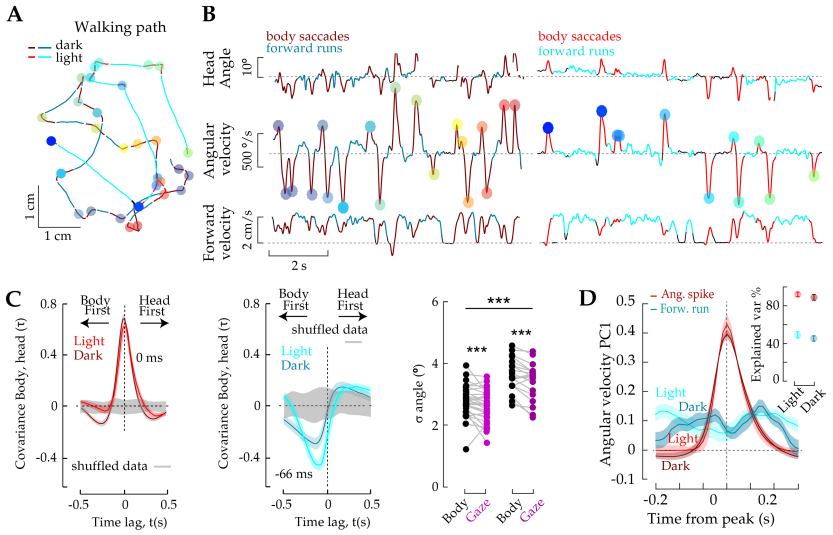

Figure 3.1: **Flies try to maximize gaze stability independent of vision.** (A) Examples of exploratory walking paths of an individual fly under clear visual conditions (light) and dark conditions. (B) Corresponding time series of head angle, forward and angular velocities. Left: exploratory walking in dark conditions. Right: exploratory walking in light conditions. Body saccades are indicated in light and dark red. Forward runs are indicated in light and dark cyan. Colored dots indicate individual body saccades. (C) Left: head-body coordination measured as the cross-covariance between head angle and body angular velocity during body saccades in light (N=33, n=1022) and dark (N=28, n=4252) conditions. Gray: cross-covariance between head angle and temporally shuffled body angular velocity. Middle: same but for forward runs. Right: Comparison between body and gaze angle variance during forward runs in light and dark conditions (***p<0.005, Wilcoxon signed-rank test). (D) Dynamics of the first principal component of body saccades in dark (dark red) and light conditions (red) or of angular velocity fluctuations during forward segments in dark (dark cyan) and light conditions (cyan). Inset: variance explained by the first PC.

3.2.2 Context-dependent visual control of locomotion

The limited contribution of the head relative to the body on gaze control (Fig. 3.1C) suggest that gaze stability increases with course stability (Warren et al., 2001; Wolf & Heisenberg, 1990). We investigated the visual contribution to course stability in both the context of body saccades and the context of forward runs. To study the relation between self-generated rotational visual signals and walking performance, we analyzed the dynamics of body saccades and angular fluctuations during forward runs in darkness, and compared them in the presence of the visual feedback. The dynamics of body saccades were identical in the two conditions (Fig. 3.1D). The lack of apparent effect of self-generated visual signals on saccade dynamics was consistent with previous work in tethered flight (Heisenberg & Wolf, 1988) and will be further explored in Chapter 4.

In contrast, forward segments were sensitive to visual feedback (Fig. 3.2). To describe this sensitivity, we calculated path straightness as a measure of walking performance. At first, local curvature is calculated with a running window of 333ms centered on each point of the fly's path. We calculated deviation as the distance between the central data point and a line defined by the edges of the window (instantaneous deviation from an ideal straight path). Straightness of a forward segment was defined as the traveled distances within the window divided by the sum of deviations. Straightness per fly is the weighted average of all the straightness per forward run, with weights given by the total distance walked in each forward run.

Flies walking in darkness display less straight paths compared to flies walking under light conditions (Fig. 3.2A, B left). In darkness, flies show larger angular deviations, suggesting that visual feedback may be actively used to control angular deviations to keep the intended straight course (Fig. 3.2B center). Although less prominent, we also observed an effect on the fly's translational speed (Fig. 3.2B right), which may be either a consequence of the angular control, or an additional effect of visual feedback on the fly's translational movements.

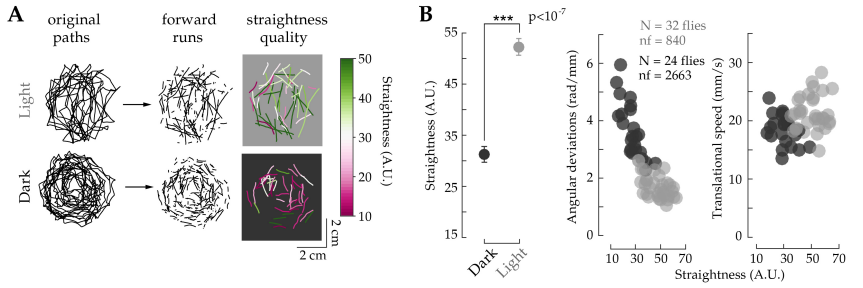

Figure 3.2: **Visual control of the straightness of forward runs.** (A) Exploratory paths of a fly walking in light (top) and dark (bottom) conditions. From the original paths (left) the classifier isolated the forward runs (middle). The performance of these segments was measured by a straightness quality parameter, with high values color-coded in green and low values in magenta. (B) Left: mean straightness performance in the dark and light conditions (***p<0.005, MWW-test). Middle: the cumulative angular deviation of the fly as a function of path straightness. Right: the translational speed of the fly as a function of walking straightness.

3.3 Visual feedback rapidly controls course stability during forward runs

3.3.1 Definition of visual influence

To better characterize the contribution of visual feedback onto straightness performance, we designed a set of VR worlds, each composed of random dots of variable size or density (Fig. 3.3C). In our VR environment, the fly's visual feedback includes the dot-based stimuli and additional objects from the rig that may excite the fly's retina. To dissect the contribution of the dot-based stimuli on the fly's locomotion, we defined a parameter called 'visual influence'. We incorporated a 'reverse gain' condition where a direction in the fly's angular movement induces the same direction of the world angular displacement (Fig. 3.3A). If the dot-stimuli is detected by the fly, and if it influences her behavior, this reversed gain condition should induce circling behavior (Holst & Mittelstaedt, 1950; Sperry, 1950) where the fly's angular movements are biased to one side (Fig. 3.3B). Since natural gain and reverse gain conditions differ only in the direction of the projected visual feedback, 'visual influence' is defined as the difference in the probability of circling between the natural and reverse conditions (Fig. 3.3D, E). In this manner, visual influence only measures the effect of the different

projected stimuli on the fly behavior (Fig. 3.3E).

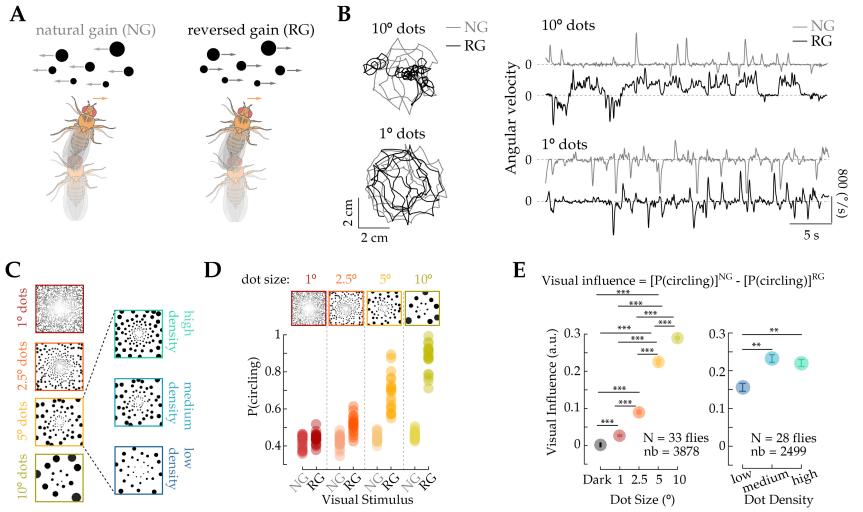

Figure 3.3: **Definition of visual influence.** (A) Schematic of the visual feedback from a rightward rotation under natural (left) and reversed (right) gain conditions. (B) Left: example exploratory path under natural gain (light gray) and reverse gain (dark gray) under 10º random dots (top) or 1º random dots (bottom). Right: corresponding angular velocity time series. (C) Visual environments with different physical attributes. (D) Circling probability (probability of consecutive rotations towards the same direction) as a function of visual environment under NG (light colors) or RG (dark colors). (E) Visual influence as a function of visual environments with varying dot size (left) of varying dot density (right), (*p<0.05, **p<0.01, ***p<0.005, MWW-test).

3.3.2 Relationship between visual influence and straightness of forward runs

A world with small dots (1º size) produced low visual influence, and flies under this condition displayed straightness performance levels closer to those observed in darkness (Fig. 3.4A, B). On the other hand, flies exploring worlds with larger visual influence showed higher performance (Fig. 3.4A, B). In fact, the more sensitive the flies were to visual feedback, the straighter their walking paths (Fig. 3.4C). Although size or density of dots induced variable influence on behavior across the population of flies, the relation between visual influence and straightness was highly correlated. (Fig. 3.4C). This finding indicates that self-generated visual signals reduce

the magnitude of body rotations and straighten forward runs when motor programs across the body are coordinated to maintain gaze stable.

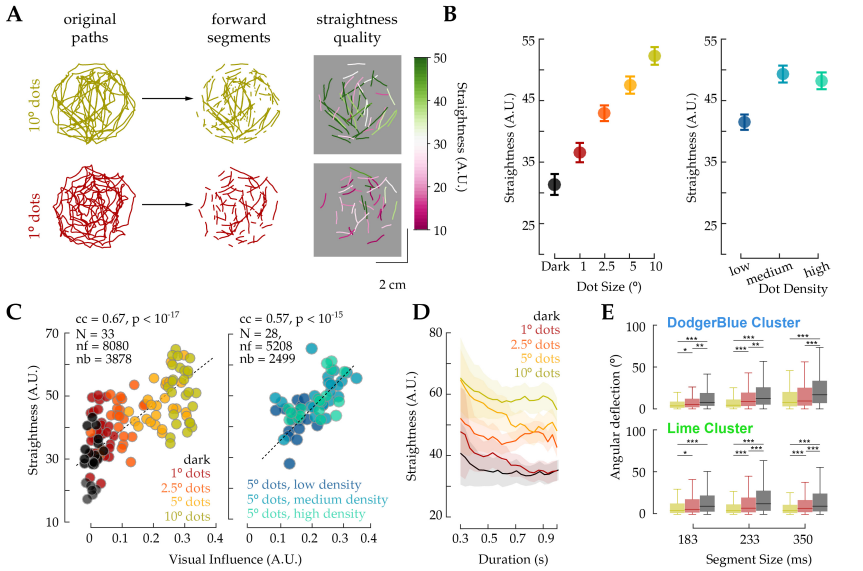

Figure 3.4: **Visual feedback rapidly controls path straightness during forward runs.** (A) Exploratory paths of a fly walking in a visual environment composed of 10° dots (top) and 1° dots (bottom) conditions. From the original paths (left) the classifier isolated the forward runs (middle). The performance of these segments was measured by a straightness quality parameter, with high values color-coded in green and low values in magenta. (B) Average straightness performance across visual environments. (C) Path straightness as a function of visual influence, with dot size (left, $p<10^{-17}$, t-test) or density (right, $p<10^{-15}$, t-test) as the changing physical attribute of the visual environment. (F) Mean path straightness as a function of the duration of forward runs under different visual environments. (G) Cumulative angular deviations in segments of different duration belonging to clusters with high forward velocity (Top: DodgerBlue, Bottom: Lime) under different visual conditions (yellow: 10° dots, red: 1° dots, black: darkness; ***p<0.001, **p<0.01, *p<0.05, MWW-Test two-sided with Bonferroni correction).

3.3.3 Visual feedback rapidly controls path straightness during forward runs

To test how fast visual feedback affects course control, we calculated path straightness as a function of the duration of forward runs across virtual

worlds (Fig. 3.4D). Strikingly, short walking bouts lasting only 300ms, or about 3 consecutive steps (DeAngelis et al., 2019; Mendes et al., 2013), were straighter under strong vs weak visual feedback. This finding is further supported by a notable effect of visual feedback on cumulative angular drift in high-forward speed clusters for temporal windows shorter than 180 ms (Fig. 3.4E).

Altogether, our findings indicate that visual feedback controls walking rapidly and in a goal-dependent manner. They further suggest that self-generated visual signals may guide leg maneuvering at a timescale close to the step cycle of the walking fly (Mendes et al., 2013). Such a fast effect of visual feedback on body dynamics suggests that self-generated visual signals operate close to the stepping timescale at which posture control systems operate.

3.4 Visual feedback prevents pairwise interlimb correlations underlying postural adjustments

3.4.1 Leg movement detection

Ultimately, the characteristics of body dynamics and its control by visual feedback depends on the movement coordination across the six legs. To understand how visual feedback controls path straightness at fast timescales, we first examined the relationship between interlimb coordination and course control.

To characterize interlimb coordination, we used machine learning tools to track each leg's tip position in two dimensions. We subtracted the background of all high resolution video frames. Pixels that belonged to the fly were estimated with a combination of edge detector operations and morphological transformations, until a connected object with dimensions similar to the fly was detected. The centroid and orientation of the object were used to translate and rotate the frame in order to keep a vertical fly at the center of the frame. Next, we cropped a window of 400x400px around the fly and stored it in a new aligned video (Fig. 3.5A). We used DeepLabCut (Mathis et al., 2018) to estimate the location of the following features from the high resolution aligned videos: top of the head, left eye, right eye, neck, tip of the thorax, tip of the abdomen, tip of left front leg, tip of right front leg, tip of the left middle leg, tip of right middle led, tip of left hind leg and tip of

right hind leg. These features were thresholded based on the accuracy of estimation parameters and aligned to the low resolution tracking data (Fig. 3.5A).

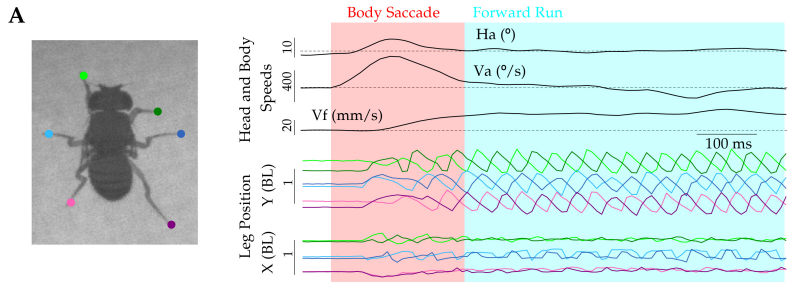

Figure 3.5: **Leg movement detection.** (A) Left: example DeepLabCut labeling of leg position. Right: from top, time series of the head angle, the angular and forward velocities, and leg positions in the body axis direction (Y) and in the orthogonal axis direction (X). Red shade: body saccade, cyan shade forward run.

3.4.2 Leg movement properties during forward runs

In order to examine the relation between the spatio-temporal properties of interlimb coordination and course control, we first divided forward runs based on the magnitude and direction of deviations from a straight course normalized by traveled distance (Fig. 3.6A). On average, flies walked with a near perfect tripod coordination irrespective of the magnitude and direction of the ongoing drift, as measured by the amount of legs in swing phase at each time (Fig. 3.6B) and also as measured by the inter-leg phases across all legs (Fig. 3.6C). Inter-leg phase was calculated by dividing the time delay in the cross-covariance between leg position signals and the period as measured in the auto-covariance of those signals. Swing-stance transitions for each leg were calculated by detecting the local maxima (swing to stance) and local minima (stance to swing) in the leg position aligned to the body orientation (Fig. 3.5A).

The observed tripod configuration was consistent with the steady and high forward velocity during forward segments (Fig. 2.2C, 3.1B), and confirmed previous work in Drosophila and other insects (Mendes et al., 2013; Wosnitza et al., 2013). Thus, body angular deviations from straight course

are not caused by variations in the temporal structure of interlimb coordination, instead, they may be caused by leg kinematic properties.

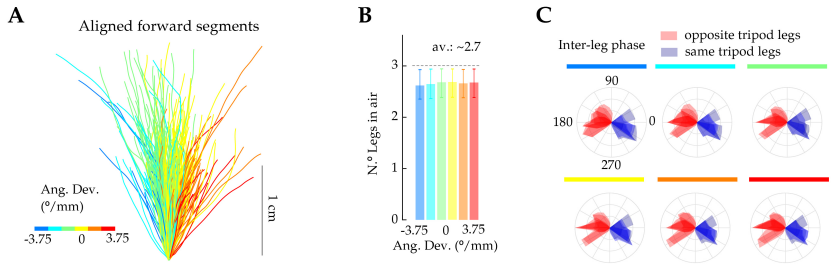

Figure 3.6: **Inter-leg coordination during forward runs.** (A) Example set of forward runs aligned at the starting position. Color code corresponds to the magnitude of the cumulative angular deviation during each segment. (B) Number of legs in the air at each frame during forward runs with paths with different amounts of angular deviation (N = 52 flies, n = 15754 forward runs). A perfect tripod gait corresponds to 3 legs in the air at all times (dashed line). (C) Inter-leg phase relation as a function of angular deviation during forward runs. Blue shades: leg phases between legs belonging to the same tripod, red shades: leg phases between legs belonging to opposite tripods (N = 52 flies, n = 15754 forward runs).

3.4.3 Course deviations are caused by spatial aspects of leg movement

We proceeded to examine whether variations in single-leg kinematics affect body angular deviations. We extracted the location lateral (orthogonal to the body axis) and longitudinal (parallel to the body axis) of the anterior and posterior extreme positions of each leg relative to the body (AEP and PEP, respectively). The distribution of the lateral and longitudinal locations of AEP and PEP were broad and can vary up to 0.3 body lengths, irrespective of the magnitude and direction of body drift, with the AEP's distribution wider than the PEP distribution (Fig. 3.7A).

The lateral AEP of front legs changed systematically with path deviations (Fig. 3.7A). This effect was clearer at a single-step level, where correlations between lateral leg placement and body angular deviations were more prominent for front than middle legs and it was not observed in hind legs (Fig. 3.7B, left). Front legs showed no correlation between the longitudinal AEP and body angular deviations, whereas the middle and hind legs showed

variable correlations (Fig. 3.7B, right). In agreement with our previous observation that temporal aspects of leg movement and inter-leg coordination are very stable within forward runs, we found no relationship between angular deviations and swing or stance times for any of the legs (Fig. 3.7C). These findings indicate a specific relationship between each leg's placement and body deviations, suggesting that variability in limb kinematics causes self-paced path deviations during forward runs.

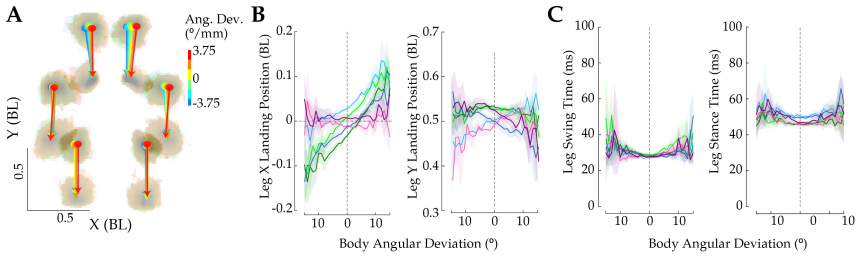

Figure 3.7: **Course deviations are caused by spatial aspects of leg movement.** (A) Spatial distributions of the location of leg landing and lift-off with respect to the body center during forward runs, color coded by the magnitude of the path's angular deviations. Arrows represent the movement from the center of the landing distribution to the center of the lift-off distribution. (B) Leg X and Y landing position in a single step (N = 52 flies, n = 42524 steps) as a function of the body angular deviation detected in that step. Individual legs follow the color code shown in Fig. 3.5A. (C) Leg swing and stance times in a single step as a function of the body angular deviation detected in that step (N = 52 flies, n = 42524 steps).

3.4.4 Interlimb spatial correlations underlie postural adjustments

Notably, the lateral placement of a front leg in a single step (FLx) is not sufficient to explain the body angular deviations. In consecutive steps, if an initial displacement is not followed by a syndirectional FLx from the contralateral leg, body angular deviations don't occur (Fig. 3.8A). In contrast, if the initial displacement is followed by a correlated FLx, the magnitude of the correlation directly relates to the magnitude of the body angular deviation (Fig. 3.8A). These relationships can also be observed when plotting the lateral placement of different legs in consecutive steps with varying body angular displacements. Consecutive front leg lateral placement is highly correlated in steps with high angular displacement and not correlated in

steps that don't generate body angular deviations (Fig. 3.8B, left). A similar but weaker relationship was found between the pair of middle legs (Fig. 3.8B, middle).

To further explore whether the effect observed in the middle legs follows as a consequence of the effect observed in front legs (through a type of targeting response) we performed the same analysis between ipsilateral front and middle legs. We found that an initial front leg lateral displacement is correlated with follow up middle leg lateral displacement, independently whether body angular deviations occur (Fig. 3.8B, right). We therefore conclude that the correlations found for middle legs may be just a consequence of the front leg correlations, possibly through a new type of targeting response.

Changes in FLx over a step can displace the fly's center of stability (COS) away from its center of mass (COM) (Fig. 3.8C), thereby momentarily decreasing posture stability (Szczecinski et al., 2018; Ting et al., 1994). Therefore, variability in leg placement on a step can decrease body stability momentarily (Fig. 3.8C). To recover stability, posture control systems could either adjust lateral foot placement in the next step, like in humans (Bauby & Kuo, 2000), or dynamically engage viscoelastic properties of the musculoskeletal system as observed in the cockroach (Jindrich & Full, 2002). Our data is consistent with the first possibility: FLx displacements were typically followed by contralateral FLx displacements in the same direction (Fig. 3.8A). That is, posture control induces strong spatial correlations between the pair of front legs in consecutive steps in response to posture instability. Because front leg spatial correlations predict body angular deviations (Fig. 3.8A), posture control essentially promotes unintended body rotations while attempting to keep the fly more balanced.

3.4.5 Visual feedback prevents pairwise interlimb spatial correlations

The front-leg pairwise correlations are strongly correlated with body angular deviations regardless of visual conditions (Fig. 3.8A). However, the interlimb correlation was stronger in darkness and gradually decreased with more salient visual feedback (Fig. 3.8D). Consistently, posture stability recovery was more robust in darkness than when visual feedback was available (Fig. 3.8E). By doing so, visual feedback effectively tunes down rapid

posture control systems and maintains a less stable walking at expense of a straighter walking path, and a more stable gaze (Fig. 3.4, 3.8E).

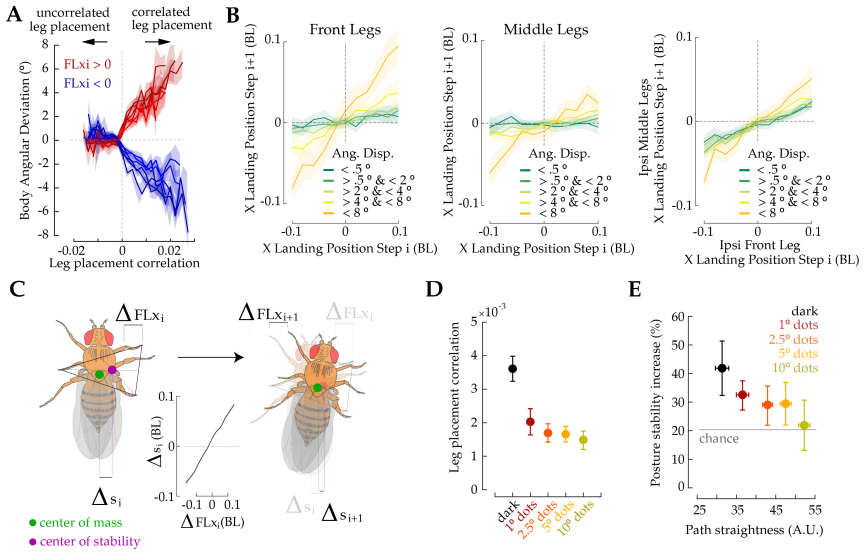

Figure 3.8: **Visual feedback prevents pairwise interlimb spatial correlations.** (A) Body angular deviation as a function of the correlated lateral movement of both front legs in consecutive steps. Plots were divided by the direction of the initial lateral movement (red: rightward, blue: leftward) and the visual environment (different shades). (B) Left: front leg X-landing position as a function of the contralateral front leg X-landing position in the preceding step for steps originating different body angular displacements. Middle: middle leg X-landing position as a function of the contralateral middle leg X-landing position in the preceding step for steps originating different body angular displacements. Right: middle leg X-landing position as a function of the ipsilateral front leg X-landing position in the preceding step for steps originating different body angular displacements. (C) Schematic of the relationship between dynamic posture instability (Δs) and the lateral placement of front legs (ΔFLx) and how a correlated lateral movement in the next step can reduce such postural instability at the expense of causing an angular deviation in the fly's path. (D) Average front leg placement correlation in different visual conditions (N = 52 flies, n = 42524 high quality steps). (E) Increase in posture stability (%Δs) following an initial front leg deflection, as a function of average path straightness in different visual conditions (colored). Gray: chance level of. increase in posture stability estimated by shuffling the sequence of steps.

3.5 External visual perturbations induce body rotations with specific interlimb coordination

Next, we asked whether visual perturbations leading to body rotations induced similar interlimb coordination. We induced visual perturbations either by OMR visual stimuli (Fig. 3.9A), or by RG (Fig. 3.3A). During both RG and OMR, flies turn either at high forward velocity or with saccades in the direction of the stimulus rotation. In this section we will focus on the biased forward runs (Fig. 3.9C), and will explore the properties of saccades in the next chapter. During biased forward runs flies turn with near perfect tripod gait (Fig. 3.9D, E).

The body angular deviations were correlated with the front legs' lateral AEP and anti-correlated with the hind legs' lateral AEP (Fig. 3.9B, F). In contrast, the longitudinal AEP was the same under RG (Fig. 3.9G). The consistent anti-correlation between the hind legs' lateral AEP and the body angular deviations during open- and closed-loop visual perturbations was never observed in natural conditions (Fig. 3.7B, 3.9B, "static"condition). Furthermore, we found that head-body coordination during forward runs under RG differs from the anti-correlation found under natural conditions (Fig. 3.9I). Altogether, our data suggests that, regardless of the temporal structure of gait (Fig. 3.9D, E, H), a different movement pattern across the body emerges under visual perturbations.

3.6 Visual motion-sensitive circuits are crucial for the rapid tuning of posture by visual feedback

3.6.1 Position vs. motion cues mediate the effect of visual feedback

What attributes of visual feedback were underlie the active steering control during forward segments? Steering control may rely not only on visual flow, but also on the local features of the visual feedback, a topic that has been a matter of debate (Cutting et al., 1992; Götz & Wenking, 1973; Harris & Bonas, 2002; Holst & Mittelstaedt, 1950; Katsov & Clandinin, 2008; Prokop et al., 1997; Rushton et al., 1998; Warren & Hannon, 1988; Warren et al., 2001). Several lines of evidence indicated that the global structure of the visual feedback contributed to the fly's course control. First, if a fly

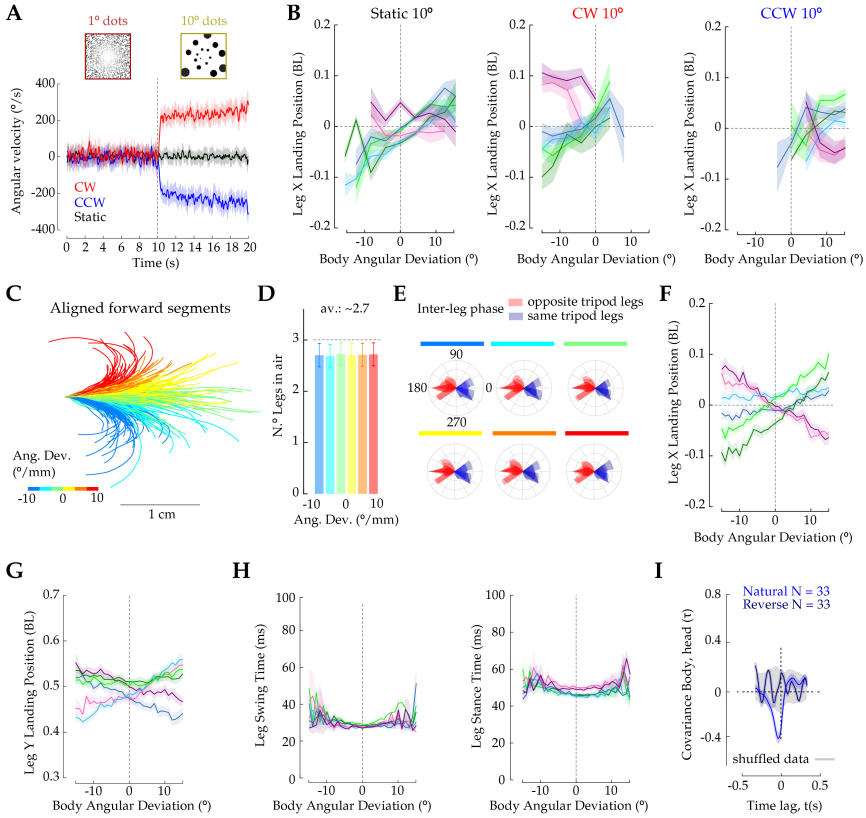

Figure 3.9: **External visual perturbations induce body rotations with specific interlimb coordination.** (A) Average angular velocity under different open-loop rotations of the visual environment (red: clockwise visual rotation, CW; blue: counterclockwise visual rotation, CCW; black: static visual stimuli) for 1° dots and 10° dots. (B) Leg X landing position in a single step in an OMR paradigm as a function of the body angular deviation detected in that step. Visual environment: 10° dots. Individual legs follow the color code shown in Fig.3.5A. Left: static stimuli, middle: CW visual rotation, right: CCW visual rotation. (C) Example set of forward segments during reversed gain conditions aligned to the starting position. Color code corresponds to the magnitude of the walking path's angular deviation during each segment. (D) Number of legs in the air at each frame during forward segments for different amounts of angular deviation (N = 28, n = 11470 forward runs). A perfect tripod gait corresponds to 3 legs in the air at all times (dashed line). (E) Inter-leg phase relation as a function of angular deviation during forward runs. Blue shades: leg phases between legs belonging to the same tripod, red shades: leg phases between legs belonging to opposite tripods for forward runs under reversed gain. (F) Leg X landing position in a single step as a function of the body angular deviation detected in that step (N = 28, n = 22329 steps). Individual leg color code as in (B). (G) Leg Y landing position in a single step as a function of the body angular deviation detected in that step (N = 28, n = 22329 steps) for forward runs under reversed gain. (H) Leg swing and stance times in a single step as a function of the body angular deviation detected in that step. (I) Head-body coordination is measured as the cross-covariance between head angle and body angular velocity during forward runs in natural and reverse conditions. Gray: cross-covariance between head angle and temporally shuffled body angular velocity.

was monitoring a single dot (a local feature of the self-generated stimuli), we would expect a bias in the individual's orientation during exploration, but we found no evidence for such a bias (Fig. 3.10A). Second, the straightness performance of the fly increased with increasing density of the dots, at least up to a certain limit (Fig. 3.10B). Such an effect of dot density on straightness performance would not be expected from a behavior based on local features of the stimulus. Third, the averaged visual influence for stimuli with dot sizes below the acceptance angle of the fly eye (5°) was about two to four times as strong as in darkness (Fig. 3.10C) (Heisenberg & Wolf, 2013). Fourth, the response amplitude of rotational flow-sensitive HS and H2 cells increased monotonically with the size of the dots (see Chapter 5), suggesting that their contribution to the behavior may increase as a function of visual influence, which in turn correlated with straightness performance (Fig. 3.4C). Altogether, our data suggest that straightness performance was influenced by the global structure of the visual feedback, suggesting that visual-flow processing pathways contributed to the control of non-saccadic rotations. In our experimental conditions, as in the real world, the local structure might additionally support straightness control.

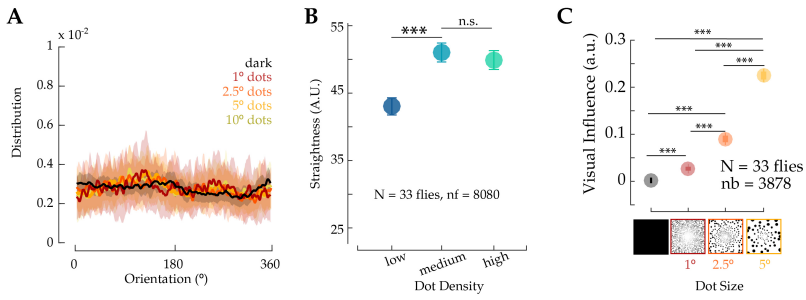

Figure 3.10: **Position vs. motion cues mediate the effect of visual feedback.** (A) Orientation preference distribution under natural gain conditions for different visual environments. (B) Path straightness of forward runs as a function of dot density (*p<0.05, **p<0.01, ***p<0.005, MWW-test). (C) Visual influence as a function of visual environment with varying dot size (*p<0.05, **p<0.01, ***p<0.005, MWW-test).

3.6.2 T4/T5 silencing specifically reduces straightness by increasing interlimb spatial correlations

Our data suggests that visual-flow processing pathways may contribute to the control of path straightness. To determine the specific visual circuits tuning down postural adjustments, we started by silencing the activity of T4/T5 cells, the first population of neurons with direction-selective visual-motion responses (Maisak et al., 2013). We expressed the silencing combination w118; Otd-nls:FLPo; pJFRC56-10xUAS >myrtdTomato-SV40> eGFPKir2.1 under the split Gal4 w118; R59E08AD; R42F06DBD. Controls included replacing the split Gal4 with an empty split Gal4 and removing the Otd-nls:FLPo from the silencing combination (Fig. 3.11A). The use of Otd-nls:FLPo restricts the expression of pJFRC56-10xUAS >myrtdTomato-SV40> eGFPKir2.1 only to neurons in the brain (Fig. 3.11A - Right). T4/T5 silenced flies displayed characteristic exploratory paths (Fig. 3.11B), suggesting that visual motion information is not required for the fixation-saccade structure of exploratory walking.

Silencing the activity of T4/T5 cells did not affect the dynamics of saccades (Fig. 3.11D). However, walking paths during forward runs under strong visual feedback were markedly less straight in experimental flies compared to controls, resembling walking in darkness (Fig. 3.11C). Moreover, this effect was not explained by an impairment in head-body coordination of decrease in object fixation response (Fig. 3.11F, G). Consistent with this observation, we found that front-leg pairwise correlations were more prominent in experimental than in control flies (Fig. 3.11E). This finding strongly suggests that pathways postsynaptic to T4/T5 cells mediate the tuning of postural reflexes to maintain walking straight and gaze stable.

3.6.3 Contributions to straightness control

T4/T5 neurons send their axons to a brain area called the Lobula Plate, where they segregate into layers, each sensitive to specific orientations of visual motion (Fig. 3.11A). Large tangential cells (LPTCs) innervate these layers and integrate visual motion in a specific direction across a large portion of the visual field. Under our experimental conditions, optic-flow was constrained to the yaw direction, making the most relevant directions of motion the progressive or front-to-back (FTB) and the regressive or back-to-front

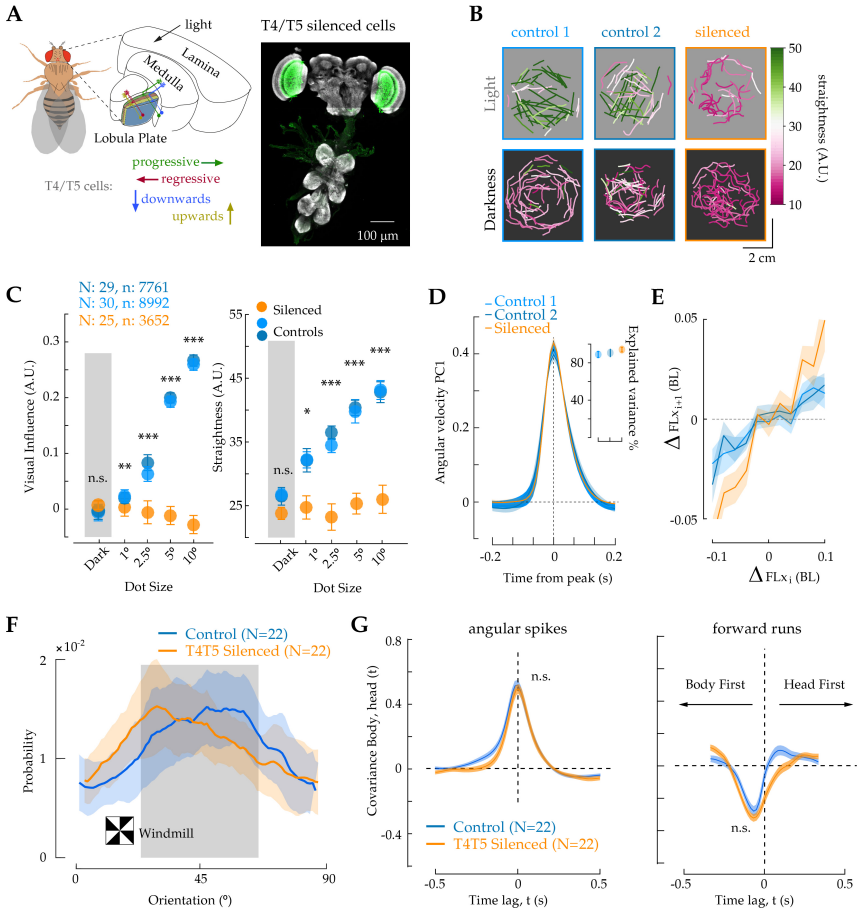

Figure 3.11: **T4/T5 silencing specifically reduces straightness by increasing interlimb spatial correlations.** (A) Left: schematic of the fly optic lobe highlighting the location of direction selective and motion sensitive T4/T5 cells. Right: Selective expression of Kir2.1:GFP in genetically identified T4/T5 cells (green). (B) Exploratory walking paths of a single control (light and dark blue) and experimental fly (orange), in light (top) and dark (bottom) conditions. Visual environment: 10º dots. (C) Left: visual influence across visual environments. Right: path straightness across visual environments. Color code same as in (B) (*p<0.05, **p<0.01, ***p<0.005, MWW-test). (D) Dynamics of the first principal component of body saccades (variance explained 90%, inset), in control (blue) and experimental flies expressing Kir2.1 in T4/T5 cells (orange). (E) Front leg X-landing position as a function of the contralateral front leg X-landing position in the preceding step for controls (blue) and T4/T5 silenced flies (orange). (F) Probability of oriented walking in NG conditions for control flies (blue) and T4/T5 silenced flies (orange) in a windmill visual environment. (G) Head-body coordination measured as the cross-covariance between head angle and body angular velocity, during body saccades (left) or forward runs (right) in control (blue) and T4/T5 silenced flies (orange).

(BTF). Before testing the contribution of T4/T5 postsynaptic neurons we first test whether both directions contributed to straightness performance. For that, we generated virtual environments where the stimulus was presented only to one eye (Fig. 3.12Aii). In this way, a stimulus projected onto the right eye in a fly rotating to the left would generate FTB visual-flow only, whereas a fly rotating to the right will generate BTF visual-flow only (note that the opposite is true under reversed gain). In these worlds, flies displayed the characteristic exploratory structure (Fig. 3.12B), and the reversed gain condition induced circling behavior regardless of the direction of self-generated visual motion (Fig. 3.12B, D). However, the dynamics of the angular velocity under the RG condition, was different for FTB or BTF stimuli (Fig. 3.12B, C). FTB flow induced a large drift of angular velocity on top of which body saccades could be observed (Fig. 3.12B, C). This large drift coincided with moment when the fly walked at high forward speed, suggesting that it may correspond to the slow angular velocity fluctuations observed during forward segments under natural gain conditions. In contrast, BTF flow induced a rather small-amplitude drift, and more prominent body saccades in the same direction (Fig. 3.12B, C). That is, FTB and BTF pathways could jointly contribute to straightness performance; however, each pathway seems to control strength of angular fluctuations differentially in the context of forward runs (Fig. 3.12C, D).

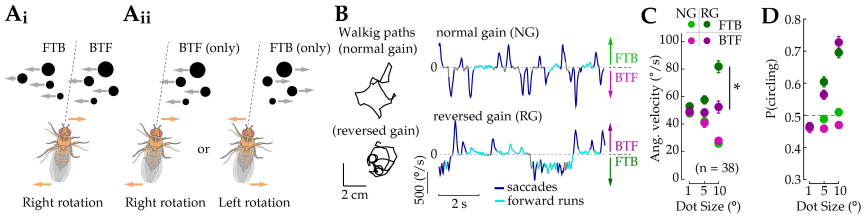

Figure 3.12: **Contributions to straightness control.** (Ai) In the VR world, a rightward rotation generates both Front-to-Back (FTB) and Back-to-Front (BTF) visual motion. (Aii) Under unilateral stimuli, a fly generates either direction of visual feedback. (B) Left: a walking-path segment of a fly in a unilateral 10°-dot size visual environment, under natural or reversed gain. Right: the angular (top trace) and forward (bottom trace) velocity time series of the corresponding example fly. (C) Mean angular deviations as a function of the visual environment's dot-size (*p<0.05, MWW-test). (D) Conditional probability of circling given FTB or BTF visual feedback in different visual environments. Dashed line represents chance.

3.6.4 Neural pathways for straightness control

A prime neural candidate to process visual feedback information for straightness control are HS cells. HS cells are a population of 3 FTB sensitive LPTCs that receive extensive synapses from T4/T5 neurons. We tested this idea by silencing the activity of HS cells with the targeted expression of Kir2.1 in HS (and in three additional VS cells (VS3-6) that were also labeled) using an intersectional strategy (Fig. 3.13A). To restrict Kir2.1 expression only in the neurons of interest we crossed w118; 8XLexAop2-FLPL; pJFRC56-10xUAS >myrtdTomato-SV40> eGFPKir2.1 and w118; R39E01-lexA; VT058487-GAL4 (Fig. 3.13A). Controls included maintaining the LexA-Gal4 combination and removing either the 8XLexAop2-FLPL or the pJFRC56-10xUAS>myrtdTomato-SV40>eGFPKir2.1 from the silencing combination. Chronic bilateral inhibition of the activity of HS cells (mean resting potential in experimental flies = -80.0±4.2 mV, mean ± SD, n=4 cells, compared to control flies = -52.8±6.2 mV, n=5 cells) affected neither straightness performance (Fig. 3.13B), nor head-body coordination (Fig. 3.13C), even when the visual feedback was constrained to the FTB direction only (Fig. 3.13D, E). This result suggested that other parallel networks might contribute to straightness performance.

Many of the LPTCs converge to a brain area called the inferior posterior slope (IPS). In there, they connect (between others) to descending neurons that directly send information to the ventral nerve cord. We selected 14 classes of descending neurons with dendrites near the IPS and silenced their activity one class at a time. Interestingly, none of the silenced DN classes had any effect in the straightness of the fly path during forward runs (Fig. 3.13F, left). Moreover, we expanded these experiments by silencing DNs innervating outside of the IPS to a total of 40 cell classes and 1300 single flies. None of the silenced cell lines displayed any defect at performing straight walking when compared to the respective control (a single line had slightly significantly better straightness than its control) (Fig. 3.13F, right).

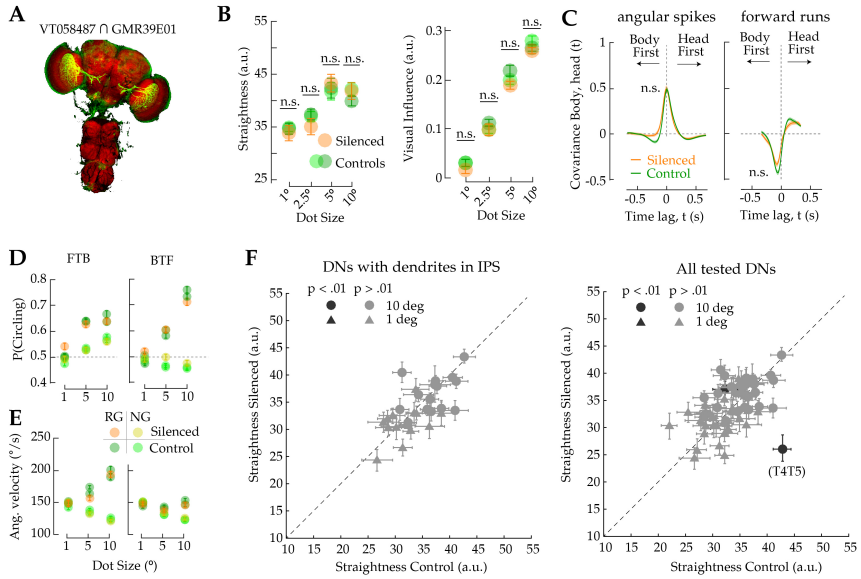

Figure 3.13: **Neural pathways for straightness control.** (A) Expression pattern of Kir2.1::EGFP, using an intersectional strategy to target HS and VS cells. (B) Left: straightness of forward runs in different visual environments for experimental (flies with HS/VS cells silenced, orange) and control flies (green). Right: visual influence of the different visual environments in experimental and control flies (D) Cross-covariance analysis between body and head (yaw) rotations in experimental (green) and in control flies (orange), considering saccadic turns (left) or rotations during forward runs (right). (D) Probability of circling under natural (light colors) and reversed gain (dark colors) conditions in experimental (orange) and control (green) flies, separated by FTB (left) and BTF (right) direction of visual feedback across different visual environments. (E) Average rotational speed during forward walking under natural (light colors) and reversed gain (dark colors) conditions, in experimental (orange) and control (green) flies, separated by FTB (left) and BTF (right) visual feedback, across different visual environments. (F) Left: Comparison between the path straightness during forward runs under silencing of specific descending neurons innervating the inferior posterior slope (IPS) and the respective control flies. Dots represent the grand-mean of flies targeting a specific class of DN exploring a 10º dot environment. Triangles represent the same but for a 1º dot environment. Right: same but for other populations of descending neurons.

3.7 Discussion

3.7.1 Neural mechanisms involved in unpredicted posture perturbations

Local circuits within the spinal cord/VNC perform rapid adjustments tailored to the step cycle to control posture in the presence of internally and externally generated noise (Büschges & El Manira, 1998; Laurent, 1991; Pearson, 2004; Tuthill & Wilson, 2016). Here, we described the presence of such noise in the variability of leg placement during forward runs, which can generate a momentary decrease in posture stability (Fig. 3.8C-E). Posture control systems respond to this perturbation via pairwise limb spatial correlations, most prominently in the pair of front legs, which cause small changes in body orientation while recovering posture stability. A similar stability recovery method has been found for vertebrates in the presence of an external push (Karayannidou et al., 2009). Although the mechanisms underlying these pairwise correlations remain unclear, we speculate that information about the position of the end point of the swing in contralateral pairs contributes to postural adjustments, likely via the activity of interneurons integrating information across the midline or segments within the VNC (Dean, 1984). Alternatively, visual descending pathways may act directly on leg sensory systems (Berg et al., 2015).

In insects, descending pathways from the brain carry task-specific signals to circuits within the VNC to regulate reactive forces, interlimb coordination, and leg placement (Cruse, 1990; Dean, 1984). Very little is known about the identity and mechanisms by which interneurons in the VNC modulate leg placement or how visual descending circuits from the brain interact with such populations of interneurons within the VNC. The findings reported here constitute an excellent framework to examine these important questions in the context of active vision and its role in goal-directed walking.

3.7.2 Active, self-paced visual control of walking

In flies, the visual control of course direction is thought to depend on compensatory systems (Götz & Wenking, 1973; Poggio & Reichardt, 1973; Strauss et al., 1997; Tammero et al., 2004; Varju, 1975; Wolf & Heisenberg,

1990). The proposed models rely on a combination of directional and non-directional components (Bahl et al., 2013; Poggio & Reichardt, 1973; Wolf & Heisenberg, 1986) which together minimize the overall angular velocities of the insect by means of compensatory turns until an internal estimate of the rate of rotation or error in position is minimized (Poggio & Reichardt, 1973; Roth et al., 2012; Strauss et al., 1997; Wolf & Heisenberg, 1990).

In flight, the directional (optomotor) component seems to depend on a negative feedback system with integrative components (Poggio & Reichardt, 1973; Roth et al., 2012; Wolf & Heisenberg, 1990). Several lines of evidence show that these models employing positional and OMR systems cannot fully explain our findings in the context of exploratory walking. First, the fly's walking course control during forward runs critically depends on visual motion pathways, in contrast to position-based oriented behaviors (Bahl et al., 2013; Wolf & Heisenberg, 1986). While flies walking in virtual worlds with discrete high-contrast edges use the position of edges to follow a course direction, and this orientation is maintained when activity in T4/T5 cells is silenced (Fig. 3.10C, 3.11F), we find no evidence for a fixation mechanism on single dots during forward runs (Fig. 3.10A). Second, during forward runs, we did not find evidence for the presence of actively generated small-amplitude turns, suggested to constitute an operant trial-and-error strategy for the operation of the optomotor system under closed-loop conditions (Strauss et al., 1997; Wolf & Heisenberg, 1990). Moreover, coordination of head-body movement during forward runs would minimize such a retinal slip signal, further suggesting that a classical optomotor strategy may not be implemented under our experimental conditions. Third, and importantly, we find that visual feedback operates by preventing the occurrence of larger body rotations rather than generating compensatory turns. Fourth, optomotor mechanisms could potentially support gaze stability in flying insects, however, the sufficiency of OMR to guarantee straight walking has been questioned given the low gain of the animal's response to external perturbations while walking (Collett et al., 1993; Lönnendonker & Scharstein, 1991). Similarly, we found that under our experimental conditions, the gain of the OMR averaged 0.56 during walking. Reversing the gain of the virtual reality system or presenting an OMR stimulus induced additional components of limb placement that are not observed under natural conditions, which likely contribute to compensatory turns. In addition, body rotations during

forward runs under reverse gain promoted different head-body coordination than the one observed under natural conditions further reflecting the distinct mechanisms in place in these two conditions.

We propose that parallel mechanisms exist for course control that are controlled by self- (visual feedback, closed-loop condition) vs. externally generated visual motions signals (open-loop condition), and that may respond to different requirements of the locomotive behavior. While external perturbations, such a gust of wind or asymmetries in the locomotor apparatus induced by limb damage, may rely on optomotor mechanisms for proper course control, the fast action of visual feedback reported here is of extreme importance in the context of self-paced variability during walking, where every step is prone to multiple sources of noise (Bernstein, 1967).

It takes about 35ms or half the stance period during forward runs (Fig. 3.7C) (DeAngelis et al., 2019; Mendes et al., 2013) for visual motion signals to excite postsynaptic neurons to T4/T5 cells (T. Fujiwara, personal communication). Thus, to control leg placement, visual feedback could act upon the swinging leg if descending signals to the ventral nerve cord (VNC) travel fast with minimal delay. T4/T5 cells connect to populations of tangential and columnar projection interneurons (Wu et al., 2016). Many of these projection neurons receive extra-retinal information that further accelerates visual processing (**chiappe2010**; Seelig et al., 2010). In addition, visual projection neurons extend their axons to regions densely innervated by descending neurons (Namiki et al., 2018). Therefore, a combination of fast visual motion processing and direct descending pathways could account for the rapid tuning of postural reflexes by visual feedback. Alternatively, visual feedback may not directly control leg sensorimotor circuits in a step-by-step manner but rather affect a VNC program with a decreased gain of postural control systems. Future experiments will focus on examining these alternatives.

The rapid control of walking direction and gaze stability by visual feedback during forward runs has several important implications. Given that visual feedback prevents spatial correlations specifically at the leg landing moment, a timing signal may exist to indicate the phase of the step cycle within circuits processing visual feedback. In addition, visual feedback is motor-context specific, as it occurs only during forward runs while the fly attempts to keep its gaze stable, and it is unclear how information about motor context is integrated with visual motion signals to control course

direction when the fly seeks to stabilize gaze position.

In summary, the stability of gaze during forward runs is achieved by circuits that link visual feedback to the control of leg placement via visual motion-sensitive descending neurons that may operate at a precise moment of the step cycle. Thus, we propose that gaze stability during walking depends on a goal-directed interaction between the brain and VNC circuits to drive flexible tuning of posture control during a continuous walking behavior via a moment-by-moment control, or through a switch of locomotive programs that are less sensitive to postural control systems.

3.8 Acknowledgements

Experiments in this chapter were designed with Eugenia Chiappe, who is also involved in the writing of the publication related to this chapter. John Tuthill and Stephen Huston for earlier discussions on this work; Michael Reiser and members of the lab for comments on the manuscript. We thank Kenta Asahina, Michael Dickinson, Michael Reiser, and Gerald Rubin for kindly sharing flies. This work was supported by the Champalimaud Foundation and the research infrastructure Congento, LISBOA-01-0145-FEDER-022170, co-financed by Fundação para a Ciência e Tecnologia (Portugal) and Lisboa2020, under the PORTUGAL 2020 Agreement (European Regional Development Fund). This work was also supported by Fundação para a Ciência e Tecnologia FCT PD/BD/105947/2014 (T.C.), by the Marie Curie Career Integration Grant PCIG13-GA-2013-618854 (M.E.Ch), and by the European Research Council Starting Grant ERC-2017-STG-759782 537 (M.E.Ch).

Chapter 4

Self-Motion Integration Modulates Behavior Decisions

4.1 Overview

In the previous chapter we showed a major role of visual self-motion signals in the control of gaze stability during forward runs. At the same time, analysis of the dynamics of body saccades under different visual conditions revealed that they are not under the direct influence of the same feedback signals, further suggesting their ballistic nature.

In this chapter we will further examine the control of body saccades at multiple levels. At first we will break down the execution of body saccades into its movement components across different body parts. Flexibility in body saccade execution is used to adjust these versatile movements according to the goals of the fly. Furthermore, we will follow the different elements modulating body saccades to discover a novel neural pathway that links the integration of self-motion information to saccade decisions.

4.1.1 Saccades as a multipurpose motor program

As previously described, singular saccades are fast movements of the eye, head or body that shift the animal's gaze in the shortest time possible

(Bender & Dickinson, 2006a; Grossberg & Kuperstein, 2011; Muijres et al., 2015). Even though they are generally described as a "simple"movement, these actions are used in different situations like search, escape, approach or visual stabilization (Cellini & Mongeau, 2020). In vertebrates, many brain areas including the retina, superior colliculus, parietal cortex, cerebellum, visual cortex, frontal cortex and the oculomotor nuclei have been involved in the generation or modulation of saccades (Grossberg & Kuperstein, 2011). Many of these brain areas are widely integrative and process context dependent multimodal information, adding evidence to the flexible use of saccades under multiple contexts. Contrary to most vertebrates that only rotate the eyes and/or head to saccade, insects rotate their whole body during saccades (Geurten et al., 2014; Land, 1999; Schilstra & Van Hateren, 1998). Flight saccades are generally divided as endogenous (spontaneous) or exogenous (triggered) (Cellini & Mongeau, 2020; Censi et al., 2013). While this division is likely to be present for walking body saccades (Geurten et al., 2014), their nature has been largely uncharacterized.

Exogenous (or stimulus-evoked) saccades have been linked to attractive or aversive responses to multiple sensory inputs, from visual to olfactory to mechanosensory (Bender & Dickinson, 2006b; Budick et al., 2007; Duistermars & Frye, 2008; Tammero & Dickinson, 2002). Interestingly, even small changes in sensory input from the same modality can lead to completely different saccade outputs. For example, flies show attraction by saccading towards vertical bars but show repulsion by saccading against shortened versions of the same stimuli (Maimon et al., 2008). Similarly, changes in behavioral state like arousal or starvation can modulate the probability of approach towards the same sensory stimulus (Corrales-Carvajal et al., 2016). The context-dependent nature of stimulus evoked saccades suggests that they are more than just a reflexive movement. Body saccades may instead depend on a process of multimodal integration and action selection tailored to elicit the most appropriate movement depending on the animal's goals. In line with this hypothesis, studies in free flying animals have found that the movements that generate reflexive ballistic escape responses have different properties than those that generate flight saccades (Muijres et al., 2015; Muijres et al., 2014).

Spontaneous saccades have been previously suggested to be the manifest of an underlying search strategy (Maye et al., 2007; Reynolds & Frye, 2007), but consistent evidence for this theory is still lacking. Recent work

in Drosophila has identified a descending neuron (AX) whose activity is correlated to both spontaneous and visually evoked saccades in flight (Schnell et al., 2017). The existence of this neuron suggests that both exogenous and endogenous saccades might converge at the level of either action selection or command in the fly's nervous system. It is still unknown how neurons such as AX acquire their tuning properties and, more generally, how internal signals relate to the triggering or modulation of spontaneous saccades.

4.2 Variability vs. stereotypy during saccades

4.2.1 Body saccades have conserved dynamics over a wide velocity range

To investigate the nature of body saccades during exploratory walking, we recorded flies exploring a large arena surrounded with warm walls under a virtual tether condition (Chapter 2, Cruz et al., 2021). As shown in Chapter 2, flies organize their walking behavior in fixation-saccade structure (Fig. 4.1A). While forward runs span a small range of forward velocity and angular velocities (Fig. 4.1B), body saccades can span a wide range of both forward and angular velocities (Fig. 4.1B, C, D). The wide range of body saccades contrasts with their highly conserved underlying rotational dynamics, with a single principal component explaining over 90% of all saccade shape variability (Fig. 4.1E, 2.3).

The dichotomy between flexibility and stereotypy within the same motor action raises the question of how motor programs are organized during saccades to allow for these two distinct features.

4.2.2 Leg movement correlates of the flexible and conserved aspects of body saccades

We hypothesize that the conserved yet widely variable characteristic of body saccades is supported by a combination of both flexible and stereotyped properties of leg movement. We used high resolution video information together with machine learning tools to track the tip position of each of the six legs in two dimensions (Chapter 2, Cruz et al., 2021; Mathis et al., 2018). To analyze the relationship between saccade direction/amplitude and different properties of leg movement, we isolated all body saccade

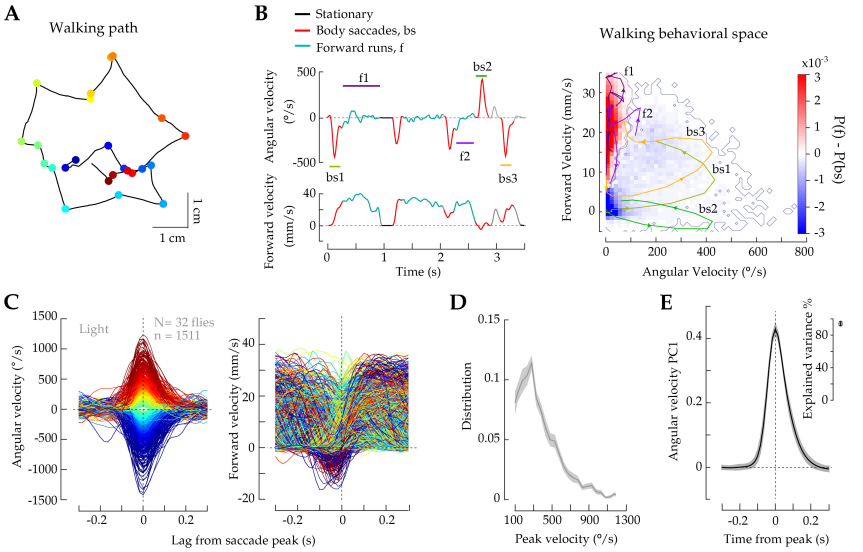

Figure 4.1: **Body saccades have conserved dynamics over a wide velocity range.** (A) Example of exploratory paths of an individual fly, colored dots correspond to body saccades. (B) Left: Time series of a walking segment with body saccades ("bs", red) and angular velocity fluctuations ("f", cyan). Right: Probability of angular velocity fluctuations over saccades as a function of the behavioral space of the fly. Color-code: red indicates regions with very low probability of body saccades, while blue indicates the reverse. Color-coded trajectories highlight different examples of trajectories of body saccades (bs1-3), and of separate forward segments (f1-2) within the behavioral space of the fly. (C) Left: population of identified body saccades from WT flies, triggered at peak angular velocity. Color code indicates the amplitude and sign of saccades, with blue hues labeling high-amplitude clock-wise saccades, and red hues labeling high-amplitude, counter-clockwise saccades. Right: forward velocity, triggered at saccade peak angular velocity. Note that high-amplitude saccades (red/blue traces) are associated with negative forward velocity, indicating events where the fly pivots or walks backwards to turn direction. Smaller amplitude saccades (yellow/cyan traces) are associated with re-orientation behaviors at onset of a walking bout, with increasing forward velocity. (D) Distribution of the amplitude of saccadic peak velocity in darkness. (E) Dynamics of the first principal component of body saccades in darkness Inset: variance explained by PC1.

events using the algorithm from (Fig. 2.3). The events were binned with respect to the amplitude of their angular deviations (Fig. 4.2A). Independently on the direction and magnitude of body saccades, the average amount of legs in the air during these events was around two, suggesting a tetrapod configuration during this locomotion mode (Fig. 4.2B). This result further indicates that the variability in body saccade amplitude is not caused by variations in temporal coordination of the gait pattern, but could result from the kinematic properties of leg movement.

To test the role of kinematic properties of leg movement during body saccades, we repeated the analysis from (Fig. 3.7A). The direction and amplitude of body saccades strongly correlates with the lateral landing position of both front legs and the middle leg contralateral to the body saccade direction (Fig. 4.2C). The correlation was not observed for any of the other legs or for the lift-off positions. The flexible lateral placement of these specific legs is likely to cause a lateral force during the stance phase that provides the torque for the fast body rotation.

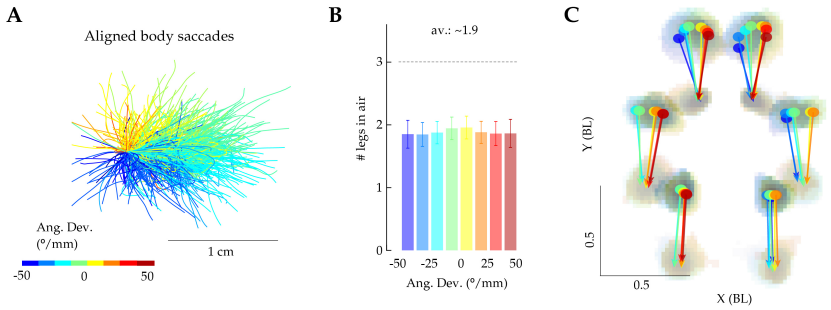

Figure 4.2: **Leg correlates of the flexible aspects of body saccades.** (A) Example set of angular spikes aligned in the starting position and orientation. Color code corresponds to the amount of angular deviation during each segment. (B) Amount of legs in the air at each frame during forward segments for different amounts of angular deviation. A perfect tripod gait corresponds to 3 legs in the air at all times (dashed line). (C) Spatial distributions of leg landing and lift-off with respect to the body center during angular spikes and color coded by the amount of angular deviations. Arrows represent the movement from the center of the landing distribution to the center of the lift-off distribution.

The previous analysis provided a static view of landing and lift-off positions during body saccades. This view suggests that specific legs may be contributing more to the variability of body saccades than others. Still, this simple analysis lacks information regarding the dynamics of leg movement

and is therefore unfit to test whether the stereotyped saccade dynamics roots on stereotyped aspects of leg movement. We applied hierarchical clustering on the movements of all six legs during saccades in order to identify which stereotyped temporal aspects of leg movement could underlie the stereotyped body dynamics during saccades. Specifically, we used euclidean linkage and the ward criteria on the movements of all six legs during body saccades with peak angular velocities larger than 400/*s*. Leg movements were aligned to the peak of the body saccade (Fig. 4.3A). Cutting the dendrogram to obtain 8 clusters revealed that the differences in the pattern of leg movements across clusters majorly reflected the translational state of the fly (Fig. 4.3A, B) or the phase of the front legs at the peak of the saccade (Fig. 4.3A, C). Different choices for the final amount of clusters provided qualitatively similar results.

Furthermore, we find that different clusters of leg dynamics give rise to the exact same body movements during saccades (Fig. 4.3A, right). While the movement phase of both front and contralateral middle leg is not locked to the body rotation, the movement of the ipsilateral hind and middle leg was highly conserved. The latter stayed in stance for most of the initial part of the rotation, serving as pivot to the body rotation (Fig. 4.3B, C).

In summary, we identified two major leg movement patterns during body saccades: a conserved stance of ipsilateral hind and middle leg during peak rotation, and a flexible lateral placement of front and contralateral middle legs that is not phase locked to the body rotation. These two movement patterns simultaneously support the wide range of amplitudes for body saccades and their underlying conserved dynamics. The flexibility in amplitude and direction of body saccades suggests that this mode of rotation can be used in multiple contexts during exploratory walking, both as a spontaneous event or in response to external factors such as temperature or vision.

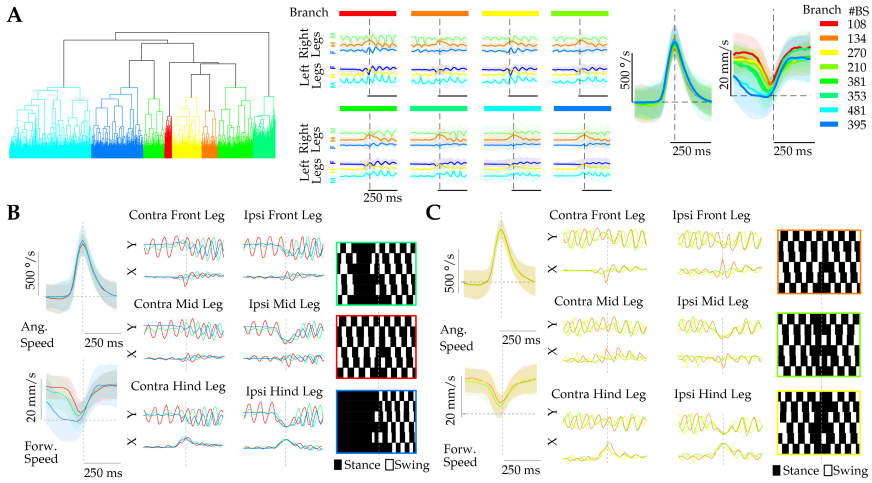

Figure 4.3: **Leg movement correlates of the conserved aspects of body saccades.** (A) Left: dendrogram from the hierarchical clustering of the leg movements during body saccades. Middle, average time series of leg movement for all the branches. Right: angular and forward velocity time series for all the branches. (B) Three example branches of leg movements giving rise to the same body angular movement. These clusters differ in the forward velocity preceding the body saccades. Left: angular and forward velocity time series. Middle, average time series of leg movement. Right: swing-stance profiles for all legs. (C) Three example branches of leg movements giving rise to the same body angular and forward movement. These clusters differ in the phase of front and contralateral middle and hind legs. Left: angular and forward velocity time series. Middle: average time series of leg movement. Right: swing-stance profiles for all legs.

4.3 Saccade modulation by endogenous and exogenous factors

4.3.1 Temperature modulates body saccade amplitude and direction in specific regions of the arena

We next investigated which external factors modulate the variability in body saccade amplitude and direction in our experimental conditions. A major element of our experimental arena is the warm wall and the temperature gradient cerated by it. To examine how temperature affects the properties of body saccades we divided the analysis in three different regions of the arena, each at specific distances from the warm walls (Fig. 4.4A).

We found that, independent of visual conditions, flies increase the amplitude of body saccades as they approach the arena walls and that this effect is most prevalent in Zone 1, the warmest part of the arena (Fig 4.4B, top). Furthermore, the direction of saccades depends on the relative orientation of the fly with regard to the arena wall, but only when the flies are in the wall's vicinity (Fig. 4.4C, Zone 1). This modulation of body saccade direction guarantees that flies will always turn in the direction that will take them away from the wall, independent of visual conditions.

A substantial amount of saccadic turns happen when flies are closer to the center of the arena (Fig. 4.4B, bottom), suggesting that body saccades do not happen just as a reaction to the temperature stimulus. The direction of these central body saccades can't be explained by the orientation relative to the wall (Fig. 4.4C, Zone 2,3), and their amplitude is much less modulated by the distance to the walls (Fig. 4.4B, Zone 2,3). This apparent lack of modulation occurs even under dark conditions, ruling out exogenous factors as major modulatory factors for the population of body saccades happening closer to the center of the arena, suggesting endogenous factors as their major drivers (Censi et al., 2013).

4.4 Self-motion information during forward runs modulate the following saccadic turn

4.4.1 Angular deviations during forward runs largely consist of unilateral drifts.

During forward runs flies intend to keep a straight trajectory in order to maintain a stable gaze (Chapter 3; Cruz et al., 2021). Having a stable gaze is beneficial for the animals to reduce motion blur as well as to isolate translational optic-flow for extraction of spatial information from the environment (Kim & Dickinson, 2017; Koenderink, 1986; Land, 1999; Müller & Wehner, 1988; Pfeffer & Wittlinger, 2016; Tolman et al., 1946; van Breugel & Dickinson, 2014). When visual feedback becomes more ambiguous, the ability of flies to keep a straight trajectory deteriorates (Chapter 3; Cruz et al., 2021) (Fig. 4.5A, B). The reduction in straightness during forward runs is associated with the emergence of unilateral drifts in the fly's orientation (Fig 4.5C). The unilateral character of these drifts, even under strong visual conditions, indicate that they are not being rapidly compensated for.

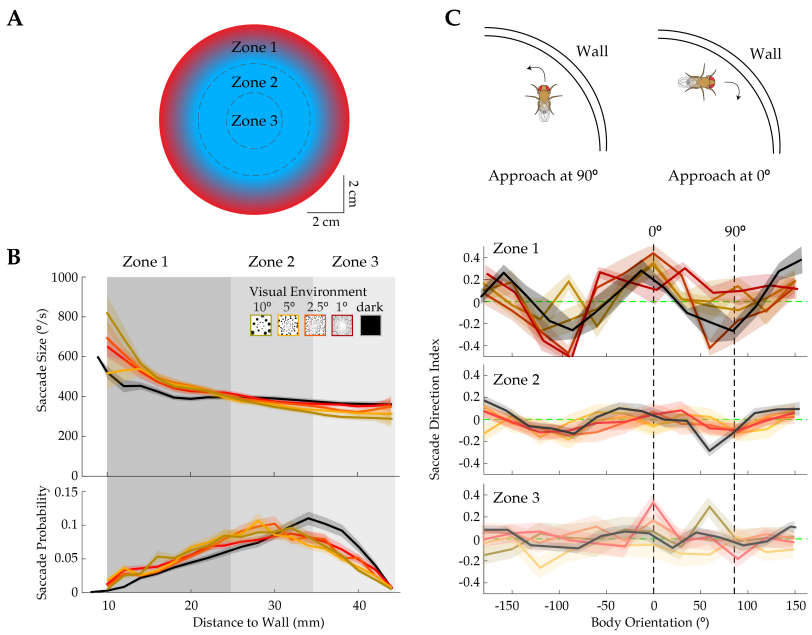

Figure 4.4: **Temperature modulates body saccade amplitude and direction in specific regions of the arena.** (A) Definition of zones in the arena. (B) Top: average saccade amplitude as a function of the distance from the arena walls in dark conditions (black) or in varying visual environments (colors). Bottom: body saccade density as a function of the distance from the wall in dark conditions (black) or in varying visual environments (colors). (C) Bias in saccade direction as a function of the fly body orientation. All data was aligned to the top-right quadrant of the arena (see schematic). If flies approach at 0° their probability of a leftward saccade increases, whether if they approach at 90° their probability of a rightward saccade increases. This modulation disappears as the flies saccade further from the walls in both darkness (black) and in varying visual environments (colors).

The apparent lack of compensation raises the question whether the fly is detecting the drifting orientation and whether it affects its future behavior.

4.4.2 Angular drifts during forward segments modulate the following saccadic turn

A large proportion of forward runs are followed by body saccades (74% in darkness). We isolated the body saccades following forward segments (henceforth named post drift saccades or PDS, Fig. 4.6A). We found that a drift during a forward run is likely followed by a PDS contralateral to

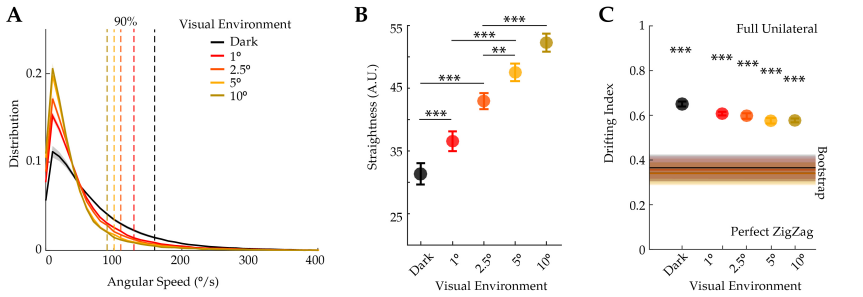

Figure 4.5: **Angular deviations during forward runs largely consist of unilateral drifts.** (A) Distributions of angular speeds during forward runs under different visual environments. 90% of the angular deviations are smaller than the value illustrated by the dotted lines. (B) Average straightness as a function of visual environment during forward runs. (C) Probability of unilateral body drifts defined as the sum of all angular deviations divided by the sum of the absolute value of all angular deviations as a function of visual environment. Shaded area correspond to the same quantification using shuffled data. The non-zero value illustrate the fact that flies have preferred turning sides, however that can't explain the body drift during forward runs.

the drift direction (Fig. 4.6B). Moreover, the larger the magnitude of drift, the larger the probability of a PDS contralateral to the drift direction (Fig. 4.6C). A smaller but significant modulation is also present when comparing the saccade amplitude and the magnitude of the preceding drift (Fig. 4.6D). This result suggests that flies accumulate information about how much they are deviating during a forward segment and may use it to flexibly modulate the properties of the following body saccade, perhaps with the intent to mitigate the effects of the deviation or improve the spatial coverage of the arena.

4.4.3 Drift-saccade modulation does not depend on vision or temperature

The probability of the preceding drift to influence the direction of the following saccade increases with the drift magnitude (Fig. 4.6C). We wondered the kind of information used to estimate the drift value in order to modulate its following action.

In darkness, the only allocentric cue the fly can use to modulate its behavior is the temperature generated by the hot walls. Previous analysis showed that the effect of the temperature is present in the proximity of

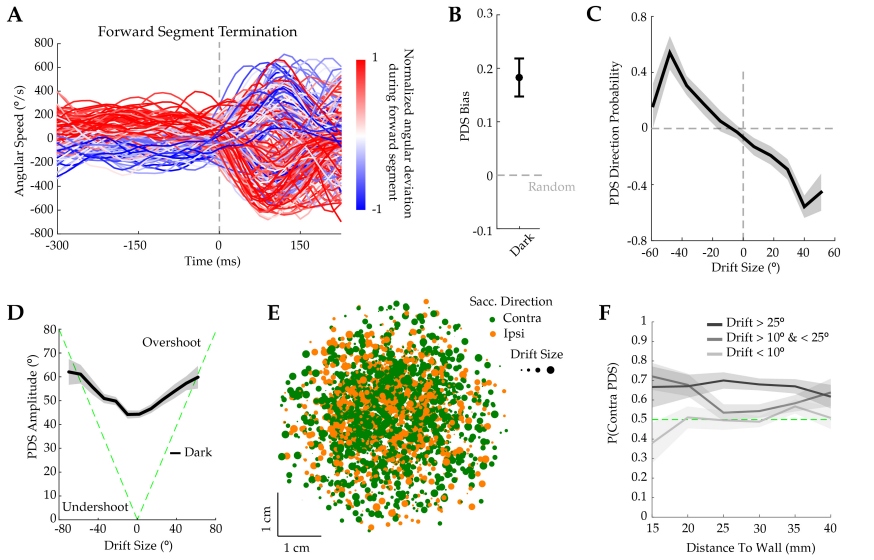

Figure 4.6: **Angular drifts during forward segments modulate the following saccadic turn.** (A) Transitions between forward runs and body saccades color coded by the magnitude and direction of drift during the forward run. (B) Bias of PDS based on preceding body drift. (C) Bias of PDS versus preceding body drift across visual conditions. (D) Absolute post saccade size versus preceding body drift. (E) Spatial location of PDS. (F) Probability of contralateral PDS as a function of preceding drift size and distance to the wall.

the walls, but not towards the center of the arena. To investigate if the increased probability of a PDS contralateral to the drift direction could be explained by the proximity to the walls, we extracted the position of all PDS. We observed that PDS can be elicited uniformly across the arena (Fig. 4.6E). Proximity to the walls does not modulate the probability of a PDS to be contralateral to a previous drift, being the amount of angular drift the fly experienced prior to eliciting the body saccade still the major factor at modulating its direction (Fig. 4.6F).

4.4.4 Drift-saccade modulation depends on a specific drift integration time window

In dark conditions flies have to rely on idiothetic cues alone to estimate the drift during forward runs. Under those conditions flies have to integrate egocentric representations of angular deviations in order to get a full

estimate of the drift during the forward run. We next investigated the properties of the integration, namely whether the drift integrator is a perfect or a leaky integrator. To tackle this question, we started by dividing the full population of transitions between forward runs and body saccades by the direction of the PDS. Next, we determined the length of the time window preceding the PDS in which angular deviations are distinguishable between the two saccade directions. Contrary to a perfect integration, in a leaky integration we expect that events further in the past would have a lesser impact, and therefore less distinguishable. Our results are consistent with a leaky integration of angular deviations, where only the angular deviations in the 500ms preceding the PDS are predictive of the direction of the body saccade (Fig. 4.7A).

We further confirmed this result by selecting forward runs of similar size that only had angular deviations more than 500ms before the body saccade or that only had angular deviations less than 500ms before the body saccade (Fig. 4.7B). Our data shows that only the angular deviations happening within the preceding 500ms to the body saccade, and not the ones before, are able to modulate its direction (Fig. 4.7B).

4.4.5 Visual motion is sufficient but not necessary for self-motion integration

Self-motion information about ongoing body drift can arise from both visual and other idiothetic self-motion cues like vestibular, proprioceptive signals or efference copies. Experiments under darkness or in visual environments that produce very weak to no visual feedback show that vision is not necessary to bias PDS. Furthermore, while vision decreases the amounts of drift during forward runs (Chapter 3, Cruz et al., 2021), the relationship between drift size and PDS bias is largely independent of visual conditions (Fig. 4.8A).

While vision is not necessary for the modulation, it could still be used for monitoring drift. To test this hypothesis, we reversed the gain of the virtual environment, creating a conflict between visual and non-visual self-motion information (Fig. 3.3). Under natural gain, drift generates a contralateral visual rotation of the environment with respect to the fly. In contrast, under reverse gain the visual rotation is now ipsilateral to the drift. If visual

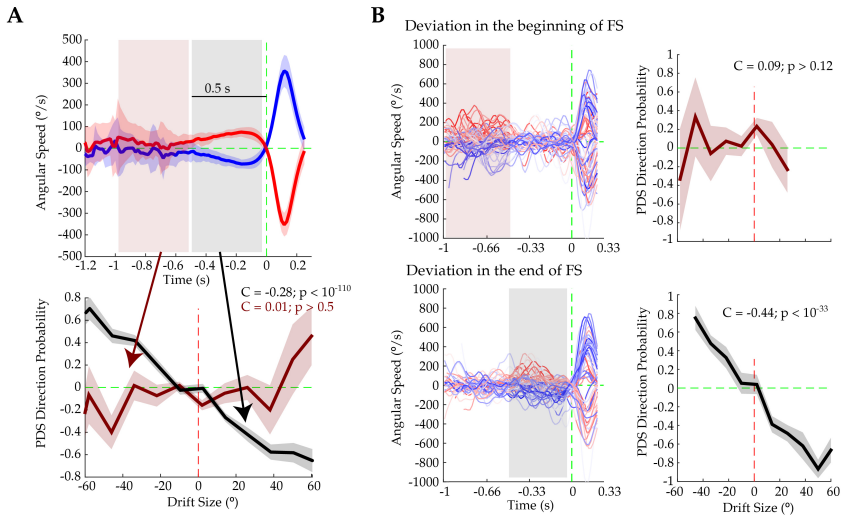

Figure 4.7: **Drift-saccade modulation depends on a specific drift integration time window.** (A) Top: average time series of the transitions between forward runs and body saccades divided by the direction of the PDS. Shaded black represents when preceding drifts are different (500ms). Shaded red area represents when preceding drifts are equal. Bottom: bias of post saccades versus preceding body drift during either the shaded red or shaded black intervals. (B) Top: average time series of the transitions between forward runs and body saccades for forward runs with drift only >500ms before the saccade, and associated bias of post saccades versus preceding body drift. Bottom: average time series of the transitions between forward runs and body saccades for forward runs with drift only <500ms before the saccade, and associated bias of post saccades versus preceding body drift.

feedback is used to measure body rotation, we predict a change of the relationship between drift and saccade bias as the visual feedback becomes stronger in reverse gain. In line with this hypothesis, we found that as the dot size of the visual environment increases the relationship between drift direction and PDS bias reverses (Fig. 4.8B). These results suggest that under natural conditions visual feedback information about the drift is redundant to that originating from idiothetic sources, however if some external source causes the fly to deviate from its path (like a gust of wind or limb damage), visual feedback can become a major component of the drift estimation to bias the PDS.

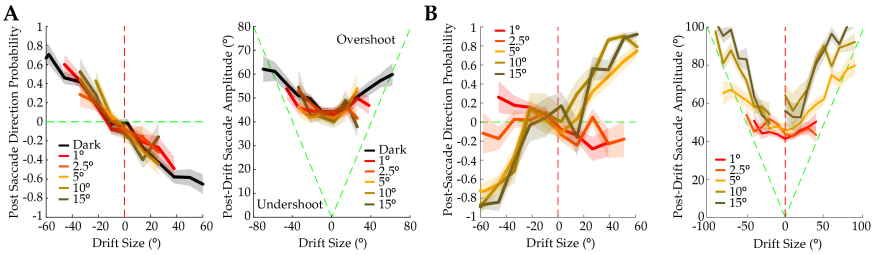

Figure 4.8: **Visual motion is sufficient but not necessary for self-motion integration.** (A) Left: Bias of PDS versus preceding body drift across visual conditions. Right: Absolute post saccade amplitude versus preceding body drift across visual conditions. Body drift was calculated in the time window <500ms previous to saccade. (B) Same as (A) but under reverse gain conditions (Fig. 3.3).

4.5 IPS circuit for visuomotor integration driving saccadic turn decision

Our results collected with wild type flies (WTTB) suggest that a multimodal signal representing angular deviations passes through a leaky integrator to represent ongoing drift during forward runs. The drift representation is then used to flexibly modulate either the selection or the command of the next body saccade taken by the fly. The behavioral results reported here make for a promising system to investigate how self-motion feedback is neurally integrated and how self-motion sensitive neural pathways interact with the process of action selection or modulate command signals.

In the next sections, we will leverage our knowledge of self-motion sensitive circuits together with the genetic and tracing tools for Drosophila to elucidate possible neural pathways that mediate the drift-saccade modulation.

4.5.1 T4/T5 silencing does not disrupt drift-saccade modulation

Even though natural visual feedback is not necessary to bias PDS, unexpected visual feedback can affect the drift-saccade modulation. As shown before, T4/T5 cells are the main neural pathway providing visual feedback information to the fly brain (Fig. 3.11). Consistent with previous results, silencing of T4/T5 (see Section 3.6.2 and Fig. 3.11 for silencer expression pattern) in natural conditions does not significantly affect the relationship between drift direction and PDS either in darkness or in visual conditions

(Fig. 4.9A). On the other hand, in reverse gain, the reversal of the relationship between drift direction and PDS bias observed in control flies does not occur in T4/T5 silenced flies (Fig. 4.9B). Our results suggest that, while T4/T5 activity is not necessary for drift-saccade modulation, it may still be involved in the visual monitoring of drift.

4.5.2 Role of LPTCs for drift-saccade modulation

T4/T5 postsynaptic cells integrate self-motion information from both visual and idiothetic sources, and project into steering control centers of the brain (Chapter 5, Fujiwara et al., 2017). These properties make them a promising starting point to investigate the possible neural basis for multimodal integration of drift information. Silencing of HS and VS cells (see Section 3.6.4 and Fig. 3.12 for silencer expression pattern), two classes of LPTCs postsynaptic to T4/T5 did not affect the relationship between drift direction and body saccade bias (Fig. 4.9C), suggesting that silencing a single class of LPTCs is not sufficient to disrupt the modulation.

T4/T5 connect to multiple LPTCs classes (Hausen, 1987), however current genetic tools do not allow to specifically target multiple LPTCs simultaneously. An imperfect approximation to the removal of all LPTCs can be done using the mutant OmbH31 that specifically targets glial cells in the lobula plate. Under this mutation, even though T4/T5 are still present, LPTCs do not develop (Heisenberg et al., 1978). Mutant flies still explore the arena with a normal fixation-saccade pattern but the relationship between drift direction and saccade bias is completely disrupted even under dark conditions (Fig. 4.9D).

4.5.3 Silencing of interneurons connecting self-motion integration centers (IPS) to premotor areas (LAL) abolishes drift-saccade modulation

Despite the OmbH31 mutation being characterized as very specific (Heisenberg et al., 1978), mutations in the context of testing circuit function are always difficult to interpret. Therefore, in the next set of experiments, we targeted neurons that integrate information across LPTC classes and that could serve as bottlenecks of self-motion information. One of such bottlenecks is the inhibitory interneuron bIPS (Erginkaya, 2022). bIPS receives

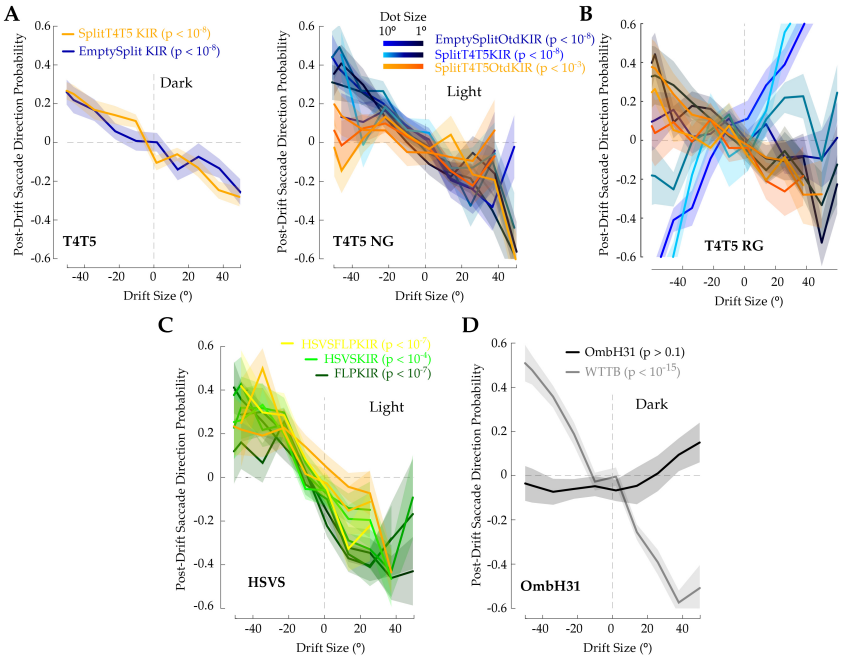

Figure 4.9: **Role of lobula plate neurons to PDS modulation.** (A) Left: bias of PDS versus preceding body drift in darkness for T4T5 silenced (orange) and control flies (blue). Right: bias of PDS versus preceding body drift in different visual conditions for T4T5 silenced (orange) and control flies (blue) under natural gain. (B) Bias of PDS versus preceding body drift in different visual conditions for T4T5 silenced (orange) and control flies (blue) under reverse gain. (C) Bias of PDS versus preceding body drift in different visual conditions for HSVS silenced (yellow) and control flies (green). (D) Bias of post saccades versus preceding body drift in darkness for wild type (gray) and OmbH31 mutants (gray).

inputs from multiple classes of LPTCs and other interneurons in the ipsilateral inferior posterior slope (IPS), and projects to the contralateral IPS where it also connects to multiple LPTCs, interneurons, projection neurons and descending neurons (Fig. 4.10A, C). Together with Mert Erginkaya, who traced and acquired the genetic lines labeling the neuron, and Nélia Varela, who performed some of the behavior experiments, we expressed the heat-sensitive cation channel dTRPA1 to activate this inhibitory neuron and mimic a silencing of all it's postsynaptic partners. Similar to OmbH31 mutants, the activation of bIPS disrupts the relationship between drift direction and body saccade bias (Fig. 4.10C, D). We used two different Gal4 lines for the neural activation with similar effects. Further evidencing the role of

the visuomotor circuit in the IPS for integration of self-motion information to modulate saccadic decisions.

Based on EM-informed circuit mapping, we focused on descending and projection neurons postsynaptic to bIPS. Our first target postsynaptic to bIPS was DNp15, a single neuron per brain hemisphere that is the major descending target of multimodal self-motion inputs from LPTCs, bIPS and other interneurons in the IPS (Erginkaya, 2022; Suver et al., 2016). We silenced DNp15 by expressing the silencing combination w118; Otd-nls:FLPo; pJFRC56-10xUAS>myrtdTomato-SV40>eGFPKir2.1 under the split Gal4 SS0556. Controls included replacing the split Gal4 with an empty split Gal4. Silencing DNp15 did not affect the drift related bias in PDS either in darkness or with visual feedback (Fig. 4.10B). This result suggests that DNp15 is not part of the pathway transmitting self-motion information to modulate the PDS.

Finally, another major simultaneous target of LPTCs and bIPS is the projection neuron PS047 that receives self-motion information from LPTCs, ascending neurons and other interneurons in the PS, and projects into the LAL (Erginkaya, 2022). The silencing of these interneurons disrupts the relationship between drift direction and the bias in PDS (Fig. 4.10E, F), as observed under bIPS activation. This strongly suggests that multimodal self-motion information being integrated in the PS may be passed on to the LAL where it could directly interact with saccade command signals (Schnell et al., 2017), or be passed on to higher action selection centers like the central complex (Hulse et al., 2021).

4.6 Discussion

4.6.1 Self-motion integration for the modulation of motor commands

Animals can detect deviations from their intended paths through external or internal cues. Across species, visual feedback is a particularly important cue for monitoring deviations (Borst, 2014; Warren et al., 2001). However, in more naturalistic locomotor scenarios, vision can become unreliable. Thus, other cues that do not depend so much on external conditions, such as proprioception and vestibular feedback, will play a major role. Indeed, visual flow-sensitive neurons have been shown to combine visual and

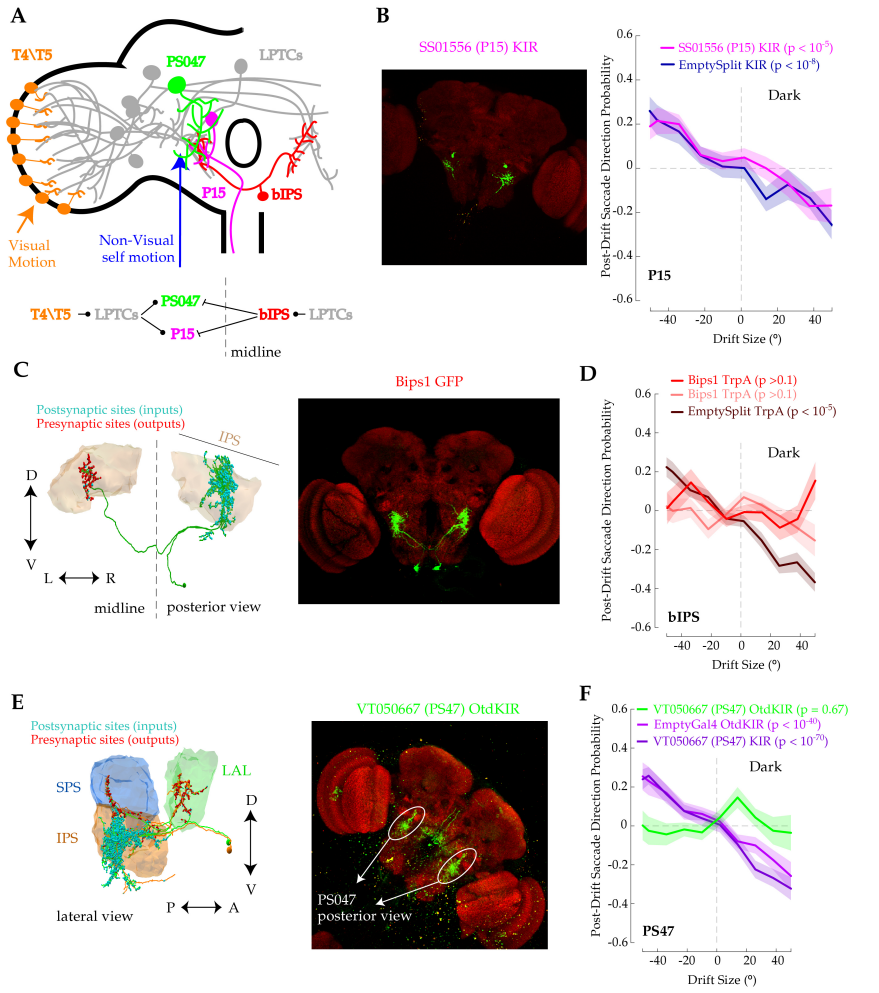

Figure 4.10: **Silencing of IPS neurons abolishes drift-saccade modulation.** (A) Schematic of the location of the tested neurons that could be part of the drift monitoring: T4/T5 (orange), LPTCs (grey), bIPS (red), DNp15 (magenta), PS047 (green). (B) Left: staining of the KIR2.1::EGFP expression under SS01556. Right: bias of PDS versus preceding body drift in darkness for DNp15 silenced (magenta) and control flies (dark blue). (C) Left: posterior view of an EM reconstruction of a right-sided bIPS neuron. Right: staining of EGFP expression under bIPS1 line. (D) Bias of PDS versus preceding body drift in darkness for bIPS expressing the TrpA channel (red) and control flies (dark red) using two different genetic lines labeling the bIPS neurons. (E) Left: lateral view of an EM reconstruction of a right-sided PS047 neuron. Right: staining of the KIR2.1::EGFP expression under VT050667Gal4. (F) Bias of PDS versus preceding body drift in darkness for PS47 silenced (green) and control flies (purple).

vestibular feedback in non-human primates (Bradley et al., 1996; Britten & van Wezel, 1998; Gu et al., 2008). Here, we show that in free walking flies, angular drifts can be detected by both visual and idiothetic cues. While visual feedback becomes of major importance to decreases the amounts of angular drift during forward runs (Chapter 3, Cruz et al., 2021), its role in modulating actions that result from this drift becomes redundant under unperturbed conditions.

A major area in the fly brain that integrates both visual and idiothetic representations of angular deviations is the lobula plate, specifically the LPTCs (Borst & Haag, 2002; Fujiwara et al., 2017). While the properties of self-motion integration in these neurons will be further explored in Chapter 5, here we suggest that LPTCs (or their immediate outputs) are partially responsible for self-motion signals to be integrated for the drift representation (Fig. 4.9). LPTC membrane potential has a faithful representation of instantaneous angular deviations (Chapter 5, Fujiwara et al., 2017; Schnell et al., 2014), suggesting that the drift signal is integrated in downstream circuits.

Here we take advantage of the recent EM tracing and reconstruction tools have been made available for Drosophila (Dorkenwald et al., 2022; Scheffer et al., 2020) to advance our knowledge of the largely unexplored downstream circuits. Using these tools, the organization of IPS circuits that LPTCs project to starts to be unveiled, revealing a highly recurrent connectivity in this brain region (Erginkaya, 2022). One possibility is that this recurrent circuit organization may potentiate the integration of the angular deviation signals before they are casted to other areas. Physiological recordings from identified projection neurons like PS047 will be important to get a clearer picture of the processing happening in this brain area.

Two hypothesis arise for how the modulation of the PDS by the integrated preceding drift can emerge: (1) it can result from a direct interaction between the integrated drift signal and saccade command signals; (2) the drift signal can be passed on into higher action selection centers in the fly brain that would select a new command. PS047s have their axon terminals in the LAL, a brain region that has been previously linked to steering movements and flight saccades (Rayshubskiy, 2020; Ridgel et al., 2007; Schnell et al., 2017). Preliminary activation experiments in LAL interneurons reveal their ability to elicit body saccades in free walking flies. However, the LAL

also receives strong modulation by multiple other premotor areas including the central complex. Further behavior, anatomical and physiological experiments will be necessary to elucidate the mechanisms by which the self-motion drift signals modulate the future actions taken by the fly.

4.7 Acknowledgements

Experiments in this chapter were designed with Eugenia Chiappe. Circuit tracing using EM datasets and generation of split gal4 lines was done by Mert Erginkaya and Nélia Varela with help from Aljoscha Nern. bIPS activation experiment was performed by Mert Erginkaya and Nélia Varela. All immunostainings were performed by Nélia Varela. We thank Wynne Stagnaro, Terufumi Fujiwara, Mert Erginkaya and Corinna Gebehart for valuable input on these experiments, text and analysis. This work was supported by the Champalimaud Foundation and the research infrastructure Congento, LISBOA-01-0145-FEDER-022170, co-financed by Fundação para a Ciência e Tecnologia (Portugal) and Lisboa2020, under the PORTUGAL 2020 Agreement (European Regional Development Fund). This work was also supported by Fundação para a Ciência e Tecnologia FCT PD/BD/105947/2014 (T.C.), by the Marie Curie Career Integration Grant PCIG13-GA-2013-618854 (M.E.Ch), and by the European Research Council Starting Grant ERC-2017-STG-759782 537 (M.E.Ch).

Chapter 5

Neural Multimodal Self-Motion Integration

5.1 Overview

In the previous chapters, we used a new virtual reality system for freely exploring flies to investigate how self-motion information is used to both control gaze stability as the animal runs forward, as well as to modulate future actions of the fly. Key for both behavior effects is the simultaneous integration and interaction between multiple types of self-motion information such as visual, proprioceptive or vestibular. In this chapter, we will use whole-cell patch-clamp recordings from self-motion sensitive cells during tethered locomotion to investigate how multimodal self-motion signals are processed during and to support locomotion. We found that LPTCs in addition to visual self-motion signals also receive non-visual (motor) signals that produce a faithful representation of the fly's rotations. Visual and motor signals form congruent representations that are optimally integrated to robustly encode the fly's rotations and support steering.

5.1.1 Internal representations of locomotor movements

Locomotion generates optic-flow fields (coherent retinal image shifts induced by instantaneous self-motion). The brain could use these signals to monitor movement (Lappe et al., 1999; Pfeffer & Wittlinger, 2016; Warren et al., 2001). However, vision alone is inadequate to accurately estimate locomotion. Retinal image flow can be confounded by changes in gaze as a result of eye or head movements, by moving objects in the visual field, or by the distance of nearby objects in the scene to the moving retina (Schnell et al., 2010). Nonetheless, locomotion also produces other sensory signals and internal copies of motor commands (corollary discharge signals). Thus, the brain could effectively combine vision with other sensorimotor information to estimate self-movement more accurately. Indeed, in some areas of the extrastriate cortex of non-human primates, optic-flow sensitive neurons combine vestibular and eye movement information (Bradley et al., 1996; Koenderink, 1986) supporting the idea that these regions may be involved in processing heading information (Britten & van Wezel, 1998). However, these studies have been carried out under non-walking conditions, which constrain the interpretation of the nature of these neural representations. For example, at present it is not known whether optic-flow sensitive neurons receive explicit information about the locomotion of the animal, which could inform other navigational or motor circuits about the movement of the body through space. Recent work from mice suggests that this might be the case (Keller et al., 2012; Roth et al., 2016; Saleem et al., 2013). However, the role of these visual circuits in locomotion control remains unclear.

5.1.2 Multimodal self-motion integration

Sensory systems are inherently uncertain, either because of the physical nature of the stimulus or noise in the neural circuits that carry the sensory information (Faisal et al., 2008). To curtail such limitations, neural systems integrate across different sources of information to create more robust and stable percepts (Murray & Wallace, 2012). Although multiple studies have been dedicated to characterize the principles of neural multimodal integration under passive conditions (Butler et al., 2010; Gu et al., 2008), it is still unclear how these principles translate to active behavior. Moreover, the link between the multitude of interaction rules and animal behavior remains largely elusive (Stein & Stanford, 2008).

Neurons with convergence of multimodal information have been found across species (Stein & Meredith, 1993). Early research focused largely on a brain area called the superior colliculus (SC), a structure involved in gaze orientation (Sparks, 1986). Specifically, in a population of cells in the SC, visual, auditory and other sensory sources interact to generate multimodal responses that have been described as super-additive, additive or sub-additive depending on the receptive field (Stanford et al., 2005), according to the principle of reverse effectiveness (Meredith & Stein, 1986; Perrault Jr et al., 2003, 2005). Importantly, these findings led to further exploration of the anatomical basis for the multisensory integration as well as its development (Jiang et al., 2001; Wallace et al., 1993; Wallace & Stein, 1997). Regardless, even though some parallels between multimodal activity and behavior have been suggested (Stein et al., 1988), the basic computational rules and their links to the control of locomotion remained unclear.

Multiple behavioral studies have suggested that human and other mammals combine multisensory stimulus in a Bayes-optimal fashion (Ernst & Banks, 2002; Fetsch et al., 2012; Raposo et al., 2012). Within this framework, the integration of multiple signals serves the purpose of minimizing the uncertainty of an estimation given noisy sensory information (Knill & Richards, 1996). Furthermore, these findings were qualitatively linked to the observation of divisive normalization (Ohshiro et al., 2011, 2017). This general network computation found in multiple multimodal areas was proposed to widen the effective range of the integration (Carandini & Heeger, 2012). Nevertheless, questions about the lack of a consistent integration rule across the neural population remain. Additionally, the behavioral relevance of the cells that integrate multimodal integration according to Bayes-optimal rules versus the ones that don't remains unclear. Moreover, the generality of the findings for the animal's general perception outside the passive conditions of the task is still unknown.

Self-motion estimation is crucial for successful navigation and course correction. Such abilities are present throughout the animal kingdom and depend on the ability of animals to continuously track their movement direction and speed (Laurens & Angelaki, 2018). In insects, two major brain areas have been associated with self-motion estimation, the central complex, linked with spatial memory and navigation (Turner-Evans & Jayaraman, 2016), and the lobula plate linked with course correction (Borst & Haag, 2002). The central complex uses multimodal information (vision

and wind and motor and more? Okubo et al., 2020; Seelig and Jayaraman, 2015) to generate internal representations of the animal's orientation in space through a ring attractor network (Kim, Rouault, et al., 2017; Turner-Evans et al., 2020). Here we will focus on the lobula plate tangential cells, which use optic-flow patterns to estimate the fly's egocentric movement through a set of matched filters (Kohn et al., 2018; Krapp & Hengstenberg, 1996). More recently, a population of LPTCs (HS cells) has been found to house multiple non-visual behavior-related modulations (Chiappe et al., 2010; Kim et al., 2015b; Maimon et al., 2010), including a non-visual self movement representation congruent to their visual responses when the fly is walking (this chapter, Fujiwara et al., 2017). While the convergence of visual and non-visual signals in HS cells is more likely additive than subtractive (Fujiwara et al., 2017), the computational and functional purpose of such interaction remains unclear. Moreover, it is not yet known how universal the multimodal interaction within LPTCs is and how it links to the fly's course control.

5.2 Lobula Plate circuit as a multimodal hub of self-motion information

5.2.1 LPTC activity in darkness encodes angular velocity

Previous imaging experiments from LPTCs (HS cells) in walking flies have revealed a strong and quantitative effect of the locomotion of the fly in the visual response of these cells (Chiappe et al., 2010). To test whether HS cells receive more detailed information about the fly's locomotion we needed to record their activity with a better temporal resolution. To this end, Terufumi Fujiwara performed whole-cell patch-clamp recordings to examine the relationship between the dynamics of HS cells' activity and the fly's behavior while walking in darkness (Fig. 5.1A, B) for both wild derived and blind flies (Fig. 5.1A, C). In both cases genetic access to HS cells was guaranteed by expressing UAS-2XEGFP under R81G07-Gal4 (Fig. 5.1B). For more detailed methods for this section's electrophysiology experiments consult Fujiwara et al., 2017.

HS cells depolarized every time flies spontaneously walked. In addition, a right-side HS cell was further depolarized when the fly turned to the left, whereas a left-side HS cell was further depolarized when the fly turned

to the right (Fig. 5.1D, E). The same effect was observed in both wild type (DL background) and blind flies (NorpA background), contrary to the possibility that these signals could result from any residual visual input. The apparent non-visual turn direction selectivity matched the HS cell optic-flow response resulting from the fly's turn.

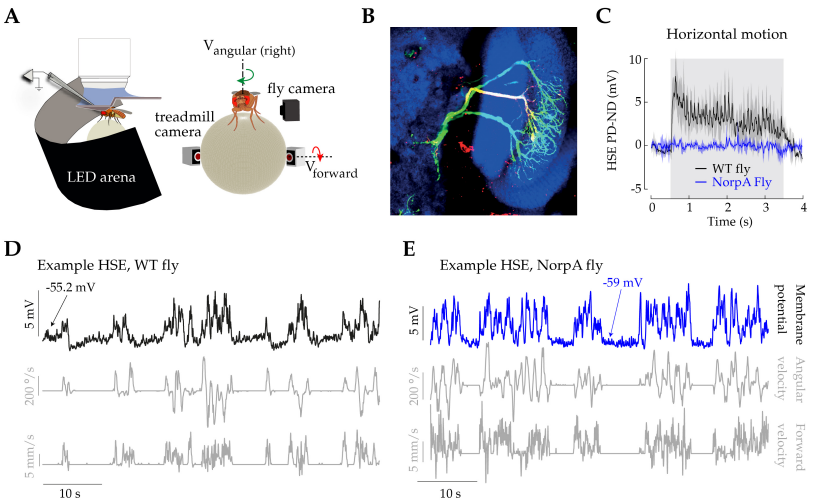

Figure 5.1: **LPTC activity in darkness encodes angular velocity.** (A) Schematics of the experimental set-up (left) and of the behavioral recording system (right). (B) Triple immunostaining for the EGFP signal (green) driven by the R81G07Gal4 line, for the biocytin signal (red) from the recorded HS cell, and for the bruchpilot protein (brp, blue), staining for synaptic neuropil. The dash line delineates the border of the lobula plate. (C) Direction-selective (DS) responses to a wide-field horizontal moving grating (gray shade) for a WT HSE (black) and a blind fly HSE (blue). (D) Example of a 1-min simultaneous recording from a WT fly of the MP of a right-side HSE cell (top trace) and the fly's walking (middle trace, angular velocity; bottom trace, forward velocity). (E) Same for a left-side HSE cell from a blind fly.

5.2.2 Faithful decoding of rotations from HS activity in darkness

In addition to the rotational selectivity, the neural response while walking in darkness reveals a general depolarization independent on the rotation of the fly (behavior state) and a small depolarization dependent on the forward movement of the fly (Fujiwara et al., 2022). We built a simple model to describe how HS cells integrate the three different motor-related signals. We used three assumptions to fit the data to a linear model that used a

weighted sum to combine the motor-related inputs: the motor-related signals originate from independent sources; HS cells linearly transform their input signals into output changes in MP (Haag & Borst, 1998); and the behavioral-state signal can be represented by a binary ON/OFF function.

The linear model was obtained by summing the convolved time series of the behavioral components p_j with the linear filters ψ_j of length L_ψ:

$$MP_{pred}(t) = \sum_j \sum_{t-\frac{L_\psi}{2}}^{t+\frac{L_\psi}{2}} p_j(\tau)\psi_j\left(\tau - \left(t - \frac{L_\psi}{2}\right)\right)$$

Or in matrix form: $MP_{pred} = P\Psi$. To reduce the amount of variables to fit, we used principal component decomposition in the behavior matrix P, choosing only the first components accounting for 99% of all variability. We used the reduced behavior matrix P_{PC} to obtain the reduced filters Ψ_{PC} by minimizing the square error using the software package CVX.

$$R_{err} = \|P_{PC}\Psi_{PC} - MP\|$$

Finally, the reduced filters were projected from the PC space back to the time series space.

We used 75% of the data to create the linear filters for each cell. For the prediction, a set of universal linear filters was obtained by linearly weighting (based on the amount of the walking) the filters of individual HS cells. By convolving these filters with the remaining 25% of the data set, we predicted the corresponding MP trace for each cell. The model performance was quantified by cross-correlating the observed and the predicted MP in temporally matched versus temporally unmatched behavior-MP pairs.

The obtained angular linear filters had opposite signs for left- and right-side cells (Fig. 5.2A), as expected from the proposed direction selectivity (Fig. 5.1D, E). The behavioral-state component filter had a positive peak that was close to a zero-time lag and displayed longer tails relative to the forward velocity filter (Fig. 5.2A). Using these filters, we can predicted the dynamics of the MP of HS cells (Fig. 5.2B). The angular and forward velocity shifted the MP along the corresponding axes of the 2D-tuning map in a speed-sensitive manner (Fig. 5.2C). The behavioral-state component contributed as expected from the design of this input vector (Fig. 5.2C). The combined predicted 2D-tuning map was very similar to the measured one (Fig. 5.2D), except for backward walking. A comparison between a

three-component versus a two-component model (without a forward velocity term) revealed that the performance of the former was marginally superior to that of the latter (Fig. 5.2E). Typically, the three-component model outperformed the two-component model in walking segments with small angular deviations (Fig. 5.2B). These results, together with the very good performance of the three-component model, suggest that HS cells are sensitive to non-visual representations of both the angular and forward components of walking.

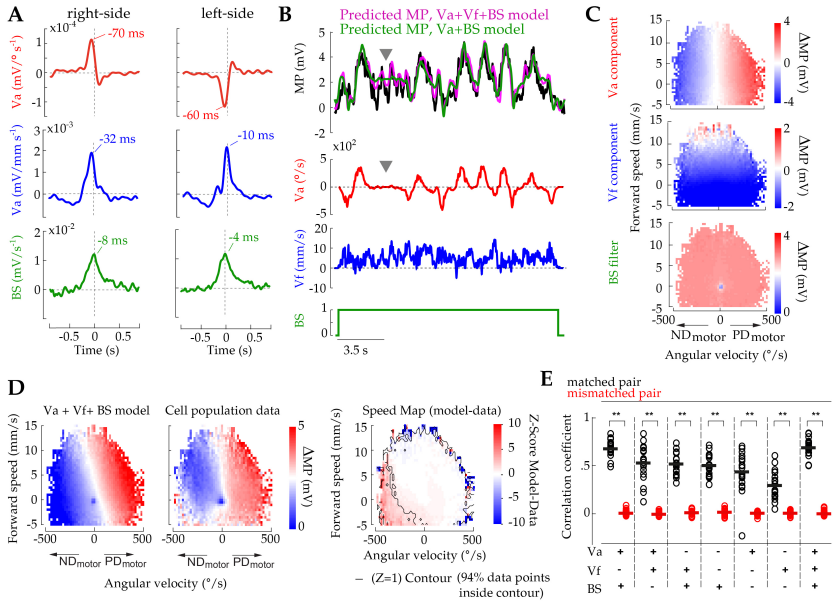

Figure 5.2: **HS activity in darkness is largely explained by a 3-component linear model.** (A) Linear filters for angular (Va, red) and forward velocities (Vf, blue) and the behavioral state (BS, green). (B) Top: the observed (black) and predicted *MP* for an example cell obtained with a 3-component model (Va + Vf + BS, magenta) and for a two-component model (Va + BS, green). Bottom three rows: the corresponding behavioral inputs. Arrowheads highlight a segment with low angular velocity. (C) Predicted velocity 2D-tuning maps for different single-components. (D) Left: 2D-tuning predicted from the three-component model. Middle: observed 2D-tuning from the population of recordings (N = 19 cells). Right: The difference between the predicted and the observed 2D-tuning maps z-scored. 94% of the data points lie within the Z = 1 contour, indicating the high similarity between the velocity maps. (E) Mean cross-correlation coefficients per cell between observed and predicted *MP* for different models (black, matched pairs; red, mismatched pairs; lines: mean values, **: P<0.001, Z>3.78, N=19 cells, Wilcoxon signed-rank test).

To further test this idea, we wondered whether an observer could decode

the walking behavior of the fly from the bilateral activity of the population of HS cells. We used recordings for one side and predictions for the opposite-side *MP* using the 3-component model and the fly's behavior (Fig. 5.3A) to construct population activity maps (Fig. 5.3B). We found that the angular and forward velocities of the fly mapped along the differential (horizontal axis) or common bilateral activity of HS cells (vertical axis), respectively (Fig. 5.3B). We implemented a linear model (same procedure as described above) using bilateral or unilateral HS *MP* to predict the angular and forward velocities of the fly. The decoder using bilateral activity was able to reliably predict the fly's walking velocity, (Fig. 5.3C, E) and its performance was superior to that of a decoder using unilateral activity (Fig. 5.3E). Moreover, the decoding of angular velocity was much more accurate than that of forward velocity. Thus, the bilateral population dynamics of HS cells represent faithful, quantitative information about the rotations of the walking fly in the dark.

5.2.3 Matching of visual and non-visual direction selectivity in LPTCs

We previously found that non-visual self-motion representations exist in the yaw-sensitive HS cells, but not in the roll/pitch sensitive VS cells (Fig. 5.1; Fujiwara et al., 2017). To investigate how pervasive are the non-visual self-motion representations within different classes of yaw-sensitive LPTCs, we performed whole-cell patch-clamp recordings from multiple LPTC classes while animals walked in an air-suspended ball in darkness (Fig. 5.1). Various yaw-sensitive LPTCs have previously been described in different fly species (Hausen, 1987). Many of such LPTCs form a compact network that processes yaw-optic flow (Fig. 5.4A, B, Erginkaya, 2022) and whose main members include HS, H2, CH, H1 and FD-like neurons (including H3 and H4) (Egelhaaf, 1985). Recordings from all the aforementioned cell classes revealed direction selective non-visual self-motion signals congruent to their visual motion responses (Fig. 5.4C). These non-visual signals are further present in DNp15, a descending neuron that receives input from multiple LPTC classes and sends it to the VNC (Erginkaya, 2022; Suver et al., 2016) (Fig. 5.4A, C).

The universality of these apparently redundant visual and non-visual representations within yaw-sensitive LPTCs raises the question of what is

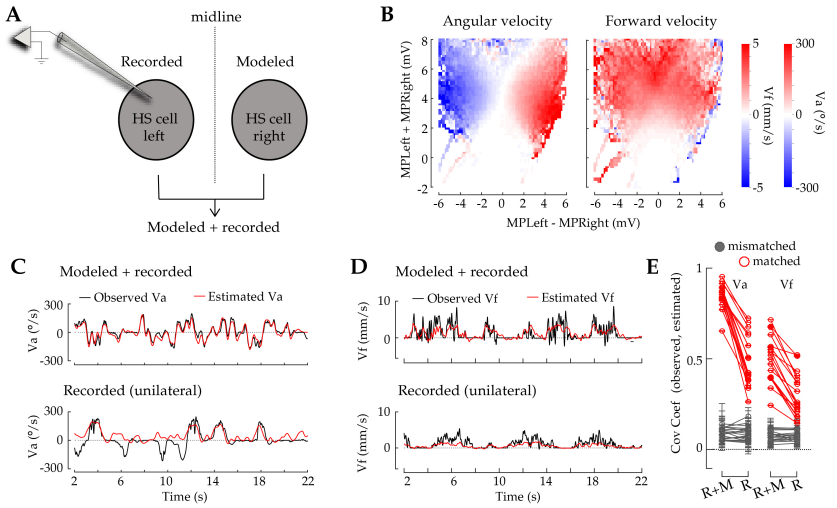

Figure 5.3: **Faithful decoding of rotations from HS activity in darkness.**(A) Recordings from HS cells on one side of the brain combined with predicted HS dynamics of the other right side using the walking behavior of the fly as input for the BS+Va+Vf model. (B) The mean angular (left) or forward (right) velocities of the fly were plotted as a function of the negative ($MP_{left} - MP_{right}$) or positive ($MP_{left} + MP_{right}$) combination of the bilateral dynamics of modeled and recorded cells. (C) Time series of real (black) and estimated angular velocity (red). Top: a linear filter estimation using bilateral modeled + recorded dynamics. Bottom: a linear filter estimation using unilateral recorded dynamics. (D) Same, but estimating forward velocity. (E) Covariance coefficients between the predicted and observed velocities using bilateral or unilateral HS cells' dynamics.

their computational purpose.

5.3 A Bayesian approach for multimodal integration

The Bayesian theory of multimodal integration was first suggested for behavioral and psychophysical studies in human and other mammals (Ernst & Banks, 2002; Fetsch et al., 2012; Raposo et al., 2012). Within this framework, the integration multiple redundant sensory signals serves the purpose of minimizing the uncertainty of an estimation given noisy sensory information (Knill & Richards, 1996).

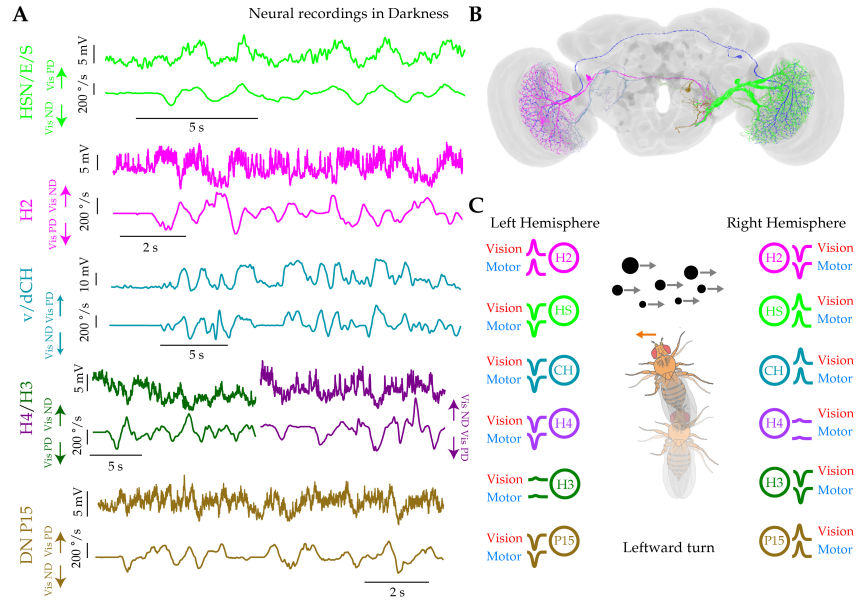

Figure 5.4: **Matching of visual and non-visual direction selectivity in yaw-sensitive LPTCs** (A) Example time series of membrane potential of different classes of LPTCs (represented by the different colors) and angular velocity during walking. Arrows represent the predicted visual response of the example cell to body rotations in a specific direction. (B) Anatomical reconstruction of the LPTC classes recorded in (A). (C) Schematic depiction of the visual and motor responses of different classes of LPTCs (colors) to a leftward turn of the fly. The rule of congruent visual and motor representations is kept for all recorded yaw-sensitive cells.

5.3.1 Maximizing the reliability of self-motion estimation

Underlying the theory of Bayesian multimodal integration is the concept that noise makes estimations probabilistic. A useful approximation is that every estimation is a sample from a Gaussian likelihood distribution with mean $\hat{S}$ and variance σ^2 (Fig. 5.5A, B).

Estimations based on independent modalities have their own Gaussian likelihood distributions. In the specific case of congruent estimations, these distributions will be centered around the same expected value (Fig. 5.5A). The Bayesian framework gives us the rules to optimally integrate the two noisy modalities and generate a more reliable multimodal estimate:

- The variance of multimodal estimates is a combination of the variance of unimodal estimates that follows the equation in (Fig. 5.5A)

- The average multimodal estimate is a linear combination or the average unimodal estimates, where the linear weights vary according to their relative variance according to the equations in (Fig. 5.5B)

In the following sections, we will be testing these predictions and consequent applicability of the Bayesian framework to explain the purpose of multimodal interactions in LPTCs.

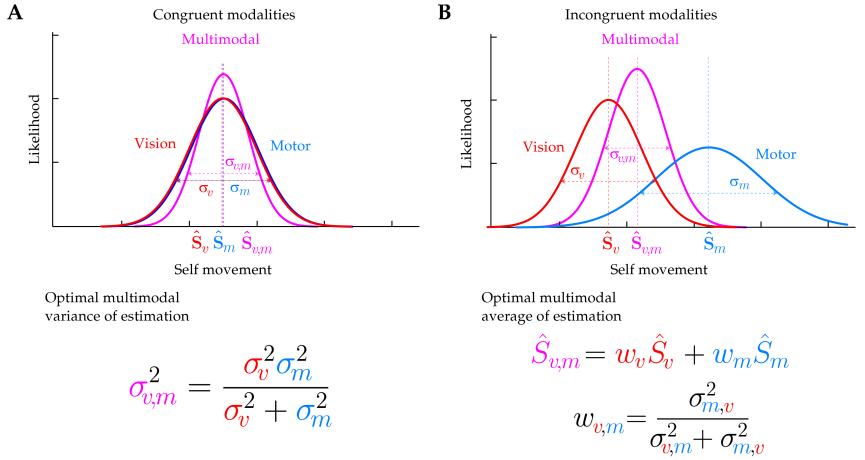

$$\sigma_{v,m}^2 = \frac{\sigma_v^2 \sigma_m^2}{\sigma_v^2 + \sigma_m^2}$$

$$\hat{S}_{v,m} = w_v \hat{S}_v + w_m \hat{S}_m$$

$$w_{v,m} = \frac{\sigma_{m,v}^2}{\sigma_{v,m}^2 + \sigma_{m,v}^2}$$

Figure 5.5: **Bayesian approach for multimodal integration.** (A) Top: red and blue curves are schematic representations of the probability distributions of independent and congruent noisy estimations of self-motion. The magenta curve represents probability distribution of the predicted optimal multimodal estimation. Bottom: equation describing the optimal multimodal variance of estimation as a function of the unimodal variances of estimation. (B) Top: same as (A) but for a non-congruent situation. Bottom: equation describing the optimal multimodal estimate as a function of the unimodal estimations. The linear weights depend on the relative reliability of unimodal cues.

5.3.2 A VR setup to study neural multimodal self-motion integration in walking Drosophila

In order to test whether the multimodal integration in LPTCs is compatible with a Bayesian integration, we first required a comprehensive set of unimodal and bimodal LPTC responses as flies spontaneously walked. We performed whole-cell patch-clamp recordings from H2 neurons (Fig. 5.6A). We genetically targeted H2 by expressing 20xUAS6xGFP using the split

combination R23C12AD; R32A11DBD under the wild type background WTDL. H2 is a single spiking neuron in each hemisphere, central to the yaw-sensitive LPTC network, known to respond to back-to-front visual rotations (Farrow et al., 2006). The recordings were performed while the fly spontaneously walked on an air-suspended ball (Fujiwara et al., 2017; Seelig et al., 2010). The rotations of the fly are measured by tracking the rotations of the ball, and this information could be transformed into movement of the visual environment projected in the floor screen. During half of the trials, the rotations of the visual environment were coupled to the fly's rotations - closed loop configuration - making the recorded H2 activity based on both visual and motor signals (Fig. 5.6A). During the other half of the trials, the rotations of the visual environment were decoupled from the fly's rotations - replay configuration - making H2 activity to be driven by either only visual signals, only motor signals or incongruent visual and motor signals (Fig. 5.6A).

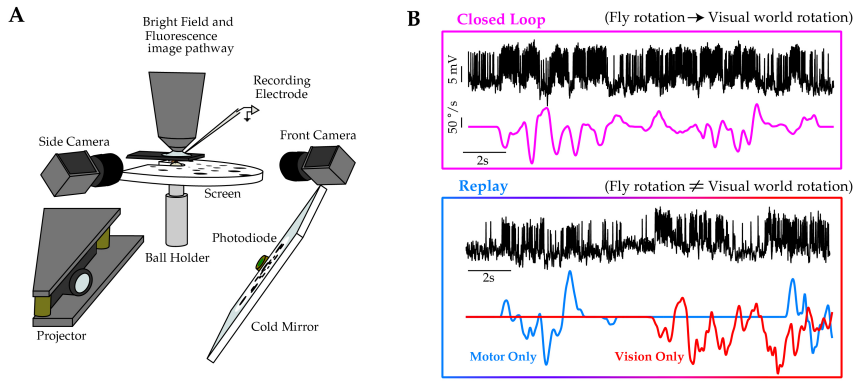

Figure 5.6: **A VR setup to study neural multimodal self-motion integration in walking Drosophila.** (A) Schematic of the developed virtual reality system that allows for whole cell patch clamp recordings while flies walk in an air suspended ball. Ball rotation can control a virtual reality environment projected ventrally to the fly. (B) Top: example time series of H2 membrane potential and fly angular velocity under closed loop (fly rotation controlling the visual world rotation). Bottom: same under replay conditions (fly rotation decoupled from replaying visual world rotations). In replay conditions we can identify moments when only visual or only motor signals are influencing H2 activity.

Briefly, flies were dissected fly and mounted under the microscope and positioned on an air-suspended ball (Seelig et al., 2010). In vivo, whole-cell patch-clamp recordings were performed using an upright microscope

(Rosenegger et al., 2014) with a 40× water-immersion objective lens (CFI Apo 40XW NIR, Nikon). The brain was perfused in external saline containing 103 mM $NaCl$, 3 mM KCl, 5 mM TES, 8 mM $trehalose$, 10 mM $glucose$, 26 mM $NaHCO_3$, 1 mM NaH_2PO_4, 4 mM $MgCl_2$ and 1.5 mM $CaCl_2$ (pH 7.3 when equilibrated with 95% O_2/ 5% CO_2; 275 mOsm). Patch pipettes (3–7 $M\Omega$) were filled with internal solution containing 125 mM aspartic acid, 10 mM $HEPES$, 1 mM $EGTA$, 1 mM KCl, 4 mM $MgATP$, 0.5 mM Na_3GTP, and 13 mM biocytin hydrazide (Life Technologies, B1603) (pH 7.3, final osmolarity: 260–265 mOsm). The neural lamella was ruptured by local application of collagenase IV (Worthington) (Maimon et al., 2010). Experiments were performed at 24 C. Current-clamp data was filtered at 4 kHz, digitized at 10 kHz using a MultiClamp 700B amplifier (Molecular Devices), and acquired with the FlyVRena software.

5.4 Optimal multimodal integration in H2

5.4.1 Visual and non-visual signals arrive to H2 through independent channels

An important and often neglected requirement for Bayesian integration is the independence between the unimodal channels. We reasoned that if visual and motor signals arrive at H2 through independent channels, we may be able to independently target the visual or the motor pathway by silencing different sets of inputs to H2. The major source of visual information to H2 are the T4/T5 cells (Fig. 5.7A). As seen before, T4/T5 cells are columnar neurons known to be the first motion-sensitive and direction selective neurons in the fly optic lobe. We expressed 10xUAS-Kir2.1::EGFP under the split combination R59E08AD; R42F06DBD combined with the recombinant R32A11-lexA,8xLexAop-GFP to simultaneous maintain genetic access to H2 cells and silence T4/T5 cells. Control flies used an empty split line instead of T4/T5 split combination. Silencing T4/T5 while recording from H2 shows a complete disruption of the neuron visual sensitivity, while keeping intact the motor sensitivity (Fig. 5.7C).

H2 cells also receive input from CH cells. CH are inhibitory cells with dendrites in the central brain and axon terminals in the lobula plate. To test the functional connection between CH and H2, we used the previous recombinant to target H2 while we performed optogenetic activation of CH

cells expressing the light gated cation channel CsChrimson under the split combination R35A10AD; VT026000DBD. We observed a large hyperpolarization in the ipsilateral H2 upon CH activation (Fig. 5.7B). Moreover, while silencing CH using 10xUAS-Kir2.1::EGFP and the previous split combination did not disturb H2 visual sensitivity, it largely reduced the inhibitory phase of H2 motor responses (Fig. 5.7C). These experiments strongly suggest that the visual and motor signals in H2 arrive from independent neural pathways, supporting the possibility of a Bayesian integration of the two signals.

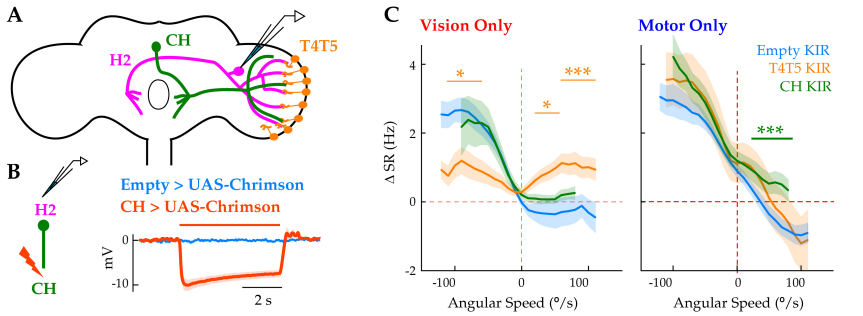

Figure 5.7: **Visual and non-visual signals arrive to H2 through independent channels.** (A) Schematic depicting the anatomical location of H2 and two of its inputs (T4/T5 and CH). (B) H2 membrane potential when CH is optogenetically activated (orange) or in control conditions (blue) reveal the inhibitory interaction between these cells. (C) Left: baseline subtracted spike rate of H2 cells as a function of visual angular speed while the fly is stationary in control (blue), T4/T5 silenced (orange) and CH silencing (green). Right: baseline subtracted spike rate of H2 cells as a function of the angular speed of the fly while the visual environment is stationary in control (blue), T4/T5 silenced (orange) and CH silencing (green).

5.4.2 Reliability of self-motion estimation under unimodal and bimodal conditions

In a Bayesian integration, the reliability (inverse of the variance) of a multimodal estimation is equal to the sum of the reliabilities of the estimations based on the individual modalities. We affected the reliability of the visual signals in H2 cells by repeating the close-loop and replay conditions under 3 different visual environments (Fig. 5.8A). All visual environments are composed of random dots with constant angular size from the fly's perspective. The visual environment with 1° dots is composed of objects much

smaller than the fly eye resolution, and expected to have minimal impact in H2 visual responses. On the other hand, the 5° and 15° dot environments should be perceived by the fly with different strengths and impacts in H2 activity.

To obtain a measurement of the reliability of self-motion discrimination we resorted to an ideal observer analysis from signal detection theory (Britten et al., 1996; Gu et al., 2008). We quantify the ability of an ideal observer to discriminate the fly's rotations based only on the H2 activity. At first, we binned the fly's rotations with bin sizes of 20°. For each bin of rotation, we compare the ability of the ideal observer to discriminate between a rotation within the bin or outside of the bin based only on the recorded firing rate. We computed discrimination performance as the area under the ROC curve for each bin of rotations and plotted the different performances in a neurometric curve (Fig. 5.8A). We finally obtain a measurement of the neuronal threshold from the standard deviation of the cumulative Gaussian fit of the neurometric curve.

$$N(Va) = \int_{-\text{inf}}^{Va} \frac{1}{\sqrt{2\pi}T^2} e^{-\frac{(x-\mu)^2}{2T^2}} dx$$

The neuronal threshold is linearly proportional to the standard deviation of the discrimination noise of the ideal observer looking at H2 activity (Gu et al., 2007; Merfeld, 2011), making it a good proxy to test how the variance of multimodal estimation relates to the variance of the unimodal ones.

5.4.3 Multimodal integration in H2 follows the variance principle from optimal integration.

In multimodal conditions, neuronal thresholds decrease as the strength of the visual environment increases, denotative of an improvement in the reliability of the estimation (Fig. 5.8A, inset). We next investigated how the improvement in reliability relates to the predicted improvement from the Bayesian framework. We repeated the ideal observer analysis in the visual only and motor only conditions to extract the neurometric threshold in the two unimodal conditions (Fig. 5.8A). Finally, we plotted the predicted Bayes-optimal multimodal threshold (Fig. 5.8B) as a function of the measured multimodal threshold for all flies and conditions. We observe our data clusters around the unit line (Fig. 5.8C), with a very good average match between the Bayes-optimal prediction and the measured values (Fig. 5.8C).

This result strongly suggests H2 is optimally integrating noisy visual and motor signals for a more reliable estimation of the fly's rotation. This role for the purpose of the multimodal signals still leaves the open question of how the neuron accomplishes the optimal integration.

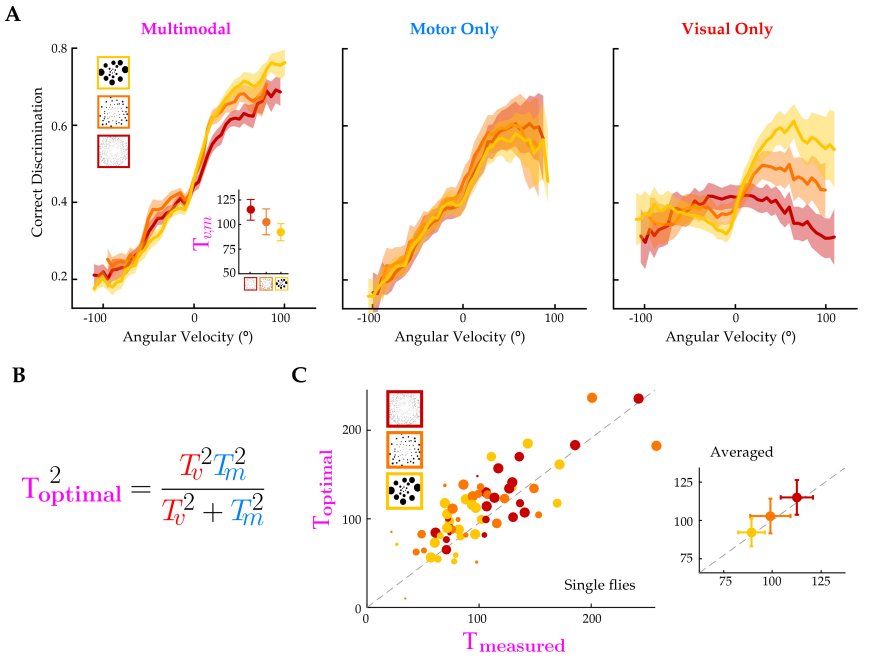

Figure 5.8: **Multimodal integration in H2 follows the variance principle from optimal integration.** (A) Neurometric curves depicting the ability of an ideal observer performing correct discrimination as a function of angular velocity. Colors represent different visual environments. Left: neurometric curves in closed loop conditions (inset correspond to the fitted neurometric threshold across visual environment). Middle: neurometric curves in motor only conditions. Right: neurometric curves in visual only conditions. (B) Relationship between the optimal multimodal neuronal threshold as a function of the measured unimodal neuronal thresholds. This relationship is derived from (Fig. 5.5A). (C) Left: optimal predicted multimodal neuronal threshold as a function of measured multimodal neuronal threshold. Each dot correspond to a single recording color coded by the visual environment and with radius proportional to its duration. Right: average optimal predicted multimodal neuronal threshold as a function of measured multimodal neuronal threshold for different visual environments.

5.4.4 Multimodal integration in H2 depends on the relative strength of its unimodal inputs.

Another prediction of the Bayesian framework is that the average unimodal estimates are linearly integrated. Moreover, the perceptual weights should depend on the relative reliability of the unimodal estimates (Fig. 5.5B). It is important to be mindful that the Bayesian theory defines the relationship between perceptual weights, which are not the same as the neural weights (Fetsch et al., 2013). The perceptual weights depend on the readout of the multimodal integration and are usually obtained through psychophysics (Landy et al., 2011). On the other hand, the neural weights are measured directly from the activity of the cells. The actual relationship between both types of weights is still not understood (Fetsch et al., 2013). While theoretical studies suggested that, within a defined set of assumptions, constant neural weights can give rise to optimal integration after population readout (Ma et al., 2006), further experimental work in the macaque MSTd has shown that neural weights are not constant and depend on cue reliability (Morgan et al., 2008). Here we attempt to obtain the neural weights and test their dependency on the visual reliability by manipulating the visual environment.

Our dataset of H2 recordings imposes a challenge in the extraction of the neural weights. The congruent interaction between visual and motor signals in natural conditions also means that all signals are attempting to execute the same estimate (Fig. 5.9A), making this condition suboptimal to fit the neural weights. For this reason we added a reverse gain condition to the experimental protocol (Fig. 3.3), in which visual and motor signals execute symmetrical estimations. The effect of reversing the gain is visible at the level of the neural tuning curves for angular speed. For more reliable visual environments the visual responses become symmetric and the shape of the multimodal tuning curve changes completely (Fig. 5.9B). We used both natural and reverse gain tuning curves to fit the neural weights (Fig. 5.9C).

Different scenarios could happen for how the neural weights might depend on the visual environment: (1) The weights could be constant and equal to 1 as suggested from Ma et al., 2006; (2) the visual weight can increase with the reliability of visual environment while the motor weight remains unchanged (signals not weighted in relative terms, Fig. 5.9D, left); (3)

as the visual weight increases the motor weight decreases (signals weighted in relative terms, Fig. 5.9D, Right). Our data is most compatible with the last possibility, where the signals are weighted in respect to their relative strength (Fig. 5.9E).

As previously stated, the relationship between the neural weights and the perceptual ones is still unclear and will depend on the readout of the neuron. Our analysis suggests that the unimodal weights in H2 are already modulated in accordance to what could be expected from an optimal integration. The neural mechanisms by which the weights are modulated and whether this modulation affects the ability of the neuron to optimally improve the reliability of estimation is still under active investigation.

5.4.5 Divisive normalization in H2 activity

The measured unimodal weights under 5 and 15 visual conditions are smaller than unit, revealing a sublinear integration of information in H2 (Fig. 5.9E). Mechanistically, a sublinear integration can arise from either single neuron properties like signal saturation of from network properties like divisive normalization.

A distinction between the two possibilities can be found in conditions where the two signals are not congruent, like the events in the Replay trials when both visual and motor signals are simultaneously present (Fig. 5.10A). In the case of saturation, simultaneously having a unimodal signal in its preferred direction and the other in its non-preferred (but excitatory) direction can never result in a combined signal smaller than the initial preferred direction unimodal signal (Fig. 5.10B, left). In the case of a divisive normalization then a combined signal smaller than the first preferred direction unimodal signal can still occur (Fig. 5.10B, right). Using only Replay trials, we binned visual, motor and multimodal responses based on the angular speed of the fly. For bins in the preferred motor direction, a simultaneous visual preferred direction creates a small further depolarization of the cell. Importantly, a simultaneous visual null direction reduces the response to a lower spike rate than the largest unimodal response, a trademark of a divisive normalization (Fig. 5.9C). We further quantified this phenomena by calculating a normalization index (Fig. 5.10D, left). As expected, the normalization index depends on the strength of the visual response (Fig. 5.10D, right).

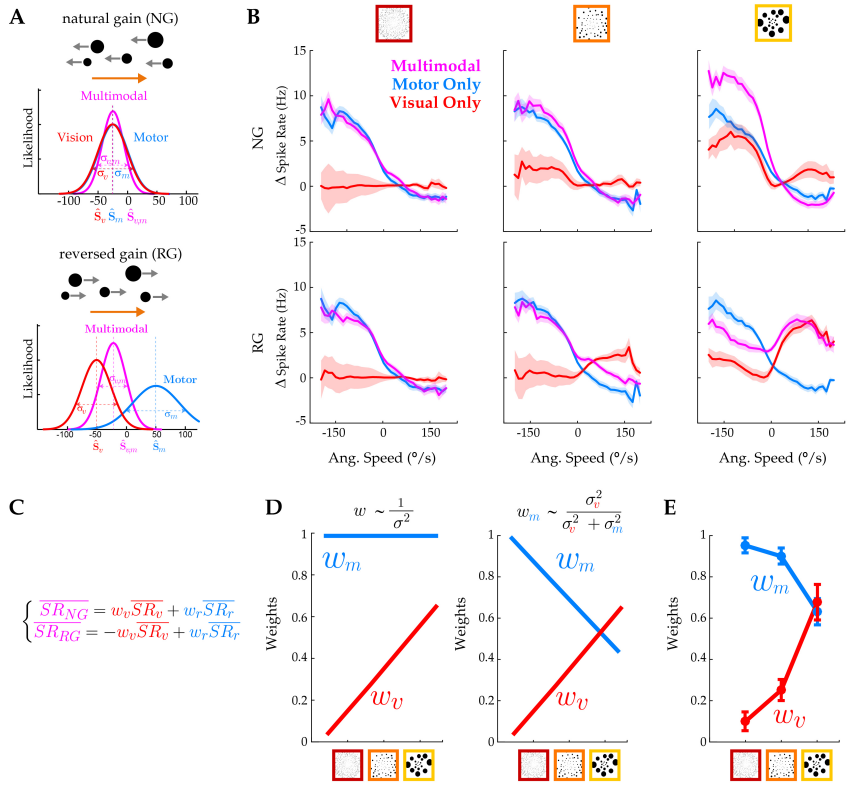

Figure 5.9: **Multimodal integration in H2 depends on the relative strength of its unimodal inputs.** (A) Schematic representations of the congruent multimodal estimation under natural gain (top) and the non-congruent multimodal estimation under reverse gain (bottom). (B) Baseline subtracted spike rate as a function of angular speed for under closed loop (magenta), motor only (blue) and visual only (red). Columns correspond to different visual environments. Top row, closed loop and visual only signals obtained under natural gain. Bottom row, closed loop and visual only signals obtained under reverse gain. (C) Equations for the linear fit to extract the neural weights based on the average spike rates in natural and reverse gain conditions. (D) Left, expected variation of weights as function of visual environment if weights depend only on the properties of their respective signal. Right, same for the case in which weights depend on relative value of the signals. (E) Measured weights based on the equations in (C).

Divisive normalization has been hypothesized to depend on the activity of inhibitory interneurons that integrate information from the multiple elements of the network. We identified a large network of inhibitory neurons that integrate information across different LPTCs and other cells and connect extensively to H2 either at the axonal or dendritic level (Fig. 5.9E). Future work will test the role of these inhibitory neurons in shaping the normalization and their role in composing the optimal integration in H2.

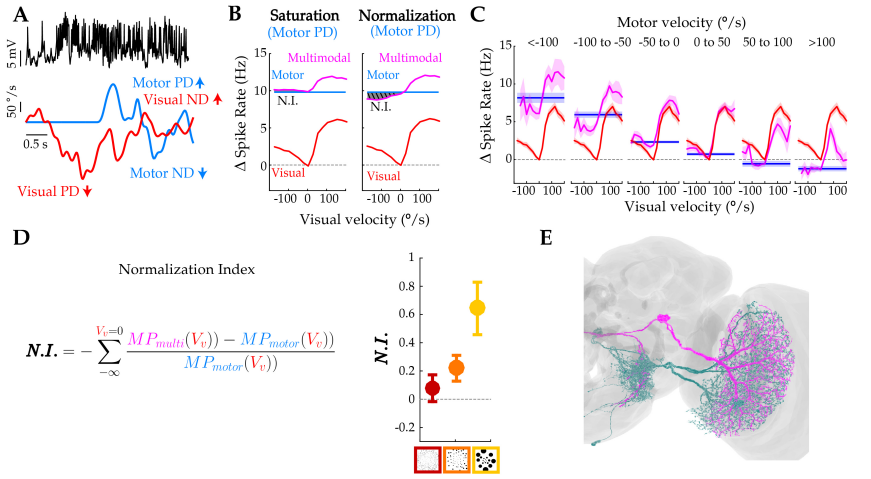

Figure 5.10: **Divisive normalization in H2 activity.** (A) Example time series of H2 membrane potential and fly angular velocity under replay conditions. (B) Schematic prediction of the multimodal activity based on a saturation or a normalization scenario. Note that for stable motor PD, the major difference between the two is the combination of motor PD and visual ND. (C) Baseline subtracted spike rate in motor only (blue), visual only (red) and replay multimodal (magenta) conditions binned according to the angular velocity of the fly. For each bin the baseline subtracted spike rate was plotted as a function of the visual velocity. (D) Definition of normalization index and how it depends on visual environment. (E) Anatomical reconstruction in FlyWire of the putative inhibitory interneurons connected to H2.

5.5 Optimal multimodal integration can support the performance of straight walking.

To link the rules for multimodal self-motion estimation measured in LPTCs with the previously observed straightness performance of free walking flies, we built a model agent to test whether a simple control system

could explain the fly's behavior during forward segments.

A rigid-body agent alternates between immobility and activity when it has sequences of forward runs and saccades (Fig. 5.11A, C). Similar to real flies, the agent explores a simulated 90mm circular arena with hot walls. The distribution of the length of activity bouts is similar to the real flies' distribution (Fig. 5.11C). Saccades are modeled as highly stereotyped rapid events in the angular velocity of the agent (Fig. 2.3). The probability and amplitude of a saccade depends on the distance to the arena wall as for real flies. The time intervals within an activity bout without saccades are considered forward segments (Fig. 2.3). Forward segments have constant translational speed of 20mm/s. In addition, the model contains $1/f$ noise during forward runs representing both internal and external sources (Dickinson et al., 2000; Franklin & Wolpert, 2011). In the full version of the model, there are two rotational control loops (Fig. 5.11B). The first one based on a copy of the angular velocity of the agent (motor feedback), which was filtered by a temporal kernel (Fujiwara et al., 2017). The second rotational controller is based on visual-flow. Four channels containing arrays of a "two-quadrant"type Hassenstein-Reichardt (HR) correlator are used to detect self-generated visual motion cues (Eichner et al., 2011). Importantly, to comply to the Bayesian rules of multimodal integration, the estimates from each rotational control loop are sampled from a noisy distribution with variance σ^2. The relative values of σ define the weights of each of the control loops and have to be found through fitting the real free walking data.

To find the model that most approximated the behavioral data, we started by simulating data in the dark using various noise levels and motor weights. We found that for the set of models that best approximated the behavior of real flies, the relation between motor weight and noise level was linear (Fig. 5.11D), thereby reducing the amount of free parameters for the second set of simulations. We then simulated the agent with various levels of visual weight and noise level under different visual environments (Fig. 5.11D) in the reverse gain condition. For each model, the distance between the simulated and the measured straightness was calculated for all visual environments. The model with the smallest distance to the data was selected as the best fitted model.

Our agent model reproduced the paths and velocities of real flies in

both natural or under visual perturbation conditions without further modifications (Fig. 5.11E). Moreover, our model can quantitatively predict the straightness performance of real flies in the natural situation (Fig. 5.11F). Altogether, our data shows that a simple control agent optimally integrating a visual and a non-visual estimation or the angular deviations could largely explain the behavior of the fly, and suggests that multimodal interactions in such a simple control system can increase course control robustness.

5.6 Discussion

5.6.1 Neural basis of multimodal signals

Previous studies have found that LPTCs receive locomotor-related signals that amplify their visual responses when flies walk or fly (Chiappe et al., 2010; Maimon et al., 2010), but not when they stand still. The behavior modulation further affected the cell's tuning depending on locomotor state, increasing their response gain to higher image speeds (Chiappe et al., 2010), an effect thought to be mediated by the neuromodulator octopamine (Suver et al., 2012). This type of coarse behavioral state modulation within sensory areas is transversal across species, and it is thought to be important for attention and adaptation of visual processing (Fujiwara & Chiappe, 2017; Maimon, 2011). Here we investigated at very high detail the relationship between the animal locomotion and the activity of optic-flow sensitive neurons. We found for the first time that optic flow-processing neurons receive locomotor-related, non-visual signals that faithfully encode information about the animal's movement through space, even in the absence of visual information (Fujiwara et al., 2017). The non-visual signals were found not only in a single cell type, but throughout the population of LPTCs sensitive to yaw optic-flow. The same type of non-visual signals were not found either when animals were flying (Kim et al., 2015a) or when recording from LPTCs sensitive to other rotational axis, suggesting that they may fulfill a specific role during angular movements in walking (Fujiwara et al., 2017).

While T4/T5 cells have been shown to be the source of visual motion signals (Schnell et al., 2012), the source of the so-called motor signals in LPTCs is still under active investigation. Experiments manipulating known self-motion sensing organs like the antenna or the halteres or removing synaptic

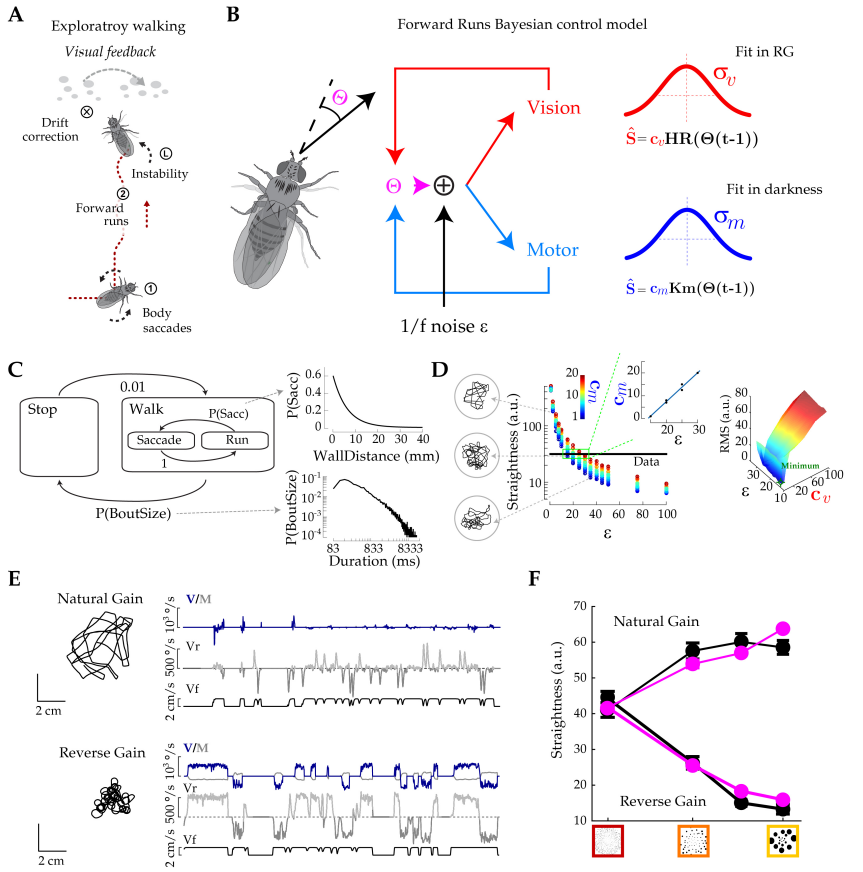

Figure 5.11: **Agent model simulations based on optimal multimodal integration can explain the performance of straight walking.** (A) Schematic of the general behavioral organization of the model agent (saccade-fixation with visuomotor drift correction during forward runs). (B) Schematic of the control loops that estimate angular deviations through either visual or motor signals that are optimally integrated to generate corrections. (C) Schematic of the state flow of the modeled agent, and the associated distributions for activity bout size and for saccades estimated from the real data (inset plots). (D) Fitting of the modeled agent to the behavioral data. Left: simulated straightness under dark conditions, as a function of noise level (NL) and motor weight (MW, color-coded). In the regime where simulations match the flies' straightness, MW linearly correlates with NL (inset). Right: distance (RMS, color-coded) between simulated and real-data straightness as a function of NL and visual weight (VW). (E) Example of simulated paths (left) with corresponding time series of the angular, and forward velocities, and the contribution of the visual and motor components of the controller, under natural (top) or reversed (bottom) gain. Visual environment: 10 random dots. (F) Straightness of real (black) and agent (magenta) flies for natural and reverse Gain, using reverse gain data for calibration.

activity from leg mechanosensory neurons did not disrupt the angular velocity related signals. Moreover, a turn towards the preferred direction of H2 causes an instantaneous depolarization in this cell (Cruz et al., 2019), suggesting that efference copies rather than sensory feedback may play the major role in shaping LPTC motor responses.

Or data further suggests that the interconnectedness of the LPTC network further propagates the motor responses through the network, as exemplified by the null direction in H2 arising from CH activity. We hypothesize that motor signals may arrive into the LPTC network from only a few sets of neurons. These signals are then internally propagated through the network. Exploration of neural connectivity using new electron microscopy datasets (Dorkenwald et al., 2022; Scheffer et al., 2020) reveals that the IPS is a target of multiple cell classes arising from motor centers like the LAL or the VNC (Erginkaya, 2022). Future work will investigate which motor channels may provide the motor signals into the LPTC network.

5.6.2 Normative, phenomenological and mechanistic approaches for neural computation

The most common approach to make sense of the computations in single neurons or neural populations is to describe how their activity relates to external events. This phenomenological approach can vary from qualitative to quite sophisticated quantification and tackles the important question of what the phenomena is. Here we extensively used this approach to describe the non-visual activity of LPTCs (Fig. 5.1, 5.2, 5.3, 5.4). This approach can help us understand the general properties of the neural response, but is generally insufficient to explain the purpose of those computations.

In contrast with phenomenological explanations, normative theories try to understand the properties of neural response in terms of a function or goal. Normative theories lay on the assumption that the system is trying to optimize a determined objective under some constraints. The process of optimization then establishes the rules for the optimal neural computations that can then be compared with real data. As with the phenomenological approach, the comparison between theory and data can have different degrees of quantification. The usefulness of normative models lies in this comparison, providing information about how well the system performs a defined function and which constraints it may be subjected to. Here we

also extensively used this approach to test the function of the multimodal integration in LPTCs (Fig. 5.5, 5.6, 5.7, 5.9). This approach can help us understand the purpose and constraints for the neural computation, but is rather insufficient to explain how the real system implements such computation.

The final method to understand neural computation is the mechanistic approach. This approach usually breaks down a system to its component parts and processes in order to understand how their interaction can give rise to a certain computation. Mechanistic models can also range from purely qualitative to heavily quantitative. The usefulness of this approach lies in its ability to make predictions about causal relationships between different components of the same system which could be tested experimentally. A common use of mechanistic approaches in systems neuroscience is to break down a computation as the result of different interacting neural populations. Through recording and manipulation of the component neural populations we gain detailed insight over how they interact to generate the final computations. Here, we briefly used this approach to investigate the neural populations bringing multimodal signals into LPTCs and shaping their multimodal integration (Fig. 5.8, 5.10). This approach can help us understand how biologically the neural computation emerges in the system, but is rather insufficient to properly describe it or to explain its purpose.

All the aforementioned approaches are complementary ways to gain understanding over a neural computation (Levenstein et al., 2020). Moreover, general theories of circuit function may include not only one but multiple of these complementary approaches. A complete theory of the function of a specific circuit must include elements of all three approaches. To merge the different levels of description in the same system is a very difficult task that is not accessible for most systems. For example, many mechanistic theories can require a detailed level of circuit manipulation only available for model organisms, or many normative theories require a deep knowledge about the contexts or intentions of the animals that may be difficult to access in untrained animals. Nevertheless, one of the most important goals of neuroscience is to bridge these levels of understanding, namely the neural mechanisms that underlie computations that govern animal behavior.

Over the last years, one of the most successful systems at utilizing multiple approaches to gain understanding of its function has been the Drosophila central complex. The large amount of existent anatomical information allied

to powerful genetic tools allowed to merge descriptive (Seelig & Jayaraman, 2015), normative (Skaggs et al., 1994), and mechanistic (Hulse et al., 2021) information to understand how the neural circuit operates to create a stable internal heading representation for navigation. It further allowed answer the question of how ring attractor dynamics can be implemented in a biological system (Turner-Evans et al., 2020).

We argue that our system presents an excellent opportunity to understand neural multimodal self-motion integration from multiple approaches. We performed a detailed description of visual and motor signals within the LPTC network and observed a strong match between the properties of H2 multimodal responses and the predictions from a normative Bayesian integration theory. Furthermore, given the anatomical knowledge and genetic tools available in Drosophila, we can manipulate specific neural populations providing different types of input to the system. In the future we will continue to manipulate elements of the circuit to try to understand the mechanisms underlying the optimal multimodal integration.

5.7 Acknowledgements

Experiments in this chapter were designed with Eugenia Chiappe. Terufumi Fujiwara performed all recordings from HS cells and most classes of LPTCs and first described the walking-related signals in HS cells. André Marques performed some of the model agent simulations and is continuously expanding the model agent. Terufumi Fujiwara and Nélia Varela generated the recombinant LexA line and the split CH line. I personally thank Terufumi Fujiwara for introducing me to the world of electrophysiology and whole-cell patch-clamp recordings, for the countless questions and hours of troubleshooting, and mostly for his infinite friendship, patience and wisdom. This work was supported by the Champalimaud Foundation and the research infrastructure Congento, LISBOA-01-0145-FEDER-022170, co-financed by Fundação para a Ciência e Tecnologia (Portugal) and Lisboa2020, under the PORTUGAL 2020 Agreement (European Regional Development Fund). This work was also supported by Fundação para a Ciência e Tecnologia FCT PD/BD/105947/2014 (T.C.), by the Marie Curie Career Integration Grant PCIG13-GA-2013-618854 (M.E.Ch), and by the European Research Council Starting Grant ERC-2017-STG-759782 537 (M.E.Ch).

Chapter 6

Discussion

6.1 Overview

In this thesis, we have investigated the role of self-motion signals in modulating the control of locomotion at multiple levels. We designed and built novel VR tools that allowed for high control over self-motion feedback during free and spontaneous locomotion, as well as high precision monitoring of the animal's behavior. We also identified the coarse structure of locomotion that could be linked to the underlying internal goals of the fly. The behavior patterning revealed moments when flies intended to keep a stable gaze, allowing us to quantify performance under spontaneous behavior. We studied in high detail how self-motion information affected such performance, by balancing the animal's general goal with posture stability requirements. The behavior patterning also includes well defined turning actions (i.e. body saccades) that could be flexibly used under different goals. We found a novel influence of self-motion signals to modulate those actions. Furthermore, we partially identified a new neural pathway that could support this modulation. This neural pathway links the integration of self-motion signals during natural locomotion and action-selection/command centers in the fly brain.

Finally, we gained a deeper understanding of the computations underlying self-motion integration outside of purely sensory areas. We found that multiple sources of congruent self-motion information converge in single neurons. Electrophysiological recordings in one of these neurons shows that it optimally integrates the unimodal signals to improve the reliability of self-motion estimation. These findings have important implications for our understanding of how animals use self-motion information to achieve high-performance locomotion given the hardships created by natural scenarios.

Even though each individual chapter contained a discussion of the presented results, in this section we will explore how insights provided by this work can expand our understanding of how animals control their walking.

6.2 Dealing with noise at multiple levels

Noise infiltrates every element of the control of locomotion, from the perception of sensory information to the physical interaction between the body and the environment (Faisal et al., 2008). As a foundational aspect of real systems, noise likely had a prominent role in shaping neural sensorimotor systems and animal behavior. Here, we tried to tackle the question of how locomotor control systems deal with noise at multiple levels.

The first level we considered was that of body posture. Keeping posture stable (both dynamic or static stability) is a priority for all moving systems. The loss of such stability can lead to falling or to a decrease in performance that can be intolerable in real life scenarios. We described that in free walking Drosophila, noise in the lateral placement of certain legs can decrease the lateral stability of the body. Moreover, the stepwise decrease in body stability can bias the lateral leg placement in the following step in order to recover the lost stability. It is still unknown the cause of the original deviation in leg lateral placement. We propose that it's caused by involuntary factors like motor system noise or micro inhomogeneities in the arena floor. Similar posture stabilization mechanisms also exist in other species (Karayannidou et al., 2009), and are likely part of a larger plethora of lower-level posture control mechanisms promoting stability during locomotion. Our results call into attention that in order to understand how locomotor commands from the brain operate in natural conditions, one must first acknowledge the full set of lower-level locomotor commands underlying the

stability of the animal's body.

The second level we considered is that of action selection. Most turning events near the walls of our experimental arena are associated with sensory variables like temperature. However, we found that most of the turning decisions of the fly are not associated with external variables but rather relate to internal factors. Intrinsic turning decisions during exploration have previously been proposed to be somehow stochastic, associated to a noise process (see Section 2.6). We showed that part of the variability in these events is related to an internal monitoring of self-motion. In particular, we found that drifts in body orientation modulate the next saccade to the direction contralateral to the drift. Our findings suggest that more detailed analysis of spontaneous behavior is required to understand its variability without having to resort to representing it as noise. A better understanding of the variability of spontaneous behavior will also improve our appreciation of the internal motivations and computations driving the animal's behavior.

Finally, the third level we considered is the level of neuronal representations of self-motion. Neuronal representations of any variable are subject to sensory noise (related to sensory transduction) and neuronal noise (Faisal et al., 2008). Moreover, the quality of the representation also depends on environmental conditions that affect the quality of the information. Here we found that neurons previously thought to encode optic-flow based estimations of self-motion (LPTCs) actually integrate self-motion information from multiple sources. Integration across different sources of information is thought to create more robust (less noisy) and stable percepts (Murray & Wallace, 2012). Our recordings show multimodal integration properties compatible with those predicted from Bayes-optimal framework (Ernst & Banks, 2002). Within this framework, the integration of multiple signals serves the purpose of minimizing the uncertainty of an estimation given noisy sensory information (Knill & Richards, 1996). Our findings propose that under natural conditions, self-motion sensitive neurons may operate differently in comparison to immobilized or artificial situations in order to improve the reliability of their representations. This way of reducing noise may be of major importance to guarantee locomotor performance in real scenarios.

6.3 The multiple context-dependencies of visuomotor processing

Context- or state-dependent modulation of neural processing has been demonstrated in a variety of sensorimotor systems across species. Between others, neuronal responses can be modulated by physiological state (e.g. hunger; Root et al., 2011; Savigner et al., 2009), arousal state (e.g. sleep; Campbell and Tobler, 1984; Hendricks et al., 2000) and also by other brain states such as behavioural state (e.g. walking or flying; Fujiwara and Chiappe, 2017). In particular, locomotion states can be responsible for multiple effects, from increasing the response of visual neurons (Niell & Stryker, 2010; Vinck et al., 2015), to suppressing auditory responses (Schneider et al., 2014; Zhou et al., 2014) to modulating other brain functions such as learning (Albergaria et al., 2018). These different expressions of a locomotor state have been associated with different mechanisms from neuromodulation (Polack et al., 2013) to specifically targeted motor signals (Schneider et al., 2014).

In Drosophila, as in mammals, visual processing is modulated by behavioral state. Visual responses in LPTCs (specifically HS cells) were known to increase during both flight and walking (Chiappe et al., 2010; Maimon et al., 2010). As with the mammalian visual cortex, neuromodulatory input plays an essential role in this modulation during Drosophila flight (Suver et al., 2012). We found that, during walking, the behavior state modulation was only one of the multiple locomotion related signals in LPTCs. By performing whole-cell patch recordings, we could access locomotor signals at a temporal resolution inaccessible with calcium image. This allowed us to analyze at greater detail the nature of these signals. We finally described them as having three components: (1) a slow behavior state signal, (2) a turn direction selective signal that includes a faithful representation of the fly's rotations, and (3) a fast forward-speed dependent modulation. While the turn direction selective signal is present through multiple LPTCs, the presence of the other signals is less clear. Our results are compatible with the turn direction selective signal forming a non-visual representation of self-motion that is optimally integrated with the neuron's visual sensitivity to generate reliable estimates of the fly's rotation. More recently it has also been found that the fast forward-speed dependent modulation might be related to a stride signal that flexibly recruits the cells to control the fly's

course (Fujiwara et al., 2022).

Interestingly, another locomotion-specific modulation was found in HS cells while the fly was flying (Kim, Fenk, et al., 2017; Kim et al., 2015a). These signals were specific for when the fly performed a flight saccade. These saccade-related potentials have a direction selectivity opposite to the visual direction-selective responses of the neuron, such that, in the presence of vision they could cancel response of the cell. The multiple non-visual signals converging in the same class of visual neurons represent multiple types of context modulation: from moving vs non-moving; to flight vs walking; to the single strides the animal performs. We propose that these types of contextual modulation might exist throughout multiple cell populations. Indeed recent work has observed locomotion related activity in virtually all regions of the fly brain (Aimon et al., 2022; Brezovec et al., 2022). The use of techniques like the ones presented here will help to understand the implications of this activity in the specific functions of different neural populations.

6.4 Granularity of command signals

Visual self-motion information is able to affect execution of posture stabilizing reflexes within almost single step timescale. This fast effect suggests that the sensory-motor pathway going from self-motion detection to descending pathways to execution must operate with minimal delay. We reasoned that such a fast system requires the command descending neurons to be in close proximity to the lobula plate circuit responsible to extract the self-motion information. We performed extensive silencing of single DNs, focusing at first on DNs that received information in the IPS (main output of lobula plate output neurons) and then more generally we tried almost every single DNs we had genetic access to (Fig. 3.13). Our systematic silencing of single DNs failed to reveal a necessity for any of the tested DNs for the visual effect to take place. We attributed this lack of effect to three possible reasons: (1) we just did not target the right DN, (2) the silencing allowed the fly to adapt and use a different command strategy, and (3) the behavior is mediated by multiple DNs that include some redundancy.

Little can be done regarding the first two options. However, if the behavior is mediated by multiple DNs, we could still try to test for the role of a specific neuron by causing asymmetric perturbations and therefore imbalance the population activity.

DNp15 is a particularly well placed command neuron to mediate visual self-motion estimation and steering commands given that it is the major target of yaw sensitive LPTCs. Indeed, unilateral application of ATP while DNp15 is expressing the ATP gated cation channel P2X2 causes a unilateral activation of these cells and consequent rotation of the fly to the side ipsilateral to the activation (Fig. 6.1A,B). In a different set of experiments we used heat-shock flippase to stochastically express the inward rectifier potassium channel KIR in P15 neurons. Specifically we combined hsFLP;+;pJFRC56-10xUAS>myrtdTomato-SV40>eGFPKir2.1 with the split Gal4 line SS01556. The heat shock protocol used allowed to obtain an unilateral silencing in about a third of the flies, as measured through immunostaining all flies post-experiment (Fig. 6.1C). As expected from previous silencing experiments (Fig. 3.13), when we compare the distributions of angular movements between flies with no cells silenced (No Label) and both cells silenced (Double Label) we observe no difference independently on visual conditions (Fig. 6.1D). A difference between the distributions of angular movements only starts to emerge when comparing flies with only the left cell silenced (Left Label) and flies with only the right cell silenced (Right Label) (Fig. 6.1D). This difference is consistent with a small general bias in the fly's drift direction that is specific for forward runs and does not happen for body saccades (Fig. 6.1E). The bias direction is contralateral to the side with a silenced cell, suggesting that the unbalanced left-right activity might be the cause for it to happen.

These results show a clear role for DNp15 neurons for the steering of walking flies during forward runs, however such effect was not observable under bilateral silencing. We propose that in the context of locomotion individual DNs may not work as single commands for specific behaviors as seen in (Ache, Namiki, et al., 2019; Von Philipsborn et al., 2011; Von Reyn et al., 2014; Zacarias et al., 2018), but are rather part of larger populations of partially redundant commands. Such organization would make this important behavior less dependent on a specific neuron or neuron type.

In Drosophila, genetic tools reached a granularity level in which we can routinely genetically target single pairs of neurons. This fine level of

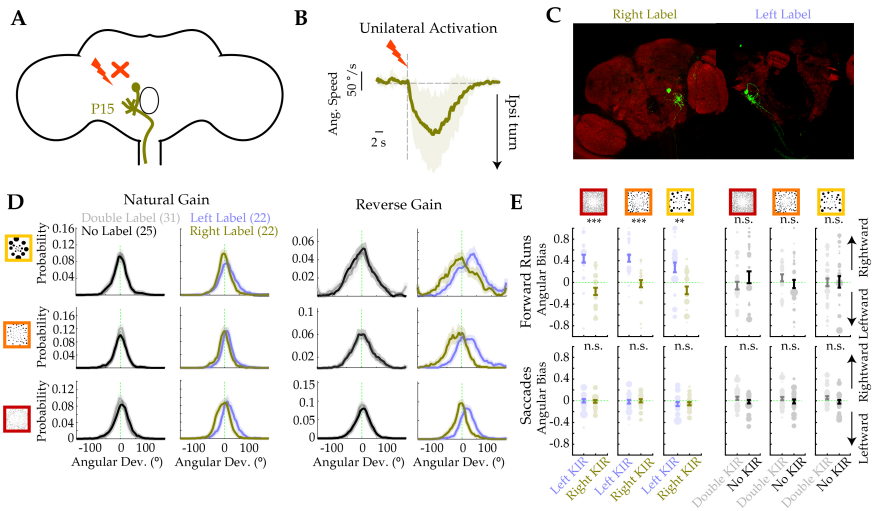

Figure 6.1: (A) Schematic of H2 and DNp15. We unilaterally silenced or activated DNp15. (B) Activation of the right-side DNp15 expressing P2X2 by local ATP injection causes a leftward angular deviation. (C) Stainings of KIR2.1:EGFP being stochastically expressed only on a left side or right side DNp15. (D) Distributions of angular deviations during forward runs across visual conditions in both natural and reverse gain. Colors represent which cells were expressing KIR2.1. (E) Rotational bias during forward runs and body saccades across visual conditions in both natural and reverse gain. Colors represent which cells were expressing KIR2.1.

granularity can however be a double edged sword when dealing with neural circuits that include some level of redundancy, and can lead us to dismiss or overlook important roles of certain neural populations.

6.5 Future Directions

In this thesis, we discussed the role of self-motion for locomotor control at multiple levels. The findings here reported have led directly to new research directions, some already initiated with collaborators in the Chiappe lab. These future directions promise to push our understanding of mechanistic implementations of neural computations and the bilateral communication between locomotor control areas.

6.5.1 Mechanistic implementation of Bayesian integration

A major benefit of the system presented in Chapter 5 to study multimodal integration is how it can link multiple approaches to understand a neural computation (see Section 5.6.2). In this future direction, we aim to establish a mechanistic model grounded on our descriptions of the system that can explain the normative properties reported here.

Some previous theoretical work has been done in linking population codes with Bayesian estimation (Ma et al., 2006). However, further evidence from the macaque MSTd (Morgan et al., 2008) showed that the expected properties did not match the experimental measurements. In contrast to Ma et al., 2006, our mechanistic model includes detailed descriptions of the activity of the neurons under multiple conditions and network properties like divisive normalization. We hope that such a model can help establish the link between the different approaches and more generally improve our understanding of why and how neural systems are wired in order to perform specific computations.

6.5.2 Neural networks for self-motion integration

In Chapter 4, we show that flies rely on internal signals alone to estimate self-motion. These idiothetic signals can arise from multiple sources like vestibular, proprioception or efference copies. While we still don't know the origin of the idiothetic signals present in the described IPS circuit, we have observed multiple candidate sources using EM datasets. One of the most exciting possibilities is ascending information (Chen et al., 2022). The IPS is target of multiple ascending neurons of unknown origin (Erginkaya, 2022). At least one of such ascending neurons is partially responsible for the forward speed modulation in HS cells (Fujiwara et al., 2022). An interesting possibility is that the angular drift signal also originates from combinations of sensory and efference copy signals arising from these ascending neurons. In this future direction we will use the behavior paradigm developed in Chapter 4 to investigate the role of ascending information going into the IPS. We hope this work will improve our understanding of the loops between brain and spinal/VNC for the control of natural locomotion.

Bibliography

Ache, J. M., Namiki, S., Lee, A., Branson, K., & Card, G. M. (2019). State-dependent decoupling of sensory and motor circuits underlies behavioral flexibility in drosophila. *Nature neuroscience*, *22*(7), 1132–1139.

Ache, J. M., Polsky, J., Alghailani, S., Parekh, R., Breads, P., Peek, M. Y., Bock, D. D., von Reyn, C. R., & Card, G. M. (2019). Neural basis for looming size and velocity encoding in the drosophila giant fiber escape pathway. *Current Biology*, *29*(6), 1073–1081.

Aimon, S., Cheng, K. Y., Gjorgjieva, J., & Kadow, I. C. G. (2022). Walking elicits global brain activity in drosophila. *bioRxiv*.

Albergaria, C., Silva, N. T., Pritchett, D. L., & Carey, M. R. (2018). Locomotor activity modulates associative learning in mouse cerebellum. *Nature neuroscience*, *21*(5), 725–735.

Anderson, O., & Grillner, S. (1981). Peripheral control of the cat's step cycle i. phase dependent effects of ramp-movements of the hip during "fictive locomotion". *Acta Physiologica Scandinavica*, *113*(1), 89–101.

Arber, S., & Costa, R. M. (2018). Connecting neuronal circuits for movement. *Science*, *360*(6396), 1403–1404.

Arber, S., & Costa, R. M. (2022). Networking brainstem and basal ganglia circuits for movement. *Nature Reviews Neuroscience*, 1–19.

Arthur, B. J., Sunayama-Morita, T., Coen, P., Murthy, M., & Stern, D. L. (2013). Multi-channel acoustic recording and automated analysis of drosophila courtship songs. *BMC biology*, *11*(1), 1–11.

Austin, D., Bowen, W., & McMillan, J. (2004). Intraspecific variation in movement patterns: Modeling individual behaviour in a large marine predator. *Oikos*, *105*(1), 15–30.

Bagarti, T. (2011). Correlated gaussian random walk models of animal dispersal. *arXiv preprint arXiv:1112.5839*.

Bahl, A., Ammer, G., Schilling, T., & Borst, A. (2013). Object tracking in motion-blind flies. *Nature neuroscience*, *16*(6), 730–738.

Bartumeus, F., da Luz, M. G. E., Viswanathan, G. M., & Catalan, J. (2005). Animal search strategies: A quantitative random-walk analysis. *Ecology*, *86*(11), 3078–3087.

Bartumeus, F., Peters, F., Pueyo, S., Marrasé, C., & Catalan, J. (2003). Helical lévy walks: Adjusting searching statistics to resource availability in microzooplankton. *Proceedings of the National Academy of Sciences*, *100*(22), 12771–12775.

Bartz, A. E. (1966). Eye and head movements in peripheral vision: Nature of compensatory eye movements. *Science*, *152*(3729), 1644–1645.

Bässler, U., & Büschges, A. (1998). Pattern generation for stick insect walking movements—multisensory control of a locomotor program. *Brain research reviews*, *27*(1), 65–88.

Bässler, U., & Wegner, U. (1983). Motor output of the denervated thoracic ventral nerve cord in the stick insect carausius morosus. *Journal of experimental Biology*, *105*(1), 127–145.

Bath, D. E., Stowers, J. R., Hörmann, D., Poehlmann, A., Dickson, B. J., & Straw, A. D. (2014). Flymad: Rapid thermogenetic control of neuronal activity in freely walking drosophila. *Nature methods*, *11*(7), 756–762.

Bauby, C. E., & Kuo, A. D. (2000). Active control of lateral balance in human walking. *Journal of biomechanics*, *33*(11), 1433–1440.

Beloozerova, I., & Sirota, M. (1993). The role of the motor cortex in the control of accuracy of locomotor movements in the cat. *The Journal of Physiology*, *461*(1), 1–25.

Bender, J. A., & Dickinson, M. H. (2006a). A comparison of visual and haltere-mediated feedback in the control of body saccades in drosophila melanogaster. *Journal of Experimental Biology*, *209*(23), 4597–4606.

Bender, J. A., & Dickinson, M. H. (2006b). Visual stimulation of saccades in magnetically tethered drosophila. *Journal of Experimental Biology*, *209*(16), 3170–3182.

Bender, J. A., Pollack, A. J., & Ritzmann, R. E. (2010). Neural activity in the central complex of the insect brain is linked to locomotor changes. *Current biology*, *20*(10), 921–926.

Berg, E. M., Björnfors, E. R., Pallucchi, I., Picton, L. D., & El Manira, A. (2018). Principles governing locomotion in vertebrates: Lessons from zebrafish. *Frontiers in neural circuits*, 73.

Berg, E. M., Hooper, S. L., Schmidt, J., & Büschges, A. (2015). A leg-local neural mechanism mediates the decision to search in stick insects. *Current Biology*, *25*(15), 2012–2017.

Berman, G. J., Choi, D. M., Bialek, W., & Shaevitz, J. W. (2014). Mapping the stereotyped behaviour of freely moving fruit flies. *Journal of The Royal Society Interface*, *11*(99), 20140672.

Bernstein, N. (1967). The co-ordination and regulation of movements. pergamo. *Press, London*.

Bidaye, S. S., Bockemühl, T., & Büschges, A. (2018). Six-legged walking in insects: How cpgs, peripheral feedback, and descending signals generate coordinated and adaptive motor rhythms. *Journal of neurophysiology*, *119*(2), 459–475.

Bidaye, S. S., Laturney, M., Chang, A. K., Liu, Y., Bockemühl, T., Büschges, A., & Scott, K. (2020). Two brain pathways initiate distinct forward walking programs in drosophila. *Neuron*, *108*(3), 469–485.

Bizzi, E., Kalil, R. E., & Morasso, P. (1972). Two modes of active eye-head coordination in monkeys. *Brain Research*.

Bizzi, E., Kalil, R. E., & Tagliasco, V. (1971). Eye-head coordination in monkeys: Evidence for centrally patterned organization. *Science*, *173*(3995), 452–454.

Bizzi, E., Mussa-Ivaldi, F. A., & Giszter, S. (1991). Computations underlying the execution of movement: A biological perspective. *Science*, *253*(5017), 287–291.

Björnfors, E. R., & El Manira, A. (2016). Functional diversity of excitatory commissural interneurons in adult zebrafish. *Elife*, *5*, e18579.

Blaj, G., & Van Hateren, J. (2004). Saccadic head and thorax movements in freely walking blowflies. *Journal of Comparative Physiology A*, *190*(11), 861–868.

Boeddeker, N., Dittmar, L., Stürzl, W., & Egelhaaf, M. (2010). The fine structure of honeybee head and body yaw movements in a homing task. *Proceedings of the Royal Society B: Biological Sciences*, *277*(1689), 1899–1906.

Bohnslav, J. P., Wimalasena, N. K., Clausing, K. J., Dai, Y. Y., Yarmolinsky, D. A., Cruz, T., Kashlan, A. D., Chiappe, M. E., Orefice, L. L., Woolf,

C. J., et al. (2021). Deepethogram, a machine learning pipeline for supervised behavior classification from raw pixels. *Elife*, *10*, e63377.

Borst, A. (2014). Fly visual course control: Behaviour, algorithms and circuits. *Nature Reviews Neuroscience*, *15*(9), 590–599.

Borst, A., & Haag, J. (2002). Neural networks in the cockpit of the fly. *Journal of Comparative Physiology A*, *188*(6), 419–437.

Borst, A., & Helmstaedter, M. (2015). Common circuit design in fly and mammalian motion vision. *Nature neuroscience*, *18*(8), 1067–1076.

Bouvier, J., Caggiano, V., Leiras, R., Caldeira, V., Bellardita, C., Balueva, K., Fuchs, A., & Kiehn, O. (2015). Descending command neurons in the brainstem that halt locomotion. *Cell*, *163*(5), 1191–1203.

Bovet, P., & Benhamou, S. (1988). Spatial analysis of animals' movements using a correlated random walk model. *Journal of theoretical biology*, *131*(4), 419–433.

Bradley, D. C., Maxwell, M., Andersen, R. A., Banks, M. S., & Shenoy, K. V. (1996). Mechanisms of heading perception in primate visual cortex. *Science*, *273*(5281), 1544–1547.

Brandt, T., Wist, E., & Dichgans, J. (1971). Optisch induzierte pseudocoriolis-effekte und circularvektion. *Archiv Für Psychiatrie und Nervenkrankheiten*, *214*(4), 365–389.

Breed, G. A., Severns, P. M., & Edwards, A. M. (2015). Apparent power-law distributions in animal movements can arise from intraspecific interactions. *Journal of the Royal Society Interface*, *12*(103), 20140927.

Brezovec, L. E., Berger, A. B., Druckmann, S., & Clandinin, T. R. (2022). Mapping the neural dynamics of locomotion across the drosophila brain. *bioRxiv*.

Britten, K. H., Newsome, W. T., Shadlen, M. N., Celebrini, S., & Movshon, J. A. (1996). A relationship between behavioral choice and the visual responses of neurons in macaque mt. *Visual neuroscience*, *13*(1), 87–100.

Britten, K. H., & van Wezel, R. J. (1998). Electrical microstimulation of cortical area mst biases heading perception in monkeys. *Nature neuroscience*, *1*(1), 59–63.

Brocard, F., Ryczko, D., Fénelon, K., Hatem, R., Gonzales, D., Auclair, F., & Dubuc, R. (2010). The transformation of a unilateral locomotor

command into a symmetrical bilateral activation in the brainstem. *Journal of Neuroscience*, *30*(2), 523–533.

Brown, C. T., Liebovitch, L. S., & Glendon, R. (2007). Lévy flights in dobe ju/'hoansi foraging patterns. *Human Ecology*, *35*(1), 129–138.

Brunn, D. E., & Dean, J. (1994). Intersegmental and local interneurons in the metathorax of the stick insect carausius morosus that monitor middle leg position. *Journal of Neurophysiology*, *72*(3), 1208–1219.

Budick, S. A., Reiser, M. B., & Dickinson, M. H. (2007). The role of visual and mechanosensory cues in structuring forward flight in drosophila melanogaster. *Journal of Experimental Biology*, *210*(23), 4092–4103.

Buelthoff, H., Poggio, T., & Wehrhahn, C. (1980). 3-d analysis of the flight trajectories of flies (drosophila melanogaster). *Zeitschrift für Naturforschung C*, *35*(9-10), 811–815.

Busch, C., Borst, A., & Mauss, A. S. (2018). Bi-directional control of walking behavior by horizontal optic flow sensors. *Current Biology*, *28*(24), 4037–4045.

Büschges, A. (1995). Role of local nonspiking interneurons in the generation of rhythmic motor activity in the stick insect. *Journal of neurobiology*, *27*(4), 488–512.

Büschges, A. (2005). Sensory control and organization of neural networks mediating coordination of multisegmental organs for locomotion. *Journal of neurophysiology*, *93*(3), 1127–1135.

Büschges, A., Akay, T., Gabriel, J. P., & Schmidt, J. (2008). Organizing network action for locomotion: Insights from studying insect walking. *Brain research reviews*, *57*(1), 162–171.

Büschges, A., & El Manira, A. (1998). Sensory pathways and their modulation in the control of locomotion. *Current opinion in neurobiology*, *8*(6), 733–739.

Butler, J. S., Smith, S. T., Campos, J. L., & Bülthoff, H. H. (2010). Bayesian integration of visual and vestibular signals for heading. *Journal of vision*, *10*(11), 23–23.

Caggiano, V., Leiras, R., Goñi-Erro, H., Masini, D., Bellardita, C., Bouvier, J., Caldeira, V., Fisone, G., & Kiehn, O. (2018). Midbrain circuits that set locomotor speed and gait selection. *Nature*, *553*(7689), 455–460.

Campbell, S. S., & Tobler, I. (1984). Animal sleep: A review of sleep duration across phylogeny. *Neuroscience & Biobehavioral Reviews*, *8*(3), 269–300.

Capelli, P., Pivetta, C., Soledad Esposito, M., & Arber, S. (2017). Locomotor speed control circuits in the caudal brainstem. *Nature*, *551*(7680), 373–377.

Carandini, M., & Heeger, D. J. (2012). Normalization as a canonical neural computation. *Nature Reviews Neuroscience*, *13*(1), 51–62.

Cellini, B., & Mongeau, J.-M. (2020). Hybrid visual control in fly flight: Insights into gaze shift via saccades. *Current Opinion in Insect Science*, *42*, 23–31.

Censi, A., Straw, A. D., Sayaman, R. W., Murray, R. M., & Dickinson, M. H. (2013). Discriminating external and internal causes for heading changes in freely flying drosophila. *PLoS computational biology*, *9*(2), e1002891.

Chen, C.-L., Aymanns, F., Minegishi, R., Matsuda, V., Talabot, N., Gunel, S., Dickson, B. J., & Ramdya, P. (2022). Ascending neurons convey behavioral state to integrative sensory and action selection centers in the brain. *bioRxiv*.

Chiappe, M. E., Seelig, J. D., Reiser, M. B., & Jayaraman, V. (2010). Walking modulates speed sensitivity in drosophila motion vision. *Current Biology*, *20*(16), 1470–1475.

Clark, D. A., Bursztyn, L., Horowitz, M. A., Schnitzer, M. J., & Clandinin, T. R. (2011). Defining the computational structure of the motion detector in drosophila. *Neuron*, *70*(6), 1165–1177.

Collett, T., Nalbach, H.-O., & Wagner, H. (1993). Visual stabilization in arthropods. *Reviews of oculomotor research*, *5*, 239–263.

Collett, T. S., & Land, M. (1975). Visual control of flight behaviour in the hoverflysyritta pipiens l. *Journal of comparative physiology*, *99*(1), 1–66.

Collett, T. (1978). Peering-a locust behaviour pattern for obtaining motion parallax information. *Journal of experimental Biology*, *76*(1), 237–241.

Collewijn, H. (1977). Eye-and head movements in freely moving rabbits. *The Journal of Physiology*, *266*(2), 471–498.

Corrales-Carvajal, V. M., Faisal, A. A., & Ribeiro, C. (2016). Internal states drive nutrient homeostasis by modulating exploration-exploitation trade-off. *Elife*, *5*, e19920.

Costa, A. C., Ahamed, T., & Stephens, G. J. (2019). Adaptive, locally linear models of complex dynamics. *Proceedings of the National Academy of Sciences*, *116*(5), 1501–1510.

Crapse, T. B., & Sommer, M. A. (2008). Corollary discharge across the animal kingdom. *Nature Reviews Neuroscience*, *9*(8), 587–600.

Cregg, J. M., Leiras, R., Montalant, A., Wanken, P., Wickersham, I. R., & Kiehn, O. (2020). Brainstem neurons that command mammalian locomotor asymmetries. *Nature neuroscience*, *23*(6), 730–740.

Crone, E. E., & Schultz, C. B. (2008). Old models explain new observations of butterfly movement at patch edges. *Ecology*, *89*(7), 2061–2067.

Cruse, H. (1985). Which parameters control the leg movement of a walking insect? i. velocity control during the stance phase. *J Exp Biol*, *116*(1), 343–355.

Cruse, H. (1990). What mechanisms coordinate leg movement in walking arthropods? *Trends in neurosciences*, *13*(1), 15–21.

Cruse, H., Dürr, V., & Schmitz, J. (2007). Insect walking is based on a decentralized architecture revealing a simple and robust controller. *Philosophical Transactions of the Royal Society A: Mathematical, Physical and Engineering Sciences*, *365*(1850), 221–250.

Cruz, T. (2013). Development and test of a virtual reality system for tethered walking drosophila.

Cruz, T., Fujiwara, T., Varela, N., Mohammad, F., Claridge-Chang, A., & Chiappe, M. E. (2019). Motor context coordinates visually guided walking in drosophila. *bioRxiv*, 572792.

Cruz, T. L., Malagón Pérez, S., & Chiappe, M. E. (2021). Rapid tuning of postural reflexes by visual feedback underlies gaze stabilization in walking drosophila. *Current Biology*, *0*(0), 0–0.

Cui, G., Jun, S. B., Jin, X., Pham, M. D., Vogel, S. S., Lovinger, D. M., & Costa, R. M. (2013). Concurrent activation of striatal direct and indirect pathways during action initiation. *Nature*, *494*(7436), 238–242.

Cullen, K. E. (2004). Sensory signals during active versus passive movement. *Current opinion in neurobiology*, *14*(6), 698–706.

Cullen, K. E. (2019). Vestibular processing during natural self-motion: Implications for perception and action. *Nature Reviews Neuroscience*, *20*(6), 346–363.

Cutting, J. E., Springer, K., Braren, P. A., & Johnson, S. H. (1992). Wayfinding on foot from information in retinal, not optical, flow. *Journal of Experimental Psychology: General*, *121*(1), 41.

Da Silva, J. A., Tecuapetla, F., Paixão, V., & Costa, R. M. (2018). Dopamine neuron activity before action initiation gates and invigorates future movements. *Nature*, *554*(7691), 244–248.

Darmohray, D. M., Jacobs, J. R., Marques, H. G., & Carey, M. R. (2019). Spatial and temporal locomotor learning in mouse cerebellum. *Neuron*, *102*(1), 217–231.

Davis, W. J., Siegler, M. V., & Mpitsos, G. J. (1973). Distributed neuronal oscillators and efference copy in the feeding system of pleurobranchaea. *Journal of Neurophysiology*, *36*(2), 258–274.

De Zeeuw, C. I., & Yeo, C. H. (2005). Time and tide in cerebellar memory formation. *Current opinion in neurobiology*, *15*(6), 667–674.

Dean, J. (1984). Control of leg protraction in the stick insect: A targeted movement showing compensation for externally applied forces. *Journal of Comparative Physiology A*, *155*(6), 771–781.

DeAngelis, B. D., Zavatone-Veth, J. A., & Clark, D. A. (2019). The manifold structure of limb coordination in walking drosophila. *Elife*, *8*, e46409.

Deliagina, T. G., Beloozerova, I., Zelenin, P., & Orlovsky, G. (2008). Spinal and supraspinal postural networks. *Brain research reviews*, *57*(1), 212–221.

Deliagina, T. G., Orlovsky, G. N., Zelenin, P. V., & Beloozerova, I. N. (2006). Neural bases of postural control. *Physiology*, *21*(3), 216–225.

Dickinson, M. H., Farley, C. T., Full, R. J., Koehl, M., Kram, R., & Lehman, S. (2000). How animals move: An integrative view. *science*, *288*(5463), 100–106.

Dittmar, L., Stürzl, W., Baird, E., Boeddeker, N., & Egelhaaf, M. (2010). Goal seeking in honeybees: Matching of optic flow snapshots? *Journal of Experimental Biology*, *213*(17), 2913–2923.

Dorkenwald, S., McKellar, C. E., Macrina, T., Kemnitz, N., Lee, K., Lu, R., Wu, J., Popovych, S., Mitchell, E., Nehoran, B., et al. (2022). Flywire: Online community for whole-brain connectomics. *Nature methods*, *19*(1), 119–128.

Drew, T., & Marigold, D. (2015). Taking the next step: Cortical contributions to the control of locomotion. *Current opinion in neurobiology*, *33*, 25–33.

Drew, T., Andujar, J.-E., Lajoie, K., & Yakovenko, S. (2008). Cortical mechanisms involved in visuomotor coordination during precision walking. *Brain research reviews*, *57*(1), 199–211.

Dubuc, R., Cabelguen, J.-M., & Rossignol, S. (1988). Rhythmic fluctuations of dorsal root potentials and antidromic discharges of primary afferents during fictive locomotion in the cat. *Journal of neurophysiology*, *60*(6), 2014–2036.

Duffy, C., & Wurtz, R. (1991). Sensitivity of mst neurons to optic flow stimuli. i. a continuum of response selectivity to large-field stimuli. *Journal of neurophysiology*, *65*(6), 1329–1345.

Duistermars, B. J., & Frye, M. A. (2008). Crossmodal visual input for odor tracking during fly flight. *Current Biology*, *18*(4), 270–275.

Duysens, J., Clarac, F., & Cruse, H. (2000). Load-regulating mechanisms in gait and posture: Comparative aspects. *Physiological reviews*.

Easter, S. S., & Johns, P. R. (1974). Horizontal compensatory eye movements in goldfish (carassius auratus).

Edwards, A. M. (2008). Using likelihood to test for lévy flight search patterns and for general power-law distributions in nature. *Journal of Animal Ecology*, *77*(6), 1212–1222.

Edwards, A. M., Freeman, M. P., Breed, G. A., & Jonsen, I. D. (2012). Incorrect likelihood methods were used to infer scaling laws of marine predator search behaviour.

Edwards, A. M., Phillips, R. A., Watkins, N. W., Freeman, M. P., Murphy, E. J., Afanasyev, V., Buldyrev, S. V., da Luz, M. G., Raposo, E. P., Stanley, H. E., et al. (2007). Revisiting lévy flight search patterns of wandering albatrosses, bumblebees and deer. *Nature*, *449*(7165), 1044–1048.

Egelhaaf, M. (1985). On the neuronal basis of figure-ground discrimination by relative motion in the visual system of the fly. 2: Figure-dectection cells, a new class of visual interneurones. *Biological Cybernetics*, *52*(3).

Eichner, H., Joesch, M., Schnell, B., Reiff, D. F., & Borst, A. (2011). Internal structure of the fly elementary motion detector. *Neuron*, *70*(6), 1155–1164.

Erginkaya, M. (2022). *Movement-dependent central processing of visual feedback for self-motion estimation in drosophila melanogaster* (Doctoral dissertation). Champalimamud Research.

Ernst, M. O., & Banks, M. S. (2002). Humans integrate visual and haptic information in a statistically optimal fashion. *Nature*, *415*(6870), 429–433.

Faisal, A. A., Selen, L. P., & Wolpert, D. M. (2008). Noise in the nervous system. *Nature reviews neuroscience*, *9*(4), 292–303.

Farrow, K., Haag, J., & Borst, A. (2006). Nonlinear, binocular interactions underlying flow field selectivity of a motion-sensitive neuron. *Nature neuroscience*, *9*(10), 1312–1320.

Ferreira-Pinto, M. J., Kanodia, H., Falasconi, A., Sigrist, M., Esposito, M. S., & Arber, S. (2021). Functional diversity for body actions in the mesencephalic locomotor region. *Cell*, *184*(17), 4564–4578.

Fetsch, C. R., DeAngelis, G. C., & Angelaki, D. E. (2013). Bridging the gap between theories of sensory cue integration and the physiology of multisensory neurons. *Nature Reviews Neuroscience*, *14*(6), 429–442.

Fetsch, C. R., Pouget, A., DeAngelis, G. C., & Angelaki, D. E. (2012). Neural correlates of reliability-based cue weighting during multisensory integration. *Nature neuroscience*, *15*(1), 146–154.

Forssberg, H., & Grillner, S. (1973). The locomotion of the acute spinal cat injected with clonidine iv. *Brain research*.

Foster, K. L., & Higham, T. E. (2014). Context-dependent changes in motor control and kinematics during locomotion: Modulation and decoupling. *Proceedings of the Royal Society B: Biological Sciences*, *281*(1782), 20133331.

Franklin, D. W., & Wolpert, D. M. (2011). Computational mechanisms of sensorimotor control. *Neuron*, *72*(3), 425–442.

Freeze, B. S., Kravitz, A. V., Hammack, N., Berke, J. D., & Kreitzer, A. C. (2013). Control of basal ganglia output by direct and indirect pathway projection neurons. *Journal of Neuroscience*, *33*(47), 18531–18539.

Fuchs, A. (1967). Saccadic and smooth pursuit eye movements in the monkey. *The Journal of Physiology*, *191*(3), 609.

Fuchs, E., Holmes, P., Kiemel, T., & Ayali, A. (2011). Intersegmental coordination of cockroach locomotion: Adaptive control of centrally

coupled pattern generator circuits. *Frontiers in neural circuits*, *4*, 125.

Fujiwara, T., Brotas, M., & Chiappe, M. E. (2022). Walking strides direct rapid and flexible recruitment of visual circuits for course control in drosophila. *Neuron*.

Fujiwara, T., & Chiappe, E. (2017). Motor-driven modulation in visual neural circuits. *Decoding neural circuit structure and function* (pp. 261–281). Springer.

Fujiwara, T., Cruz, T. L., Bohnslav, J. P., & Chiappe, M. E. (2017). A faithful internal representation of walking movements in the drosophila visual system. *Nature neuroscience*, *20*(1), 72–81.

Gal, R., & Libersat, F. (2006). New vistas on the initiation and maintenance of insect motor behaviors revealed by specific lesions of the head ganglia. *Journal of Comparative Physiology A*, *192*(9), 1003–1020.

Gandevia, S. C., & Burke, D. (1992). Does the nervous system depend on kinesthetic information to control natural limb movements? *Behavioral and Brain Sciences*, *15*(4), 614–632.

Garcia-Rill, E., & Skinner, R. (1987). The mesencephalic locomotor region. ii. projections to reticulospinal neurons. *Brain research*, *411*(1), 13–20.

Garcia-Rill, E., Skinner, R., Gilmore, S., & Owings, R. (1983). Connections of the mesencephalic locomotor region (mlr) ii. afferents and efferents. *Brain research bulletin*, *10*(1), 63–71.

Gdowski, G. T., & McCrea, R. A. (1999). Integration of vestibular and head movement signals in the vestibular nuclei during whole-body rotation. *Journal of neurophysiology*, *82*(1), 436–449.

Geurten, B. R., Jähde, P., Corthals, K., & Göpfert, M. C. (2014). Saccadic body turns in walking drosophila. *Frontiers in behavioral neuroscience*, *8*, 365.

Geurten, B. R., Kern, R., Braun, E., & Egelhaaf, M. (2010). A syntax of hoverfly flight prototypes. *Journal of Experimental Biology*, *213*(14), 2461–2475.

Gilchrist, I. D., Brown, V., & Findlay, J. M. (1997). Saccades without eye movements. *Nature*, *390*(6656), 130–131.

Goldberg, J., & Peterson, B. W. (1986). Reflex and mechanical contributions to head stabilization in alert cats. *Journal of neurophysiology*, *56*(3), 857–875.

Götz, K. G., & Biesinger, R. (1985). Centrophobism indrosophila melanogaster. *Journal of Comparative Physiology A*, *156*(3), 329–337.

Götz, K. G. (1975). The optomotor equilibrium of the drosophila navigation system. *Journal of comparative physiology*, *99*(3), 187–210.

Götz, K. G., & Wenking, H. (1973). Visual control of locomotion in the walking fruitflydrosophila. *Journal of comparative physiology*, *85*(3), 235–266.

Goulding, M. (2009). Circuits controlling vertebrate locomotion: Moving in a new direction. *Nature Reviews Neuroscience*, *10*(7), 507–518.

Graham, D. (1979). Effects of circum-oesophageal lesion on the behaviour of the stick insect carausius morosus. *Biological Cybernetics*, *32*(3), 139–145.

Grasse, K., & Cynader, M. (1982). Electrophysiology of medial terminal nucleus of accessory optic system in the cat. *Journal of Neurophysiology*, *48*(2), 490–504.

Green, J., Adachi, A., Shah, K. K., Hirokawa, J. D., Magani, P. S., & Maimon, G. (2017). A neural circuit architecture for angular integration in drosophila. *Nature*, *546*(7656), 101–106.

Grillner, S. (1981). *Control of locomotion in bipeds, tetrapods, and fish in: Brooks vb (ed) handbook of physiology-the nervous system, ii*. Waverly Press, Baltimore.

Grillner, S., Hongo, T., & Lund, S. (1971). Convergent effects on alpha motoneurones from the vestibulospinal tract and a pathway descending in the medial longitudinal fasciculus. *Experimental brain research*, *12*(5), 457–479.

Grillner, S., & Rossignol, S. (1978). On the initiation of the swing phase of locomotion in chronic spinal cats. *Brain research*, *146*(2), 269–277.

Grillner, S., & Wallén, P. (1982). On peripheral control mechanisms acting on the central pattern generators for swimming in the dogfish. *Journal of Experimental Biology*, *98*(1), 1–22.

Grillner, S. (1985). Neurobiological bases of rhythmic motor acts in vertebrates. *Science*, *228*(4696), 143–149.

Grillner, S. (2006). Biological pattern generation: The cellular and computational logic of networks in motion. *Neuron*, *52*(5), 751–766.

Grillner, S., & El Manira, A. (2020). Current principles of motor control, with special reference to vertebrate locomotion. *Physiological reviews*, *100*(1), 271–320.

Grillner, S., Hellgren, J., Menard, A., Saitoh, K., & Wikström, M. A. (2005). Mechanisms for selection of basic motor programs–roles for the striatum and pallidum. *Trends in neurosciences*, *28*(7), 364–370.

Grillner, S., & Zangger, P. (1984). The effect of dorsal root transection on the efferent motor pattern in the cat's hindlimb during locomotion. *Acta Physiologica Scandinavica*, *120*(3), 393–405.

Grossberg, S., & Kuperstein, M. (2011). *Neural dynamics of adaptive sensory-motor control: Ballistic eye movements*. Elsevier.

Gu, Y., Angelaki, D. E., & DeAngelis, G. C. (2008). Neural correlates of multisensory cue integration in macaque mstd. *Nature neuroscience*, *11*(10), 1201–1210.

Gu, Y., DeAngelis, G. C., & Angelaki, D. E. (2007). A functional link between area mstd and heading perception based on vestibular signals. *Nature neuroscience*, *10*(8), 1038–1047.

Haag, J., & Borst, A. (1998). Active membrane properties and signal encoding in graded potential neurons. *Journal of Neuroscience*, *18*(19), 7972–7986.

Haag, J., Wertz, A., & Borst, A. (2007). Integration of lobula plate output signals by dnovs1, an identified premotor descending neuron. *Journal of Neuroscience*, *27*(8), 1992–2000.

Haefner, J. W., & Crist, T. O. (1994). Spatial model of movement and foraging in harvester ants (pogonomyrmex)(i): The roles of memory and communication. *Journal of Theoretical Biology*, *166*(3), 299–313.

Haikala, V., Joesch, M., Borst, A., & Mauss, A. S. (2013). Optogenetic control of fly optomotor responses. *Journal of Neuroscience*, *33*(34), 13927–13934.

Harley, C., & Ritzmann, R. (2010). Electrolytic lesions within central complex neuropils of the cockroach brain affect negotiation of barriers. *Journal of Experimental Biology*, *213*(16), 2851–2864.

Harris, C. M., & Wolpert, D. M. (1998). Signal-dependent noise determines motor planning. *Nature*, *394*(6695), 780–784.

Harris, J. M., & Bonas, W. (2002). Optic flow and scene structure do not always contribute to the control of human walking. *Vision research*, *42*(13), 1619–1626.

Hateren, J., & Schilstra, C. (1999). Blowfly flight and optic flow. ii. head movements during flight. *Journal of Experimental Biology*, *202*(11), 1491–1500.

Hausen, K. (1987). The neural architecture of the lobula plate of the blowfly, calliphora erythrocephala. *Unpublished work*.

Hausen, K., Wolburg-Buchholz, K., & Ribi, W. (1980). The synaptic organization of visual interneurons in the lobula complex of flies. *Cell and tissue research*, *208*(3), 371–387.

Heisenberg, M., & Wolf, R. (1988). Reafferent control of optomotor yaw torque indrosophila melanogaster. *Journal of Comparative Physiology A*, *163*(3), 373–388.

Heisenberg, M., & Wolf, R. (1979). On the fine structure of yaw torque in visual flight orientation ofdrosophila melanogaster. *Journal of comparative physiology*, *130*(2), 113–130.

Heisenberg, M., & Wolf, R. (2013). *Vision in drosophila: Genetics of microbehavior* (Vol. 12). Springer-Verlag.

Heisenberg, M., Wonneberger, R., & Wolf, R. (1978). Optomotor-blindh31—adrosophila mutant of the lobula plate giant neurons. *Journal of comparative physiology*, *124*(4), 287–296.

Helmbrecht, T. O., Dal Maschio, M., Donovan, J. C., Koutsouli, S., & Baier, H. (2018). Topography of a visuomotor transformation. *Neuron*, *100*(6), 1429–1445.

Henderson, J. M. (2017). Gaze control as prediction. *Trends in cognitive sciences*, *21*(1), 15–23.

Hendricks, J. C., Finn, S. M., Panckeri, K. A., Chavkin, J., Williams, J. A., Sehgal, A., & Pack, A. I. (2000). Rest in drosophila is a sleep-like state. *Neuron*, *25*(1), 129–138.

Hengstenberg, R., Hausen, K., & Hengstenberg, B. (1982). The number and structure of giant vertical cells(vs) in the lobula plate of the blowflycalliphora erythrocephala. *Journal of Comparative Physiology A*, *149*(2), 163–177.

Herman, R. (2017). *Neural control of locomotion* (Vol. 18). Springer.

Hikosaka, O., & Wurtz, R. H. (1983). Visual and oculomotor functions of monkey substantia nigra pars reticulata. iv. relation of substantia nigra to superior colliculus. *Journal of neurophysiology*, *49*(5), 1285–1301.

Holst, E., & Mittelstaedt, H. (1950). Das reafferenzprinzip. *Naturwissenschaften*, *37*(20), 464–476.

Howe, M. W., & Dombeck, D. A. (2016). Rapid signalling in distinct dopaminergic axons during locomotion and reward. *Nature*, *535*(7613), 505–510.

Hsu, C. T., & Bhandawat, V. (2016). Organization of descending neurons in drosophila melanogaster. *Scientific reports*, *6*(1), 1–14.

Hulse, B. K., Haberkern, H., Franconville, R., Turner-Evans, D. B., Takemura, S.-y., Wolff, T., Noorman, M., Dreher, M., Dan, C., Parekh, R., et al. (2021). A connectome of the drosophila central complex reveals network motifs suitable for flexible navigation and context-dependent action selection. *ELife*, *10*, e66039.

Imai, T., Moore, S. T., Raphan, T., & Cohen, B. (2001). Interaction of the body, head, and eyes during walking and turning. *Experimental brain research*, *136*(1), 1–18.

Isa, T., Marquez-Legorreta, E., Grillner, S., & Scott, E. K. (2021). The tectum/superior colliculus as the vertebrate solution for spatial sensory integration and action. *Current Biology*, *31*(11), R741–R762.

Isakov, A., Buchanan, S. M., Sullivan, B., Ramachandran, A., Chapman, J. K., Lu, E. S., Mahadevan, L., & de Bivort, B. (2016). Recovery of locomotion after injury in drosophila melanogaster depends on proprioception. *Journal of Experimental Biology*, *219*(11), 1760–1771.

James, A., Plank, M. J., & Edwards, A. M. (2011). Assessing lévy walks as models of animal foraging. *Journal of the Royal Society Interface*, *8*(62), 1233–1247.

Jiang, W., Wallace, M. T., Jiang, H., Vaughan, J. W., & Stein, B. E. (2001). Two cortical areas mediate multisensory integration in superior colliculus neurons. *Journal of Neurophysiology*, *85*(2), 506–522.

Jindrich, D. L., & Full, R. J. (2002). Dynamic stabilization of rapid hexapedal locomotion. *Journal of Experimental Biology*, *205*(18), 2803–2823.

Joesch, M., Plett, J., Borst, A., & Reiff, D. F. (2008). Response properties of motion-sensitive visual interneurons in the lobula plate of drosophila melanogaster. *Current Biology*, *18*(5), 368–374.

Joesch, M., Schnell, B., Raghu, S. V., Reiff, D. F., & Borst, A. (2010). On and off pathways in drosophila motion vision. *Nature*, *468*(7321), 300–304.

Josset, N., Roussel, M., Lemieux, M., Lafrance-Zoubga, D., Rastqar, A., & Bretzner, F. (2018). Distinct contributions of mesencephalic locomotor region nuclei to locomotor control in the freely behaving mouse. *Current Biology*, *28*(6), 884–901.

Juusola, M., & French, A. S. (1997). Visual acuity for moving objects in first-and second-order neurons of the fly compound eye. *Journal of neurophysiology*, *77*(3), 1487–1495.

Kabra, M., Robie, A. A., Rivera-Alba, M., Branson, S., & Branson, K. (2013). Jaaba: Interactive machine learning for automatic annotation of animal behavior. *Nature methods*, *10*(1), 64–67.

Karayannidou, A., Zelenin, P. V., Orlovsky, G. N., Sirota, M. G., Beloozerova, I. N., & Deliagina, T. G. (2009). Maintenance of lateral stability during standing and walking in the cat. *Journal of neurophysiology*, *101*(1), 8–19.

Kardamakis, A. A., Saitoh, K., & Grillner, S. (2015). Tectal microcircuit generating visual selection commands on gaze-controlling neurons. *Proceedings of the National Academy of Sciences*, *112*(15), E1956–E1965.

Kareiva, P., & Shigesada, N. (1983). Analyzing insect movement as a correlated random walk. *Oecologia*, *56*(2), 234–238.

Katsov, A. Y., & Clandinin, T. R. (2008). Motion processing streams in drosophila are behaviorally specialized. *Neuron*, *59*(2), 322–335.

Katsov, A. Y., Freifeld, L., Horowitz, M., Kuehn, S., & Clandinin, T. R. (2017). Dynamic structure of locomotor behavior in walking fruit flies. *Elife*, *6*.

Keleş, M., & Frye, M. (2017). Object-detecting neurons in drosophila. *Current Biology*, *27*(5), 680–687.

Keller, G. B., Bonhoeffer, T., & Hübener, M. (2012). Sensorimotor mismatch signals in primary visual cortex of the behaving mouse. *Neuron*, *74*(5), 809–815.

Kelly, D. H. (1979). Motion and vision. ii. stabilized spatio-temporal threshold surface. *Josa*, *69*(10), 1340–1349.

Kern, R., Van Hateren, J., & Egelhaaf, M. (2006). Representation of behaviourally relevant information by blowfly motion-sensitive visual interneurons requires precise compensatory head movements. *Journal of Experimental Biology*, *209*(7), 1251–1260.

Kien, J. (1983). The initiation and maintenance of walking in the locust: An alternative to the command concept. *Proceedings of the Royal society of London. Series B. Biological sciences*, *219*(1215), 137–174.

Kim, A. J., Fenk, L. M., Lyu, C., & Maimon, G. (2017). Quantitative predictions orchestrate visual signaling in drosophila. *Cell*, *168*(1-2), 280–294.

Kim, A. J., Fitzgerald, J. K., & Maimon, G. (2015a). Cellular evidence for efference copy in drosophila visuomotor processing. *Nature neuroscience*, *18*(9), 1247–1255.

Kim, A. J., Fitzgerald, J. K., & Maimon, G. (2015b). Cellular evidence for efference copy in drosophila visuomotor processing. *Nature neuroscience*, *18*(9), 1247–1255.

Kim, I. S., & Dickinson, M. H. (2017). Idiothetic path integration in the fruit fly drosophila melanogaster. *Current Biology*, *27*(15), 2227–2238.

Kim, S. S., Rouault, H., Druckmann, S., & Jayaraman, V. (2017). Ring attractor dynamics in the drosophila central brain. *Science*, *356*(6340), 849–853.

Kita, T., & Kita, H. (2012). The subthalamic nucleus is one of multiple innervation sites for long-range corticofugal axons: A single-axon tracing study in the rat. *Journal of Neuroscience*, *32*(17), 5990–5999.

Klapoetke, N. C., Nern, A., Rogers, E. M., Rubin, G. M., Reiser, M. B., & Card, G. M. (2022). A functionally ordered visual feature map in the drosophila brain. *Neuron*, *110*(10), 1700–1711.

Knill, D. C., & Richards, W. (1996). *Perception as bayesian inference*. Cambridge University Press.

Koenderink, J. J. (1986). Optic flow. *Vision research*, *26*(1), 161–179.

Koenderink, J. J., & van Doorn, A. J. (1987). Facts on optic flow. *Biological cybernetics*, *56*(4), 247–254.

Kohn, J. R., Heath, S. L., & Behnia, R. (2018). Eyes matched to the prize: The state of matched filters in insect visual circuits. *Frontiers in neural circuits*, *12*, 26.

Krapp, H., & Hengstenberg, R. (1996). Estimation of self-motion by optic flow processing in single visual interneurons. *Nature*, *384*(6608), 463–466.

Krapp, H. G., Hengstenberg, B., & Hengstenberg, R. (1998). Dendritic structure and receptive-field organization of optic flow processing

interneurons in the fly. *Journal of neurophysiology*, *79*(4), 1902–1917.

Kretschmer, F., Tariq, M., Chatila, W., Wu, B., & Badea, T. C. (2017). Comparison of optomotor and optokinetic reflexes in mice. *Journal of neurophysiology*, *118*(1), 300–316.

Kubo, F., Hablitzel, B., Dal Maschio, M., Driever, W., Baier, H., & Arrenberg, A. B. (2014). Functional architecture of an optic flow-responsive area that drives horizontal eye movements in zebrafish. *Neuron*, *81*(6), 1344–1359.

Land, M. (1973). Head movement of flies during visually guided flight. *Nature*, *243*(5405), 299–300.

Land, M. F. (1995). The functions of eye movements in animals remote from man. *Studies in visual information processing*, *6*, 63–76.

Land, M. F. (1999). Motion and vision: Why animals move their eyes. *Journal of Comparative Physiology A*, *185*(4), 341–352.

Landy, M. S., Kording, K., & Trommershauser, J. (2011). *Sensory cue integration*. Oxford University Press.

Lappe, M., Bremmer, F., & Van den Berg, A. (1999). Perception of self-motion from visual flow. *Trends in cognitive sciences*, *3*(9), 329–336.

Laurens, J., & Angelaki, D. E. (2018). The brain compass: A perspective on how self-motion updates the head direction cell attractor. *Neuron*, *97*(2), 275–289.

Laurent, G. (1991). Sensory control of locomotion in insects. *Current Opinion in Neurobiology*, *1*(4), 601–604.

Laurent, G., & Burrows, M. (1989). Intersegmental interneurons can control the gain of reflexes in adjacent segments of the locust by their action on nonspiking local interneurons. *Journal of Neuroscience*, *9*(9), 3030–3039.

Lehrer, M., Srinivasan, M. V., Zhang, S.-W., & Horridge, G. A. (1988). Motion cues provide the bee's visual world with a third dimension. *Nature*, *332*(6162), 356–357.

Levenstein, D., Alvarez, V. A., Amarasingham, A., Azab, H., Gerkin, R. C., Hasenstaub, A., Iyer, R., Jolivet, R. B., Marzen, S., Monaco, J. D., et al. (2020). On the role of theory and modeling in neuroscience. *arXiv preprint arXiv:2003.13825*.

Liu, S., Liu, Q., Tabuchi, M., & Wu, M. N. (2016). Sleep drive is encoded by neural plastic changes in a dedicated circuit. *Cell*, *165*(6), 1347–1360.

Lönnendonker, U., & Scharstein, H. (1991). Fixation and optomotor response of walking colorado beetles: Interaction with spontaneous turning tendencies. *Physiological entomology*, *16*(1), 65–76.

Lu, J., Behbahani, A. H., Hamburg, L., Westeinde, E. A., Dawson, P. M., Lyu, C., Maimon, G., Dickinson, M. H., Druckmann, S., & Wilson, R. I. (2022). Transforming representations of movement from body-to world-centric space. *Nature*, *601*(7891), 98–104.

Lyu, C., Abbott, L., & Maimon, G. (2022). Building an allocentric travelling direction signal via vector computation. *Nature*, *601*(7891), 92–97.

Ma, W. J., Beck, J. M., Latham, P. E., & Pouget, A. (2006). Bayesian inference with probabilistic population codes. *Nature neuroscience*, *9*(11), 1432–1438.

Maimon, G. (2011). Modulation of visual physiology by behavioral state in monkeys, mice, and flies. *Current opinion in neurobiology*, *21*(4), 559–564.

Maimon, G., Straw, A. D., & Dickinson, M. H. (2008). A simple vision-based algorithm for decision making in flying drosophila. *Current Biology*, *18*(6), 464–470.

Maimon, G., Straw, A. D., & Dickinson, M. H. (2010). Active flight increases the gain of visual motion processing in drosophila. *Nature neuroscience*, *13*(3), 393–399.

Maisak, M. S., Haag, J., Ammer, G., Serbe, E., Meier, M., Leonhardt, A., Schilling, T., Bahl, A., Rubin, G. M., Nern, A., et al. (2013). A directional tuning map of drosophila elementary motion detectors. *Nature*, *500*(7461), 212–216.

Marder, E., & Bucher, D. (2001). Central pattern generators and the control of rhythmic movements. *Current biology*, *11*(23), R986–R996.

Marder, E., & Calabrese, R. L. (1996). Principles of rhythmic motor pattern generation. *Physiological reviews*, *76*(3), 687–717.

Mårell, A., Ball, J. P., & Hofgaard, A. (2002). Foraging and movement paths of female reindeer: Insights from fractal analysis, correlated random walks, and lévy flights. *Canadian Journal of Zoology*, *80*(5), 854–865.

Martin, J. P., Guo, P., Mu, L., Harley, C. M., & Ritzmann, R. E. (2015). Central-complex control of movement in the freely walking cockroach. *Current Biology*, *25*(21), 2795–2803.

Mathis, A., Mamidanna, P., Cury, K. M., Abe, T., Murthy, V. N., Mathis, M. W., & Bethge, M. (2018). Deeplabcut: Markerless pose estimation of user-defined body parts with deep learning. *Nature neuroscience*, *21*(9), 1281–1289.

Matthis, J. S., Yates, J. L., & Hayhoe, M. M. (2018). Gaze and the control of foot placement when walking in natural terrain. *Current Biology*, *28*(8), 1224–1233.

Maye, A., Hsieh, C.-h., Sugihara, G., & Brembs, B. (2007). Order in spontaneous behavior. *PloS one*, *2*(5), e443.

Mearns, D. S., Donovan, J. C., Fernandes, A. M., Semmelhack, J. L., & Baier, H. (2020). Deconstructing hunting behavior reveals a tightly coupled stimulus-response loop. *Current Biology*, *30*(1), 54–69.

Mendes, C. S., Bartos, I., Akay, T., Márka, S., & Mann, R. S. (2013). Quantification of gait parameters in freely walking wild type and sensory deprived drosophila melanogaster. *elife*, *2*, e00231.

Meredith, M. A., & Stein, B. E. (1986). Visual, auditory, and somatosensory convergence on cells in superior colliculus results in multisensory integration. *Journal of neurophysiology*, *56*(3), 640–662.

Merfeld, D. M. (2011). Signal detection theory and vestibular thresholds: I. basic theory and practical considerations. *Experimental brain research*, *210*(3), 389–405.

Meyer, A. F., O'Keefe, J., & Poort, J. (2020). Two distinct types of eye-head coupling in freely moving mice. *Current Biology*, *30*(11), 2116–2130.

Miall, R. C., & Wolpert, D. M. (1996). Forward models for physiological motor control. *Neural networks*, *9*(8), 1265–1279.

Miles, F., & Lisberger, S. (1981). Plasticity in the vestibulo-ocular reflex: A new hypothesis. *Annual review of neuroscience*, *4*(1), 273–299.

Mogenson, G., Swanson, L., & Wu, M. (1985). Evidence that projections from substantia innominata to zona incerta and mesencephalic locomotor region contribute to locomotor activity. *Brain research*, *334*(1), 65–76.

Morgan, B., & Frost, B. (1981). Visual response characteristics of neurons in nucleus of basal optic root of pigeons. *Experimental Brain Research*, *42*(2), 181–188.

Morgan, M. L., DeAngelis, G. C., & Angelaki, D. E. (2008). Multisensory integration in macaque visual cortex depends on cue reliability. *Neuron*, *59*(4), 662–673.

Muijres, F. T., Elzinga, M. J., Iwasaki, N. A., & Dickinson, M. H. (2015). Body saccades of drosophila consist of stereotyped banked turns. *The Journal of experimental biology*, *218*(6), 864–875.

Muijres, F. T., Elzinga, M. J., Melis, J. M., & Dickinson, M. H. (2014). Flies evade looming targets by executing rapid visually directed banked turns. *Science*, *344*(6180), 172–177.

Müller, M., & Wehner, R. (1988). Path integration in desert ants, cataglyphis fortis. *Proceedings of the National Academy of Sciences*, *85*(14), 5287–5290.

Murray, A. J., Croce, K., Belton, T., Akay, T., & Jessell, T. M. (2018). Balance control mediated by vestibular circuits directing limb extension or antagonist muscle co-activation. *Cell reports*, *22*(5), 1325–1338.

Murray, M., & Wallace, M. (2012). *The neural bases of multisensory processes. boca raton, fl: Crc*. Taylor&Francis.

Namiki, S., Dickinson, M. H., Wong, A. M., Korff, W., & Card, G. M. (2018). The functional organization of descending sensory-motor pathways in drosophila. *Elife*, *7*, e34272.

Niell, C. M., & Stryker, M. P. (2010). Modulation of visual responses by behavioral state in mouse visual cortex. *Neuron*, *65*(4), 472–479.

Noah, J., Quimby, L., Frazier, S., & Zill, S. (2004). Sensing the effect of body load in legs: Responses of tibial campaniform sensilla to forces applied to the thorax in freely standing cockroaches. *Journal of Comparative Physiology A*, *190*(3), 201–215.

Ohshiro, T., Angelaki, D. E., & DeAngelis, G. C. (2011). A normalization model of multisensory integration. *Nature neuroscience*, *14*(6), 775–782.

Ohshiro, T., Angelaki, D. E., & DeAngelis, G. C. (2017). A neural signature of divisive normalization at the level of multisensory integration in primate cortex. *Neuron*, *95*(2), 399–411.

Ojelade, S. A., Butts, A. R., Merrill, C. B., Champaloux, E. P., Aso, Y., Wolin, D., Cofresi, R. U., Gonzales, R. A., Rubin, G. M., Venton, B. J., et

al. (2019). Dopaminergic learning and arousal circuits mediate opposing effects on alcohol consumption in drosophila. *bioRxiv*, 624833.

Okubo, T. S., Patella, P., D'Alessandro, I., & Wilson, R. I. (2020). A neural network for wind-guided compass navigation. *Neuron*, *107*(5), 924–940.

Orger, M. B., Smear, M. C., Anstis, S. M., & Baier, H. (2000). Perception of fourier and non-fourier motion by larval zebrafish. *Nature neuroscience*, *3*(11), 1128–1133.

Orlovsky, G., & Pavlova, G. (1972). Response of deiters' neurons to tilt during locomotion. *Brain research*, *42*(1), 212–214.

Orlovsky, G. N., Orlovsky, T., Deliagina, T., & Grillner, S. (1999). *Neuronal control of locomotion: From mollusc to man*. Oxford University Press.

Patla, A. E. (1997). Understanding the roles of vision in the control of human locomotion. *Gait & posture*, *5*(1), 54–69.

Pearson, K. G. (1995). Proprioceptive regulation of locomotion. *Current opinion in neurobiology*, *5*(6), 786–791.

Pearson, K. G. (2004). Generating the walking gait: Role of sensory feedback. *Progress in brain research*, *143*, 123–129.

Perrault Jr, T. J., Vaughan, J. W., Stein, B. E., & Wallace, M. T. (2003). Neuron-specific response characteristics predict the magnitude of multisensory integration. *Journal of neurophysiology*, *90*(6), 4022–4026.

Perrault Jr, T. J., Vaughan, J. W., Stein, B. E., & Wallace, M. T. (2005). Superior colliculus neurons use distinct operational modes in the integration of multisensory stimuli. *Journal of neurophysiology*, *93*(5), 2575–2586.

Pfeffer, S. E., & Wittlinger, M. (2016). Optic flow odometry operates independently of stride integration in carried ants. *Science*, *353*(6304), 1155–1157.

Pfeiffer, K., & Homberg, U. (2014). Organization and functional roles of the central complex in the insect brain. *Annual review of entomology*, *59*, 165–184.

Pimentel, D., Donlea, J. M., Talbot, C. B., Song, S. M., Thurston, A. J., & Miesenböck, G. (2016). Operation of a homeostatic sleep switch. *Nature*, *536*(7616), 333–337.

Pitkow, X., & Angelaki, D. E. (2017). Inference in the brain: Statistics flowing in redundant population codes. *Neuron*, *94*(5), 943–953.

Poggio, T., & Reichardt, W. (1973). A theory of the pattern induced flight orientation of the fly musca domestica. *Kybernetik*, *12*(4), 185–203.

Polack, P.-O., Friedman, J., & Golshani, P. (2013). Cellular mechanisms of brain state–dependent gain modulation in visual cortex. *Nature neuroscience*, *16*(9), 1331–1339.

Popov, A., Peresleni, A., Ozerskii, P., Shchekanov, E., & Savvateeva-Popova, E. (2005). The role of the flabellar and ellipsoid bodies of the central complex of the brain of drosophila melanogaster in the control of courtship behavior and communicative sound production in males. *Neuroscience and behavioral physiology*, *35*(7), 741–750.

Pratt, D. W. (1982). Saccadic eye movements are coordinated with head movements in walking chickens. *Journal of Experimental Biology*, *97*(1), 217–223.

Preuss, T., & Hengstenberg, R. (1992). Structure and kinematics of the prosternal organs and their influence on head position in the blowfly calliphora erythrocephala meig. *Journal of Comparative Physiology A*, *171*(4), 483–493.

Prokop, T., Schubert, M., & Berger, W. (1997). Visual influence on human locomotion modulation to changes in optic flow. *Experimental brain research*, *114*(1), 63–70.

Raposo, D., Sheppard, J. P., Schrater, P. R., & Churchland, A. K. (2012). Multisensory decision-making in rats and humans. *Journal of neuroscience*, *32*(11), 3726–3735.

Rashbass, C. (1961). The relationship between saccadic and smooth tracking eye movements. *The Journal of physiology*, *159*(2), 326.

Rayshubskiy, A. (2020). *Neural control of steering in walking drosophila* (Doctoral dissertation). Harvard University.

Reichardt, W., & Poggio, T. (1976). Visual control of orientation behaviour in the fly: Part i. a quantitative analysis. *Quarterly reviews of biophysics*, *9*(3), 311–375.

Requarth, T., Kaifosh, P., & Sawtell, N. B. (2014). A role for mixed corollary discharge and proprioceptive signals in predicting the sensory consequences of movements. *Journal of Neuroscience*, *34*(48), 16103–16116.

Reynolds, A. M., & Frye, M. A. (2007). Free-flight odor tracking in drosophila is consistent with an optimal intermittent scale-free search. *PloS one*, *2*(4), e354.

Ribeiro, I. M., Drews, M., Bahl, A., Machacek, C., Borst, A., & Dickson, B. J. (2018). Visual projection neurons mediating directed courtship in drosophila. *Cell*, *174*(3), 607–621.

Ridgel, A. L., Alexander, B. E., & Ritzmann, R. E. (2007). Descending control of turning behavior in the cockroach, blaberus discoidalis. *Journal of Comparative Physiology A*, *193*(4), 385–402.

Ridgel, A. L., & Ritzmann, R. E. (2005). Effects of neck and circumoesophageal connective lesions on posture and locomotion in the cockroach. *Journal of Comparative Physiology A*, *191*(6), 559–573.

Robinson, D. (1981). The use of control systems analysis in the neurophysiology of eye movements. *Annual review of neuroscience*, *4*(1), 463–503.

Root, C. M., Ko, K. I., Jafari, A., & Wang, J. W. (2011). Presynaptic facilitation by neuropeptide signaling mediates odor-driven food search. *Cell*, *145*(1), 133–144.

Roseberry, T. K., Lee, A. M., Lalive, A. L., Wilbrecht, L., Bonci, A., & Kreitzer, A. C. (2016). Cell-type-specific control of brainstem locomotor circuits by basal ganglia. *Cell*, *164*(3), 526–537.

Rosenegger, D. G., Tran, C. H. T., LeDue, J., Zhou, N., & Gordon, G. R. (2014). A high performance, cost-effective, open-source microscope for scanning two-photon microscopy that is modular and readily adaptable. *PloS one*, *9*(10), e110475.

Roth, E., Reiser, M. B., Dickinson, M. H., & Cowan, N. J. (2012). A task-level model for optomotor yaw regulation in drosophila melanogaster: A frequency-domain system identification approach. *2012 IEEE 51st IEEE Conference on Decision and Control (CDC)*, 3721–3726.

Roth, M. M., Dahmen, J. C., Muir, D. R., Imhof, F., Martini, F. J., & Hofer, S. B. (2016). Thalamic nuclei convey diverse contextual information to layer 1 of visual cortex. *Nature neuroscience*, *19*(2), 299–307.

Rushton, S. K., Harris, J. M., Lloyd, M. R., & Wann, J. P. (1998). Guidance of locomotion on foot uses perceived target location rather than optic flow. *Current Biology*, *8*(21), 1191–1194.

Saitoh, K., Ménard, A., & Grillner, S. (2007). Tectal control of locomotion, steering, and eye movements in lamprey. *Journal of Neurophysiology*, *97*(4), 3093–3108.

Sakai, T., & Kitamoto, T. (2006). Differential roles of two major brain structures, mushroom bodies and central complex, for drosophila male courtship behavior. *Journal of neurobiology*, *66*(8), 821–834.

Saleem, A. B., Ayaz, A., Jeffery, K. J., Harris, K. D., & Carandini, M. (2013). Integration of visual motion and locomotion in mouse visual cortex. *Nature neuroscience*, *16*(12), 1864–1869.

Sareen, P., McCurdy, L. Y., & Nitabach, M. N. (2020). A neural signature of choice under sensory conflict in drosophila. *bioRxiv*.

Savigner, A., Duchamp-Viret, P., Grosmaitre, X., Chaput, M., Garcia, S., Ma, M., & Palouzier-Paulignan, B. (2009). Modulation of spontaneous and odorant-evoked activity of rat olfactory sensory neurons by two anorectic peptides, insulin and leptin. *Journal of neurophysiology*, *101*(6), 2898–2906.

Scaplen, K. M., Talay, M., Fisher, J. D., Cohn, R., Sorkaç, A., Aso, Y., Barnea, G., & Kaun, K. R. (2021). Transsynaptic mapping of drosophila mushroom body output neurons. *Elife*, *10*, e63379.

Scheffer, L. K., Xu, C. S., Januszewski, M., Lu, Z., Takemura, S.-y., Hayworth, K. J., Huang, G. B., Shinomiya, K., Maitlin-Shepard, J., Berg, S., et al. (2020). A connectome and analysis of the adult drosophila central brain. *Elife*, *9*, e57443.

Schilstra, C., & Hateren, J. (1999). Blowfly flight and optic flow. i. thorax kinematics and flight dynamics. *Journal of experimental biology*, *202*(11), 1481–1490.

Schilstra, C., & Van Hateren, J. (1998). Stabilizing gaze in flying blowflies. *Nature*, *395*(6703), 654–654.

Schneider, D. M., Nelson, A., & Mooney, R. (2014). A synaptic and circuit basis for corollary discharge in the auditory cortex. *Nature*, *513*(7517), 189–194.

Schnell, B., Joesch, M., Forstner, F., Raghu, S. V., Otsuna, H., Ito, K., Borst, A., & Reiff, D. F. (2010). Processing of horizontal optic flow in three visual interneurons of the drosophila brain. *Journal of neurophysiology*, *103*(3), 1646–1657.

Schnell, B., Raghu, S. V., Nern, A., & Borst, A. (2012). Columnar cells necessary for motion responses of wide-field visual interneurons in drosophila. *Journal of Comparative Physiology A*, *198*(5), 389–395.

Schnell, B., Ros, I. G., & Dickinson, M. H. (2017). A descending neuron correlated with the rapid steering maneuvers of flying drosophila. *Current Biology*, *27*(8), 1200–1205.

Schnell, B., Weir, P. T., Roth, E., Fairhall, A. L., & Dickinson, M. H. (2014). Cellular mechanisms for integral feedback in visually guided behavior. *Proceedings of the National Academy of Sciences*, *111*(15), 5700–5705.

Schuster, S., Strauss, R., & Götz, K. G. (2002). Virtual-reality techniques resolve the visual cues used by fruit flies to evaluate object distances. *Current Biology*, *12*(18), 1591–1594.

Schwenkgrub, J., Harrell, E. R., Bathellier, B., & Bouvier, J. (2020). Deep imaging in the brainstem reveals functional heterogeneity in v2a neurons controlling locomotion. *Science advances*, *6*(49), eabc6309.

Seelig, J. D., Chiappe, M. E., Lott, G. K., Dutta, A., Osborne, J. E., Reiser, M. B., & Jayaraman, V. (2010). Two-photon calcium imaging from head-fixed drosophila during optomotor walking behavior. *Nature methods*, *7*(7), 535–540.

Seelig, J. D., & Jayaraman, V. (2015). Neural dynamics for landmark orientation and angular path integration. *Nature*, *521*(7551), 186–191.

Shik, M., Severin, F., & Orlovsky, G. (1969). Control of walking and running by means of electrical stimulation of the mesencephalon. *Electroencephalography and clinical neurophysiology*, *26*(5), 549–549.

Shlesinger, M. F. (2009). Random searching. *Journal of Physics A: Mathematical and Theoretical*, *42*(43), 434001.

Shlesinger, M. F., & Klafter, J. (1986). Lévy walks versus lévy flights. *On growth and form* (pp. 279–283). Springer.

Sillar, K. T., & Roberts, A. (1988). A neuronal mechanism for sensory gating during locomotion in a vertebrate. *Nature*, *331*(6153), 262–265.

Sims, D. W., Humphries, N. E., Bradford, R. W., & Bruce, B. D. (2012). Lévy flight and brownian search patterns of a free-ranging predator reflect different prey field characteristics. *Journal of Animal Ecology*, *81*(2), 432–442.

Sims, D. W., Righton, D., & Pitchford, J. W. (2007). Minimizing errors in identifying lévy flight behaviour of organisms. *Journal of Animal Ecology*, *76*(2), 222–229.

Skaggs, W., Knierim, J., Kudrimoti, H., & McNaughton, B. (1994). A model of the neural basis of the rat's sense of direction. *Advances in neural information processing systems*, *7*.

Skavenski, A. A., & Robinson, D. A. (1973). Role of abducens neurons in vestibuloocular reflex. *Journal of Neurophysiology*, *36*(4), 724–738.

Sommer, M. A., & Wurtz, R. H. (2002). A pathway in primate brain for internal monitoring of movements. *science*, *296*(5572), 1480–1482.

Soodak, R., & Simpson, J. (1988). The accessory optic system of rabbit. i. basic visual response properties. *Journal of neurophysiology*, *60*(6), 2037–2054.

Sparks, D. L. (1986). Translation of sensory signals into commands for control of saccadic eye movements: Role of primate superior colliculus. *Physiological reviews*, *66*(1), 118–171.

Sperry, R. W. (1950). Neural basis of the spontaneous optokinetic response produced by visual inversion. *Journal of comparative and physiological psychology*, *43*(6), 482.

Srinivasan, M. (2011). Visual control of navigation in insects and its relevance for robotics. *Current opinion in neurobiology*, *21*(4), 535–543.

Stanford, T. R., Quessy, S., & Stein, B. E. (2005). Evaluating the operations underlying multisensory integration in the cat superior colliculus. *Journal of Neuroscience*, *25*(28), 6499–6508.

Steeves, J. D., & Jordan, L. M. (1980). Localization of a descending pathway in the spinal cord which is necessary for controlled treadmill locomotion. *Neuroscience letters*, *20*(3), 283–288.

Stein, B. E., Huneycutt, W. S., & Meredith, M. A. (1988). Neurons and behavior: The same rules of multisensory integration apply. *Brain research*, *448*(2), 355–358.

Stein, B. E., & Meredith, M. A. (1993). *The merging of the senses.* The MIT Press.

Stein, B. E., & Stanford, T. R. (2008). Multisensory integration: Current issues from the perspective of the single neuron. *Nature reviews neuroscience*, *9*(4), 255–266.

Stephenson-Jones, M., Samuelsson, E., Ericsson, J., Robertson, B., & Grillner, S. (2011). Evolutionary conservation of the basal ganglia as a common vertebrate mechanism for action selection. *Current biology*, *21*(13), 1081–1091.

Stone, T., Webb, B., Adden, A., Weddig, N. B., Honkanen, A., Templin, R., Wcislo, W., Scimeca, L., Warrant, E., & Heinze, S. (2017). An anatomically constrained model for path integration in the bee brain. *Current Biology*, *27*(20), 3069–3085.

Strausfeld, N. J. (1999). A brain region in insects that supervises walking. *Progress in brain research*, *123*, 273–284.

Strausfeld, N. J., & Hirth, F. (2013). Deep homology of arthropod central complex and vertebrate basal ganglia. *Science*, *340*(6129), 157–161.

Strausfeld, N. (1976). *Atlas of an insect brain*. Springer.

Strausfeld, N., & Okamura, J. (2007). Visual system of calliphorid flies: Organization of optic glomeruli and their lobula complex efferents. *Journal of Comparative Neurology*, *500*(1), 166–88.

Strauss, R., & Heisenberg, M. (1993). A higher control center of locomotor behavior in the drosophila brain. *Journal of Neuroscience*, *13*(5), 1852–1861.

Strauss, R., Schuster, S., & Götz, K. G. (1997). Processing of artificial visual feedback in the walking fruit fly drosophila melanogaster. *The Journal of experimental biology*, *200*(9), 1281–1296.

Stryker, M., & Blakemore, C. (1972). Saccadic and disjunctive eye movements in cats. *Vision research*, *12*(12), 2005–2013.

Suver, M. P., Huda, A., Iwasaki, N., Safarik, S., & Dickinson, M. H. (2016). An array of descending visual interneurons encoding self-motion in drosophila. *Journal of Neuroscience*, *36*(46), 11768–11780.

Suver, M. P., Mamiya, A., & Dickinson, M. H. (2012). Octopamine neurons mediate flight-induced modulation of visual processing in drosophila. *Current Biology*, *22*(24), 2294–2302.

Szczecinski, N. S., Bockemühl, T., Chockley, A. S., & Büschges, A. (2018). Static stability predicts the continuum of interleg coordination patterns in drosophila. *Journal of Experimental Biology*, *221*(22), jeb189142.

Takakusaki, K., Kohyama, J., & Matsuyama, K. (2003). Medullary reticulospinal tract mediating a generalized motor inhibition in cats: Iii. functional organization of spinal interneurons in the lower lumbar segments. *Neuroscience*, *121*(3), 731–746.

Tammero, L. F., & Dickinson, M. H. (2002). The influence of visual landscape on the free flight behavior of the fruit fly drosophila melanogaster. *Journal of Experimental Biology*, *205*(3), 327–343.

Tammero, L. F., Frye, M. A., & Dickinson, M. H. (2004). Spatial organization of visuomotor reflexes in drosophila. *Journal of Experimental Biology*, *207*(1), 113–122.

Thura, D., & Cisek, P. (2017). The basal ganglia do not select reach targets but control the urgency of commitment. *Neuron*, *95*(5), 1160–1170.

Ting, L., Blickhan, R., & Full, R. J. (1994). Dynamic and static stability in hexapedal runners. *The Journal of experimental biology*, *197*(1), 251–269.

Todorov, E. (2004). Optimality principles in sensorimotor control. *Nature neuroscience*, *7*(9), 907–915.

Tolman, E. C., Ritchie, B. F., & Kalish, D. (1946). Studies in spatial learning. i. orientation and the short-cut. *Journal of experimental psychology*, *36*(1), 13.

Turano, K., & Wang, X. (1994). Visual discrimination between a curved and straight path of self motion: Effects of forward speed. *Vision Research*, *34*(1), 107–114.

Turner-Evans, D. B., & Jayaraman, V. (2016). The insect central complex. *Current Biology*, *26*(11), R453–R457.

Turner-Evans, D. B., Jensen, K. T., Ali, S., Paterson, T., Sheridan, A., Ray, R. P., Wolff, T., Lauritzen, J. S., Rubin, G. M., Bock, D. D., et al. (2020). The neuroanatomical ultrastructure and function of a biological ring attractor. *Neuron*, *108*(1), 145–163.

Tuthill, J. C., & Azim, E. (2018). Proprioception. *Current Biology*, *28*(5), R194–R203.

Tuthill, J. C., & Wilson, R. I. (2016). Mechanosensation and adaptive motor control in insects. *Current Biology*, *26*(20), R1022–R1038.

Usseglio, G., Gatier, E., Heuzé, A., Hérent, C., & Bouvier, J. (2020). Control of orienting movements and locomotion by projection-defined subsets of brainstem v2a neurons. *Current Biology*, *30*(23), 4665–4681.

van Breugel, F., & Dickinson, M. H. (2014). Plume-tracking behavior of flying drosophila emerges from a set of distinct sensory-motor reflexes. *Current Biology*, *24*(3), 274–286.

Varju, D. (1975). Stationary and dynamic responses during visual edge fixation by walking insects. *Nature*, *255*(5506), 330–332.

Vinck, M., Batista-Brito, R., Knoblich, U., & Cardin, J. A. (2015). Arousal and locomotion make distinct contributions to cortical activity patterns and visual encoding. *Neuron*, *86*(3), 740–754.

Viswanathan, G. M., Afanasyev, V., Buldyrev, S. V., Murphy, E. J., Prince, P. A., & Stanley, H. E. (1996). Lévy flight search patterns of wandering albatrosses. *Nature*, *381*(6581), 413–415.

Viswanathan, G. M., Da Luz, M. G., Raposo, E. P., & Stanley, H. E. (2011). *The physics of foraging: An introduction to random searches and biological encounters*. Cambridge University Press.

Viswanathan, G. M., Buldyrev, S. V., Havlin, S., Da Luz, M., Raposo, E., & Stanley, H. E. (1999). Optimizing the success of random searches. *nature*, *401*(6756), 911–914.

Von Philipsborn, A. C., Liu, T., Jai, Y. Y., Masser, C., Bidaye, S. S., & Dickson, B. J. (2011). Neuronal control of drosophila courtship song. *Neuron*, *69*(3), 509–522.

Von Reyn, C. R., Breads, P., Peek, M. Y., Zheng, G. Z., Williamson, W. R., Yee, A. L., Leonardo, A., & Card, G. M. (2014). A spike-timing mechanism for action selection. *Nature neuroscience*, *17*(7), 962–970.

von Holst, E., & Mittelstaedt, H. (1950). Das reafferenzprinzip. *Naturwissenschaften*, *37*(20), 464–476.

Voss, M., Ingram, J. N., Haggard, P., & Wolpert, D. M. (2006). Sensorimotor attenuation by central motor command signals in the absence of movement. *Nature neuroscience*, *9*(1), 26–27.

Waespe, W., & Henn, V. (1987). Gaze stabilization in the primate. *Reviews of Physiology, Biochemistry and Pharmacology, Volume 106*, 37–125.

Wagner, H. (1986). Flight performance and visual control of flight of the free-flying housefly (musca domestica l.) i. organization of the flight motor. *Philosophical Transactions of the Royal Society of London. B, Biological Sciences*, *312*(1158), 527–551.

Wallace, M. T., Meredith, M. A., & Stein, B. E. (1993). Converging influences from visual, auditory, and somatosensory cortices onto output neurons of the superior colliculus. *Journal of neurophysiology*, *69*(6), 1797–1809.

Wallace, M. T., & Stein, B. E. (1997). Development of multisensory neurons and multisensory integration in cat superior colliculus. *Journal of Neuroscience*, *17*(7), 2429–2444.

Warren, W. H., & Hannon, D. J. (1988). Direction of self-motion is perceived from optical flow. *Nature*, *336*(6195), 162–163.

Warren, W. H., Kay, B. A., Zosh, W. D., Duchon, A. P., & Sahuc, S. (2001). Optic flow is used to control human walking. *Nature neuroscience*, *4*(2), 213–216.

Weir, P. T., & Dickinson, M. H. (2015). Functional divisions for visual processing in the central brain of flying drosophila. *Proceedings of the National Academy of Sciences*, *112*(40), E5523–E5532.

Wertz, A., Haag, J., & Borst, A. (2012). Integration of binocular optic flow in cervical neck motor neurons of the fly. *Journal of Comparative Physiology A*, *198*(9), 655–668.

White, E. P., Enquist, B. J., & Green, J. L. (2008). On estimating the exponent of power-law frequency distributions. *Ecology*, *89*(4), 905–912.

Whitlock, J. R., Sutherland, R. J., Witter, M. P., Moser, M.-B., & Moser, E. I. (2008). Navigating from hippocampus to parietal cortex. *Proceedings of the National Academy of Sciences*, *105*(39), 14755–14762.

Wilson, V., Boyle, R., Fukushima, K., Rose, P., Shinoda, Y., Sugiuchi, Y., & Uchino, Y. (1995). The vestibulocollic reflex. *Journal of Vestibular Research*, *5*(3), 147–170.

Wiltschko, A. B., Johnson, M. J., Iurilli, G., Peterson, R. E., Katon, J. M., Pashkovski, S. L., Abraira, V. E., Adams, R. P., & Datta, S. R. (2015). Mapping sub-second structure in mouse behavior. *Neuron*, *88*(6), 1121–1135.

Windhorst, U. (2007). Muscle proprioceptive feedback and spinal networks. *Brain research bulletin*, *73*(4-6), 155–202.

With, K. A. (2019). *Essentials of landscape ecology*. Oxford University Press.

Wolf, H., & Burrows, M. (1995). Proprioceptive sensory neurons of a locust leg receive rhythmic presynpatic inhibition during walking. *Journal of Neuroscience*, *15*(8), 5623–5636.

Wolf, R., & Heisenberg, M. (1990). Visual control of straight flight in drosophila melanogaster. *Journal of Comparative Physiology A*, *167*(2), 269–283.

Wolf, R., & Heisenberg, M. (1986). Visual orientation in motion-blind flies is an operant behaviour. *Nature*, *323*(6084), 154–156.

Wosnitza, A., Bockemühl, T., Dübbert, M., Scholz, H., & Büschges, A. (2013). Inter-leg coordination in the control of walking speed in drosophila. *Journal of experimental biology*, *216*(3), 480–491.

Wu, M., Nern, A., Williamson, W. R., Morimoto, M. M., Reiser, M. B., Card, G. M., & Rubin, G. M. (2016). Visual projection neurons in the drosophila lobula link feature detection to distinct behavioral programs. *Elife*, *5*, e21022.

Yarbus, A. L. (1967). *Eye movements and vision*. Springer-Verlag.

Yellman, C., Tao, H., He, B., & Hirsh, J. (1997). Conserved and sexually dimorphic behavioral responses to biogenic amines in decapitated drosophila. *Proceedings of the national academy of sciences*, *94*(8), 4131–4136.

Zacarias, R., Namiki, S., Card, G. M., Vasconcelos, M. L., & Moita, M. A. (2018). Speed dependent descending control of freezing behavior in drosophila melanogaster. *Nature communications*, *9*(1), 1–11.

Zeil, J. (1986). The territorial flight of male houseflies (fannia canicularis l.) *Behavioral ecology and Sociobiology*, *19*(3), 213–219.

Zhou, M., Liang, F., Xiong, X. R., Li, L., Li, H., Xiao, Z., Tao, H. W., & Zhang, L. I. (2014). Scaling down of balanced excitation and inhibition by active behavioral states in auditory cortex. *Nature neuroscience*, *17*(6), 841–850.

ITQB-UNL | Av. da República, 2780-157 Oeiras, Portugal
Tel (+351) 214 469 100 | Fax (+351) 214 411 277

www.itqb.unl.pt